INVESTIGATION OF WATER VAPOR EFFECTS ON THE DETECTION OF NITRIC ACID VAPOR WITH THE TUNGSTIC ACID TECHNIQUE

by

RALPH MICHAEL MARINARO JR.

Dissertation submitted to the Graduate Faculty of the

Virginia Polytechnic Institute and State University

in partial fulfillment of the requirements for the degree of

DOCTOR OF PHILOSOPHY

in

Environmental Science and Engineering

APPROVED:

J. M. Hughes, Chairman

G. D. Boardman

B. I. Chevone

J. P. Wightman

W. D. Conn

August, 1986

Blacksburg, Virginia

ACKNOWLEDGMENTS

This research could not have been accomplished without much support.

On a professional basis, at Virginia Tech, I have appreciated the opinions and input of my former advisor for his initial confidence and J. M. Hughes whose invaluable guidance allowed for this works completion. Also, my thanks go to committee members: Greg Boardman, David Conn, Boris Chevone, and Jim Wightman, and Department Head Dick Walker and Program Chairman Clifford Randall. Of course, in addition to these, at NASA, , , and proved essential to finalizing the redirection and regrouping which was required to complete my research at work.

Financially, I am obliged to thank Virginia Tech (ESEN, CE), the Department of Energy, the Environmental Protection Agency, the U.S. Forestry Service and the Veterans Administration for funding and NASA for the job opportunity.

Personally, as much as all the above, I would like to thank many friends I have made, in particular, , , , , , , , and .

Finally, my most devoted thanks to my family, especially my parents, , and , for their moral, financial and emotional support, to whom this work is ultimately dedicated.

TABLE OF CONTENTS

TABLE OF CONTENTS (cont.)

CONTENTS (continued)

LIST OF FIGURES

LIST OF FIGURES (cont.)

LIST OF FIGURES (cont.)

LIST OF TABLES

LIST OF TABLES (cont.)

CHAPTER I

INTRODUCTION

The recent interest in acid rain has lead to investigations of approaches to measure and quantify atmospheric processes which generate acid formation. Nitric acid vapor (HNO_3) is a major contributor to acid precipitation (National Academy of Science, 1977, and Adams, 1986). Development of analytical measurement methodology for nitric acid has come under study (Stevens, 1979 and Spicer et al., 1982). This measurement methodology becomes crucial to the understanding of the formation and transport of nitric acid in the atmosphere. Model development with atmospheric chemistry and chemical kinetics will need to be validated by accurate measurement. Atmospheric processes, such as heterogeneous removal (Fishman and Crutzen, 1978, Stedman et al., 1980) can be characterized to complete the source-to-fate scenario. Future policy issues to control acidic deposition based on such an overall understanding can then be assessed and implemented.

Nitric acid is second only to sulfuric acid in acidic input to acid rain. Occasionally, nitric acid has been found (NOAA, 1984) to be

greater than sulfuric acid as in the western U.S. According to Barnes (1979), nitric acid contribution to acid rain can be as high as 40%, based on nitrogen dioxide (NO_2) solubility and nitrate (NO_3^-) atmospheric residence time. These precursor chemical species, which are generated from combustion processes, have also been shown to react photochemically and heterogeneously to form gaseous nitric acid. The exact mechanisms for nitric acid and acid rain formation is not known, but is generally believed to be formed in transformation processes of a chemical nature within clouds (Vermeulen, 1979). One objective of nitric acid research is to define the role of atmospheric nitric acid and the precursors for its formation. The ultimate fates of these chemical species have been shown to have deleterious impacts on sensitive ecosystems.

It becomes apparent that an understanding (practical and theoretical) of the numerous pathways and mechanisms for nitric acid formation must be supported quantitatively. The formation of nitric acid depends on atmospheric conditions such as other chemical species, relative humidity, temperature, solar irradiance and their interactions to name a few. The complex interaction of these factors make attempts to model nitric acid formation difficult. Research has been aimed at investigating each or as many of these variables as possible to aid in determining the extent of each variable's effect on nitric acid formation.

Water vapor, in particular, has been shown to be associated with nitric acid (Stedman et al., 1975 and Seinfeld, 1975). Research directed to water vapor's role has provided valuable insight to nitric

acid modelling. The association of H_2O with HNO_3 may also prove to be a hinderance to effective HNO_3 measurement techniques (Goldan et al., 1983, and Eatough et al., 1985) because of changes in the chemical and physical characteristics caused by the hydration of nitric acid. Therefore, critical to the decisions to implement control strategies for the precursors of nitric acid, the need arises to make measurements of nitric acid under ambient relative humidity conditions.

Nitric acid measurements require analytical techniques which are as free from interferents as possible and just as insensitive to changes in atmospheric conditions. The relative effectiveness of all techniques for nitric acid measurement is of major concern. There has been little study and some conjecture as to the effect of atmospheric water vapor (i.e., relative humidity) on measurement methods requiring a collection medium (Goldan et al., 1983 and Eatough et al., 1985), as well as its role in nitric acid formation.

The selection of a medium to collect ambient HNO_3, which is specific for HNO_3 collection and maintains the integrity (i.e., gas versus aerosol separation) of the sample is still the major obstacle. Techniques have been reported which do this, but upon subsequent evaluation have been shown to be less effective than first reported. Therefore, either improvements need to be made on those techniques or further research is required to find a collection/analysis method which specifically measures atmospheric HNO_3.

Initial attempts to measure nitric acid using filter method techniques to separate and collect HNO_3 were thought to be successful.

Fellin et al. (1980) in laboratory studies showed minimal loss of filter collected HNO_3 under humid conditions and compared different filter media for collection capability. Upon further investigation by Goldan et al. (1983), relative humidity was correlated with increased HNO_3 loss from standard filter media (teflon/nylon filter packs). Relative humid-humidity is not the major problem with filter techniques, rather the inability to effectively separate gas and aerosol HNO_3 phases, the long sample time and large sample collection flows to collect enough HNO_3 for detection have led to research using different techniques (Knapp et al., 1986).

Other HNO_3 measurement techniques (laser, denuders) have shown promise, but do not have as strong a data base as filter techniques and lack full testing in both laboratory and ambient trials. These new techniques have the required sensitivity and specificity to prove to be effective HNO_3 detection methods, once current evaluations are completed. The effect of relative humidity on these techniques is one of the criterion in such an evaluation.

Contradictory evidence of the effect of relative humidity (RH) on the Tungstic Acid Technique (TAT) for HNO_3 measurement has been offered. Research by Wartburg et al. (1984) and Eatough et al. (1985) indicates an apparent systematic loss of HNO_3 under typical ambient RH conditions using the TAT denuder method. Braman et al. (1982 and 1985) has shown the effect of RH to be neglible for this same method. Since a comprehensive study of the effects of relative humidity on TAT measurement of nitric acid has not been done and is relevant, further research is necessary.

The hypothesis of this research is that the Tungstic Acid Technique is not affected by water vapor and is an appropriate method for atmospheric nitric acid measurement. This hypothesis is based on gas phase diffusion theory and experimentation for nitric acid. Using the Gormely-Kennedy equation, Braman et al. (1982) has shown that certain conditions must be established for high collection efficiency (85% RH) for gaseous nitric acid on tungsten VI oxide (WO_3) coated denuder tubes. Using conditions defined in that study for tube length, sample collection flow and diffusion coefficient, collection efficiency remains high. Diffusion coefficients are a function of temperature and pressure which must also be properly maintained. When all these conditions are satisfied collection of gaseous HNO_3 is high (> 90%) even in humid air. There has not been any other experimental or theoretical research specifically dealing with WO_3 and HNO_3 chemistry, making these viable future topics.

The current nitric acid measurement capabilities for polluted areas, which can be as high as 20 ppbv, have been demonstrated (Hildemann et al., 1984). More commonly, ambient HNO_3 levels range from 1-20 ppbv. In unpolluted environs (background) and at high altitudes of several thousand meters, HNO_3 concentrations can be in the parts-per-trillion (pptv) range which is below current detection limits. To date, confidence in field tested HNO_3 measurements is at best 100 pptv, and more realistically at 500 pptv. There are no proven field tested measurements for pptv HNO_3 levels using continuous methods. The benefit of denuders is in preconcentrating ambient background HNO_3 for short sample

times (< 20 minutes) to obtain measurable amounts of HNO_3. Increasing the sensitivity of the detection system and/or the collection efficiency of the denuder tubes will decrease sample time (< 5 minutes) and lower detection limits (50 pptv) approaching quasi-real time measurement capabilities for background levels of gaseous HNO_3. This was achieved in laboratory tests under dry and humid conditions in this research.

This research has shown the importance of laboratory testing instruments under real world conditions, in particular, ambient relative humidity levels for nitric acid measurement techniques. It has also shown that physical conditions (i.e. temperature) can contribute greatly to the collection efficiency of a medium used for HNO_3. Therefore, it is necessary that such conditions be considered in future HNO_3 analysis and current techniques be evaluated with respect to these and other similar effects.

This study was conducted at the National Aeronautics and Space Administration (NASA) facility at the Langley Research Center in Hampton, Virginia. NASA's interest is in global atmospheric chemistry characterization, in situ global atmospheric chemistry characterization as well as from space, which includes: species measurement, meteorology, changes in atmospheric composition, modelling and atmospheric strategies from recommendations based on these data. Upcoming NASA atmospheric research missions will include background nitric acid measurements to evaluate measurement techniques and to determine global distribution of this important contributor to acid rain. In-flight instrumentation to measure sub-part-per-billion (by volume) gaseous

nitric acid concentrations will be required. This study furthers that goal by modifying the TAT method to achieve optimum nitric acid collection, analysis and quantification required by real world effects of water vapor and temperature.

CHAPTER II

LITERATURE REVIEW

The complex nature of oxides of nitrogen (NO_x) species, makes measurements and characterization of any one individual specie difficult. Figure 1 is an attempt to summarize the source-to-fate scenario for nitrogen oxide species based on models developed by Russell et al. (1985). It shows how the primary NO_x pollutants (NO and NO_2) are involved in triggering secondary pollutant formation. A number of pathways are shown for the formation of nitric acid, which becomes a key terminal product and aerosol nitrate (NIT) generator. Accurate measurement of HNO_3 is difficult because it is reactive (both homogeneous and heterogeneous) and exists at low concentration in the overall nitrogen cycle. Attempts to characterize the role of HNO_3 in this cycle are based more on expected chemical behavior than on quantitative measurement, because data is sparse due to the lack of sensitive detection methods. The combination of chemical characterization and accurate sensitive measurement will define the actual role of atmospheric nitric acid.

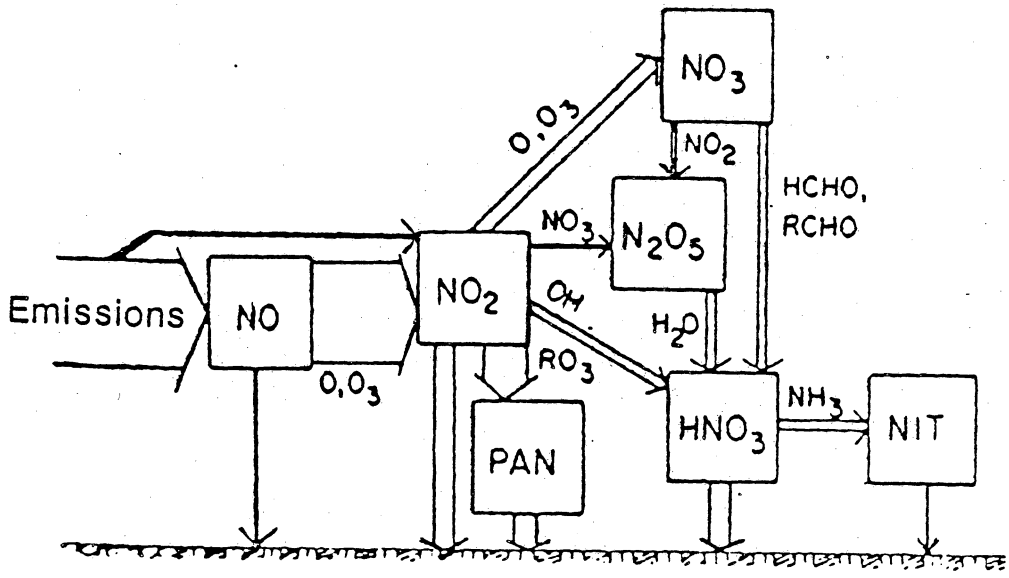

Figure 1. Schematic representation of the net flux between nitrogen oxides species, including reaction paths for aerosol nitrate (NIT) formation. The width of these arrows indicates the magnitude of the net flux during the base case 24-h trajectory simulation. Russell et al., 1985.

1. Atmospheric HNO_3

NRC (1975), Huebert and Lazrus (1980), and LeBel et al. (1983), have profiled nitric acid in the atmosphere shown in Figures 2, 3, and 4, respectively, with in-flight measurements and models in an attempt to characterize its ambient chemical behavior. There is interest in both tropospheric and stratospheric nitric acid because of its role as a termination product in many chemical processes; photochemical reactions as in Figure 5 and deposition as in Figure 6. Table I summarizes some of these processes and indicates the importance of water vapor to nitric acid formation.

Figures 7, 8, and 9 (Miller and Spicer, 1975, and Spicer and Miller, 1976) show the effect of irradiation on nitrogeneous pollutants and ozone (O_3). Some important concepts are illustrated by these studies. The greatest concentrations of nitric acid develop during prolonged exposure to light in smog chambers. In these lines, Lazrus et al. (1981) reports the greatest acidity in air occurs during the passage of a warm front (i.e. warm southerly air) being overridden by a cold front after a stagnating high pressure system has increased pollutant precursor concentrations as shown in Figure 10. Since clear skies are usually associated with high pressure systems, the meteorological scenario (i.e., high solar irradiance) which would most likely produce maximum nitric acid levels is shown in Figure 11. Relative humidity also increases prior to the passage of a front and is associated with the formation of nitric acid.

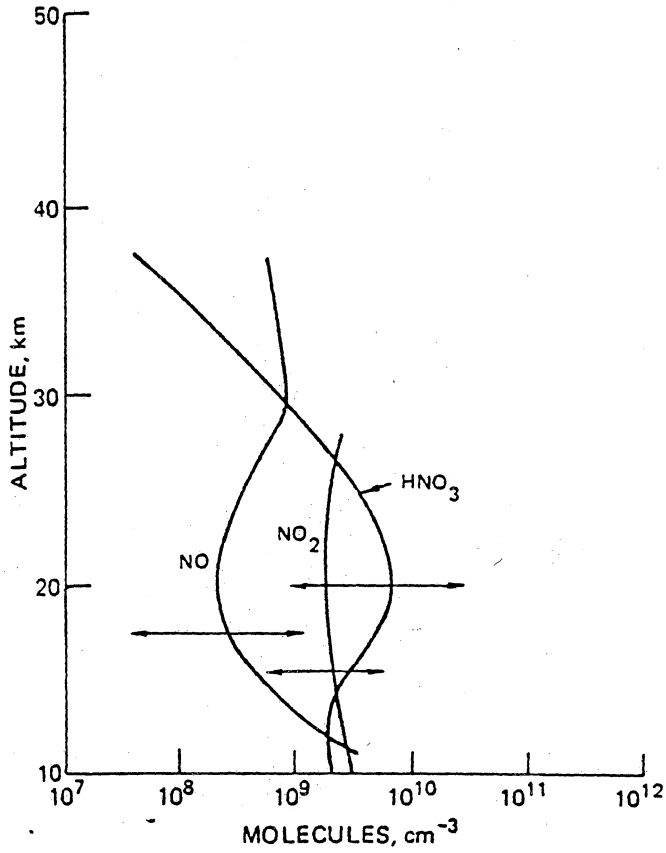

Figure 2. Concentrations of nitric oxide (NO), nitrogen dioxide (NO_2), and nitric acid in the stratosphere. National Academy of Science, 1977.

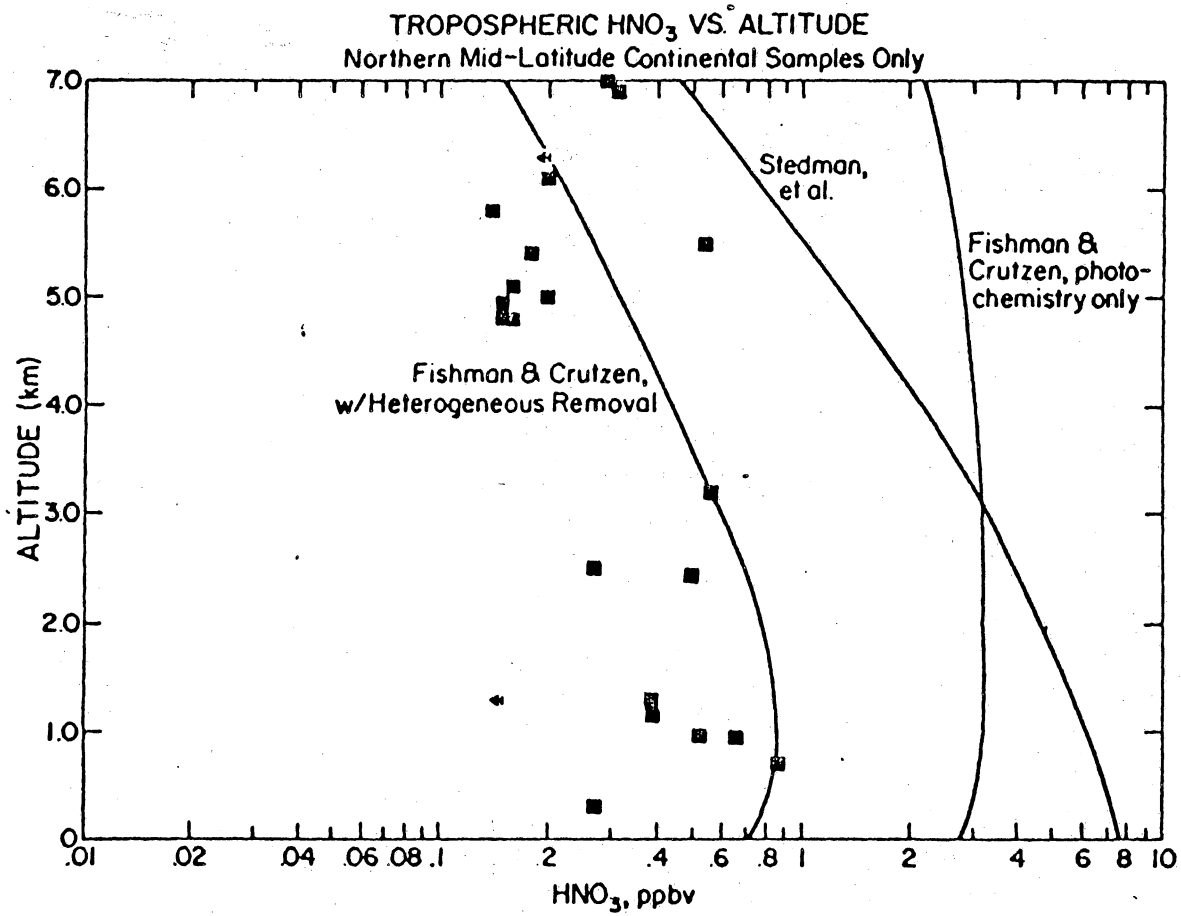

Figure 3. Tropospheric HNO_3 vs. altitude. Northern mid-latitude continental samples only. Huebert and Lazrus, 1979.

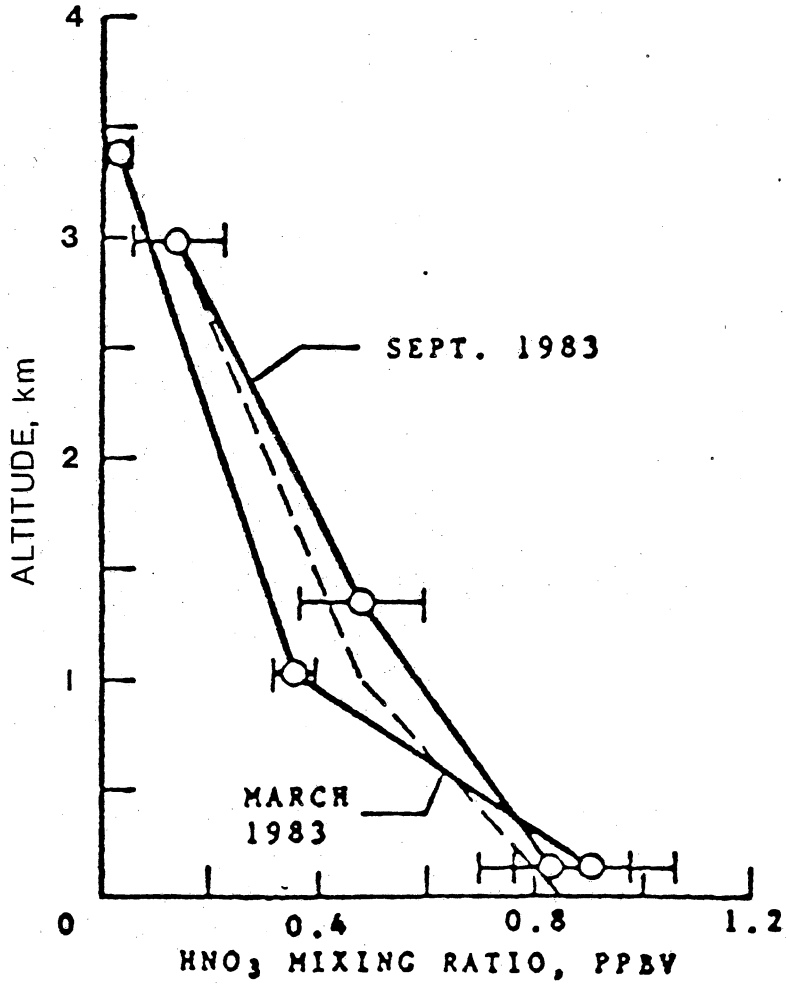

Figure 4. Vertical profiles and seasonal variation of tropospheric nitric acid over coastal Virginia and Maryland. The dashed line is the result of photochemical calculations. LeBel et al., 1983.

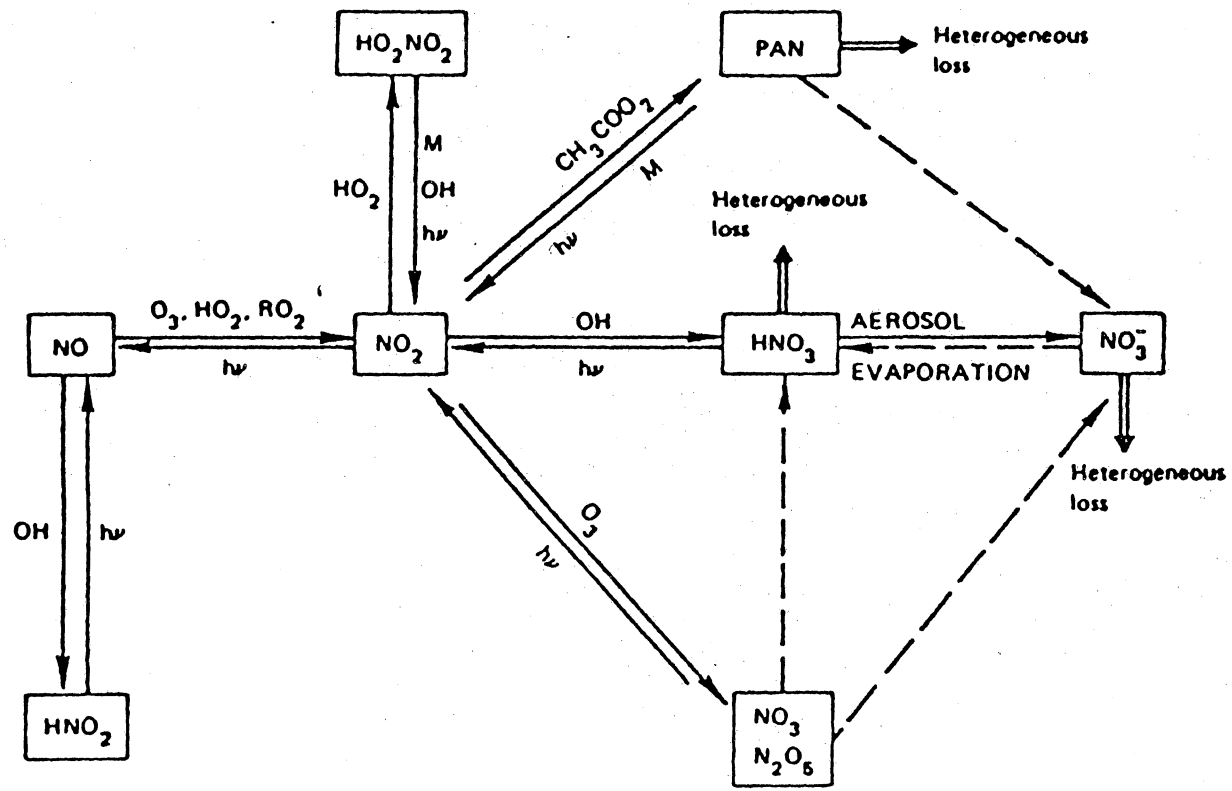

Figure 5. Photochemical transformations among odd-nitrogen species. Liu and Cicerone, 1984.

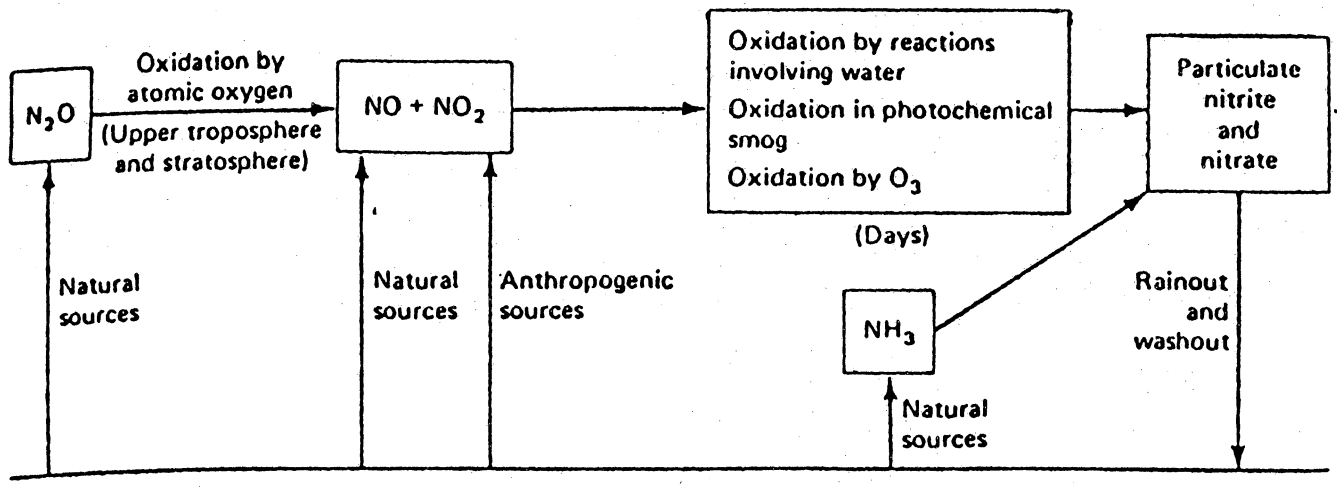

Figure 6. Nitrogen cycle for the nitrogen-containing compounds in air pollution. Seinfeld, 1985.

Table I. Nitric Acid and Nitrate Aerosol Formation Reactions. National Academy of Science, 1977.

1. Nitrogen dioxide – hydroxyl free radical reaction

$$NO_2 + HO\cdot + M \longrightarrow HNO_3 + M$$

2. Nitric acid anhydride reaction

$$NO_2 + O_3 \longrightarrow NO_3 + O_2$$
$$NO_3 + NO_2 \longrightarrow N_2O_5$$
$$N_2O_5 + H_2O \longrightarrow 2HNO_3$$

3. Homogeneous conversions of nitric acid to aerosol

$$HNO_3\ (g) + H_2O\ (g) \longrightarrow HNO_3 \text{ aerosol}$$
$$N_2O_5\ (g) + H_2O\ (\ell) \longrightarrow HNO_3 \text{ aerosol}$$
$$NH_3\ (g) + HNO_3\ (g) \longrightarrow NH_4NO_3 \text{ aerosol}$$

4. NO_x absorption into aerosol droplets

$$2\,NO_2 + H_2O\ (\ell) \longrightarrow HNO_3 + HNO_2 \quad \text{(aqueous solution)}$$
$$NO + NO_2 + H_2O\ (\ell) \longrightarrow 2HNO_2 \quad \text{(aqueous solution)}$$
$$HNO_2\ (aq.) \longrightarrow H^+ + NO_2^- \quad \text{(aqueous solution)}$$
$$NO_2^- + \tfrac{1}{2}\,O_2 \text{ (in aerosol solution)} \longrightarrow NO_3^-$$
$$NO_2^- + O_3 \text{ (in aerosol solution)} \longrightarrow NO_3^- + O_2$$

5. Hydrolysis of PANs

$$RC(=O)OONO_2 + H_2O\ (\ell) \longrightarrow RC(=O)OH + O_2 + HNO_2 \rightleftharpoons H^+ + NO_2^- \quad \text{(aqueous solution)}$$
$$NO_2^- + \tfrac{1}{2}\,O_2 \longrightarrow NO_3^-$$

6. Methyl nitrate formation

$$CH_3O\cdot + NO_2 \longrightarrow CH_3NO_3$$

Methoxy radical — methyl nitrate

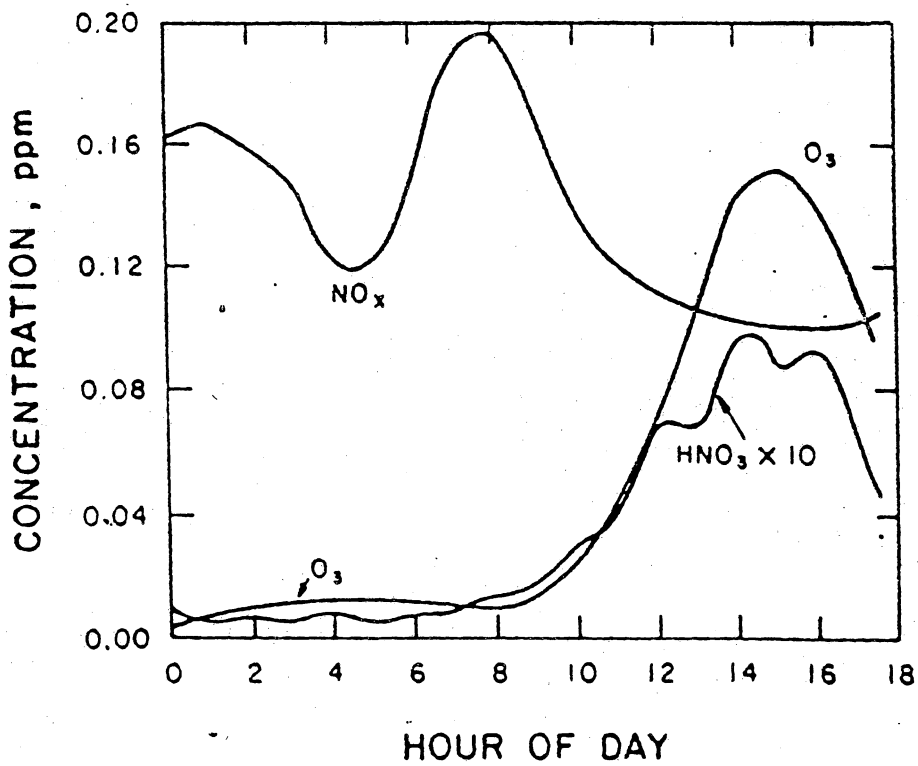

Figure 7. Composite diurnal profile of nitric acid concentration West Covina, Ca. Miller and Spicer, 1975.

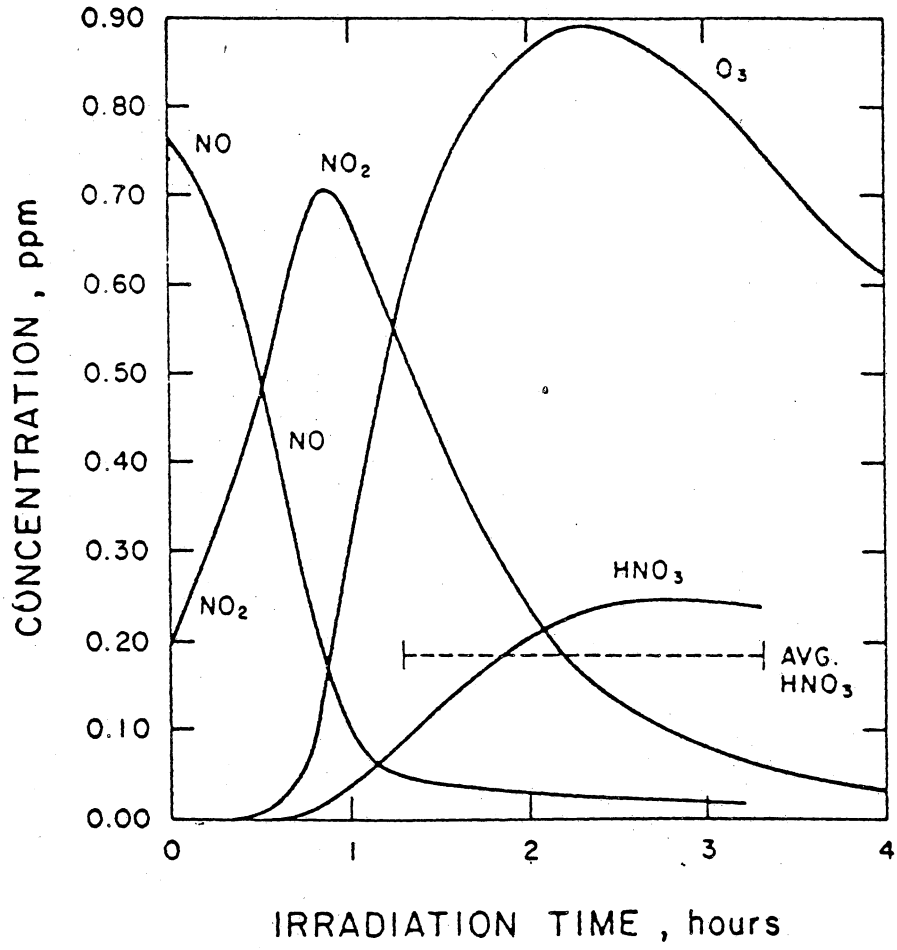

Figure 8. Profile of nitric acid formation during irradiation of synthetic auto exhaust mixture. Spicer and Miller, 1976.

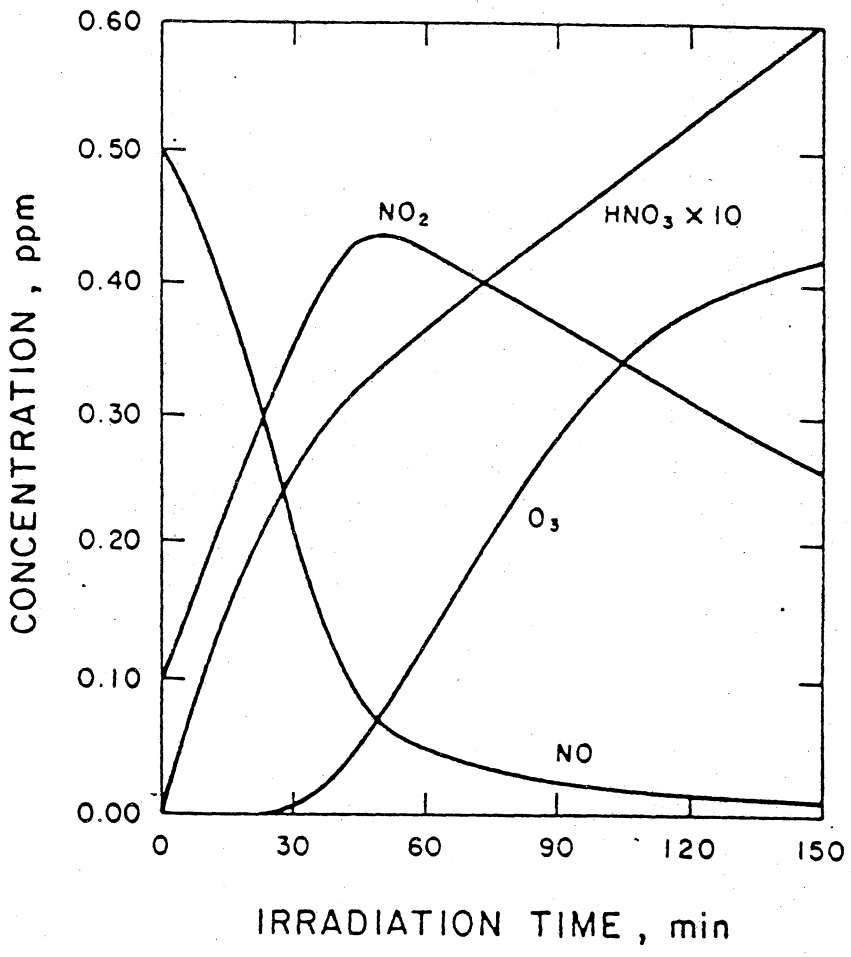

Figure 9. Profile of nitric acid formation during photooxidation of NO in humid air containing 4000 ppm CO. Spicer and Miller, 1976.

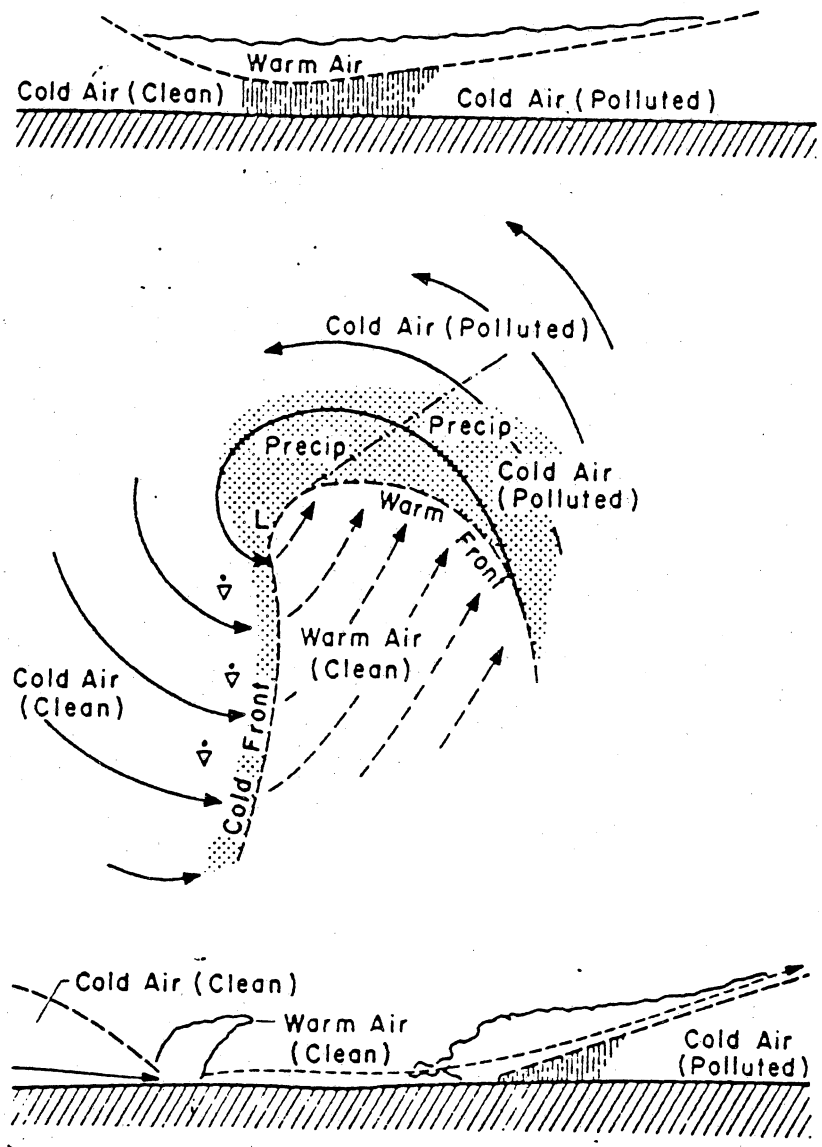

Figure 10. Idealized cyclone. In middle diagram, curved arrows are streamlines of surface airflow. Top and bottom diagrams are vertical cross sections along direction of cyclone movement north of its center and across warm sector south of its center. Lazrus et al., 1981.

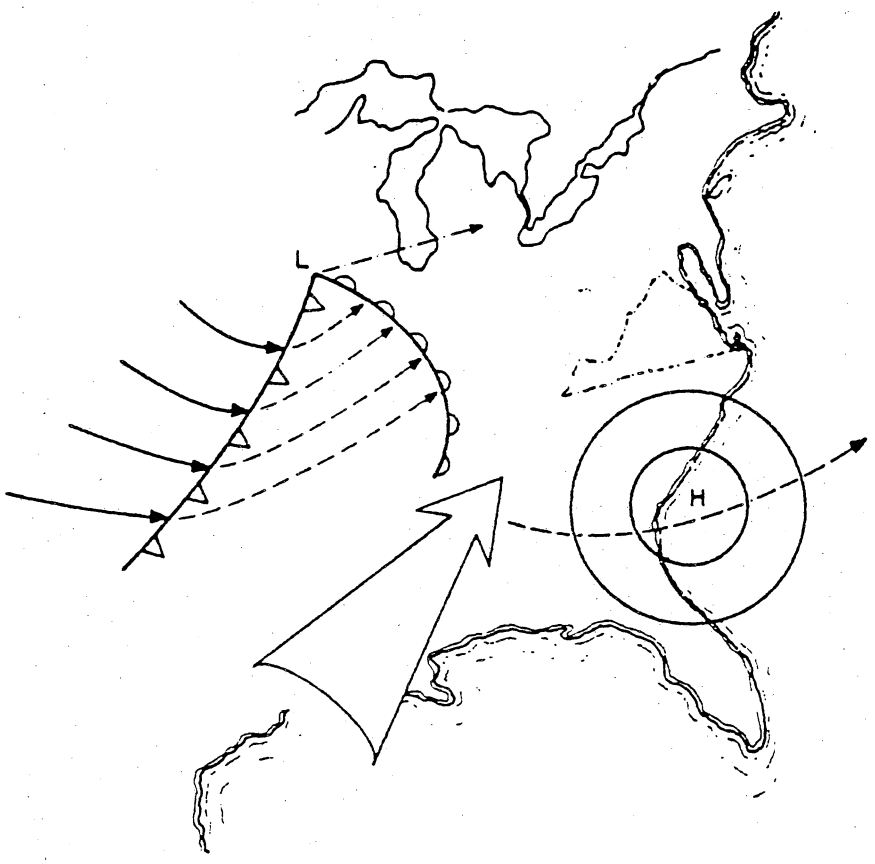

Figure 11. Meteorological conditions expected to yield the highest concentration of nitric acid for Mid-Atlantic states. Low pressure system advancing as stagnating high pressure moves offshore, resulting in a moist, southerly flow of warm air (large arrow).

In addition to this, Spicer and Miller (1976) have shown that the concentration of nitric acid can be set in the following approximate proportionality:

$$PAN/HNO_3 = NO_2/N_2O_5 \qquad (1)$$

once the concentration of NO_2 (nitrogen dioxide), N_2O_5 (nitrogen pentoxide) and HNO_3 are determined, the expected concentration of PAN (peroxyacylnitrate) can be approximated. This approximate concentration adds an important dimension to the rate of formation of nitric acid, because the formation of PAN is both a competitive reaction (for NO_2) and a potential interference to the measurement of nitric acid in the atmosphere.

When a polluted, heterogeneous atmosphere is considered, certain chemical reactions are more dominant than others. Table II summarizes those reactions which contribute to nitric acid formation in a polluted, heterogeneous atmosphere. Joseph and Spicer (1978) proposed that the formation of nitric acid in the lower atmosphere is basically due to the following reactions,

$$NO_2 + O_3 \longrightarrow NO_2 + O_2$$

$$NO_3 + NO_2 \longleftrightarrow N_2O_5$$

$$N_2O_5 + H_2O \longrightarrow 2HNO_3$$

Reaction 2a is the key propagation reaction, and reaction 3 is much faster than the back-reaction 2b (Leighton, 1961).

Table II. Reactions and Rate Constants in the Formation of Nitric Acid in a Polluted Heterogeneous atmosphere.

Reaction	Rate Constant
1. $NO_2 + O_3 \longrightarrow NO_3 + O_2$	$0.46 \times 10^{-1} ppm^{-1} min^{-1}$
2a. $NO_3 + NO_2 \longrightarrow N_2O_5$	$4.43 \times 10^{3} ppm^{-1} min^{-1}$
2b. $N_2O_5 \longrightarrow NO_2 + NO_3$	$1.38 \times 10^{1} min^{-1}$
3a. $N_2O_5 + H_2O \longrightarrow 2\ HNO_3$	$2.5 \times 10^{-3} ppm^{-1} min^{-1}$
3b. $2\ HNO_3 \longrightarrow N_2O_5 + H_2O$	? ?
4. $HNO_3 + NO \longrightarrow HNO_2 + NO_2$	$2.5 \times 10^{-4} ppm^{-1} min^{-1}$
5. $HNO_3 + HNO_2 \longrightarrow 2\ NO_2 + H_2O$	$0.2\ ppm^{-1} min^{-1}$
6. $NO + NO_2 + H_2O \longrightarrow 2\ HNO_2$	$4.3 \times 10^{-6} ppm^{-2} min^{-1}$
7. $NO_3 + NO \longrightarrow 2\ NO_2$	$1.48 \times 10^{4} ppm^{-1} min^{-1}$
8. $NO_3 + NO_2 \longrightarrow NO + O_2 + NO_2$	$0.37\ pphm^{-1} hr^{-1}$ *
9. $OH\bullet + NO_2 \longrightarrow HNO_3$	$1.5 \times 10^{4} ppm^{-1} min^{-1}$
10. $2HNO_2 \longrightarrow NO + NO_2 + H_2O$	$1.5 \times 10^{-5} ppm^{-1} min^{-1}$
11. $HONO + h\nu \longrightarrow OH\bullet + NO$	depends on light ints
12. $OH\bullet + NO \longrightarrow HONO$	$1.2 \times 10^{4} ppm^{-1} min^{-1}$
13. $3\ NO_2 + H_2O \longrightarrow 2\ HNO_3 + NO$	? ?
14. $NO_2 + RO_2\bullet \longrightarrow PAN$	$5.9 \times 10^{3} ppm^{-1} min^{-1}$ **

Hampson and Garvin, 1977, * Hampson, 1973, ** Seinfeld, 1975

Fishman and Crutzen (1978) indicate that the formation of nitric acid through free hydroxyl radical ($OH^{\bullet}$) reaction ($NO_2 + OH^{\bullet} + M \rightarrow HNO_3$) is 20 times as fast as the dissociation of nitric acid ($HNO_3 \rightarrow OH^{\bullet} + NO_2$) closest to the earth's surface (1km).

Stedman et al. (1979) have shown that the vertical distribution of water (H_2O) soluble gases in the troposphere is limited by kinetic processes and molecular diffusion. In the Stedman study, the strong correlation between the mixing ratio profile of H_2O and HNO_3 provides additional evidence that the anhydride reaction (3) is highly likely. Furthermore, Spicer and Miller (1976) have indicated that reactions 1-3 occur before the time that the $OH^{\bullet}$ level is at its maximum. More recently, Seigneur and Saxena (1984) have concluded that nitric acid is formed rapidly from the hydroxyl radical reaction during daylight hours, and the anhydride reaction at night. However, the anhydride reaction occurs through both the homogeneous and heterogeneous pathways.

2. HNO_3 Measurement

As mentioned in the Introduction, a number of analytical techniques have been reported for the measurement of nitric acid. Spicer et al. (1978) used ion chromatography (IC) and a filter collection system to measure nitric acid (as nitrate). Ross et al. (1978) using electron capture/gas chromatography (EC/GC) was able to determine nitric acid concentration in the atmosphere, also using a filter collection system. HNO_3 was collected on nylon filters, then extracted with C_6H_6 (benzene) under acidic conditions yielding $C_6H_5NO_2$, which was detected by EC/GC.

Sensitivity of this technique was approximately 0.5 ppb. The Denuder Difference Experiment (Shaw et al., 1979, 1982) uses a filter system with a magnesium oxide (M_gO coated) denuder tube and allows for compensation of artifact nitrate formation on filters, which are analyzed by either ion chromatography or by x-ray diffraction. Huebert and Lazrus (1979, 1980a, 1980b) used filters treated with tetra-n-butylammonium hydroxide and colormetric techniques (spectroscopy) to measure nitric acid.

All of the above techniques mentioned require in-lab analysis of the filter collection medium. This is not a desirable aspect for approximating real-time measurement of atmospheric nitric acid. Also, the sample times which are required for sufficient analysis levels are long (hours) when dealing with low concentrations (i.e., background). Preparation of standards, instrument calibration, treatment of filters and their extraction of sample take time and add to overall delay in determining ambient concentrations. When this is added to the time delay between sample collection and analysis (hours in flight) there is an increased potential for sample contamination and misrepresentation. Therefore, even quasi-real-time sampling is impractical, if impossible, in flight using filter techniques.

Cadle (1985) states that filter techniques continue to be used even with this lag time in data collection/analysis, because of their simplicity to effectively measure total nitrate and a large data base for comparison exists. Dual filter techniques use teflon filters for removing nitrate aerosols, backed by nylon filters which trap nitric

acid from a passing air stream (Fellin et al., 1980 and Goldan et al., 1983). The collection of nitric acid is followed by IC analysis. The HNO_3 is detected as NO_3^-. These procedures have yet to dispell errors associated with negative artifact nitrate loss (from teflon to nylon filters) and positive nitrate gain, nitric acid accumulating on aerosols trapped on teflon filter (Appel et al., 1980 and 1981, Appel and Tokiwa, 1981, Shaw et al., 1982, and Cadle et al., 1982). The former leads to positive artifact HNO_3, the latter to negative HNO_3 (on the nylon filters) determinations (Harker et al., 1977, Spicer and Schumacher, 1979, and Russell et al., 1983).

The gains and losses of the filter methods are attributed to three main causes; (1) NH_4NO_3 aerosol volatilization from teflon filters, (2) strong acid (e.g., H_2SO_4) reaction with non-volatile nitrate (e.g., $NaNO_3$) and (3) relative humidity. In the Appel studies, as much as 50% of the NH_4NO_3 collected on the teflon filter could volatilize and be collected on the nylon filter. Shaw et al. (1982) found the same effect to be approximately 25%. These results supported the theoretical work of Stelson et al. (1979) concerning the equilibria between $HNO_3 + NH_3 \longleftrightarrow NH_4NO_3$. Similarly, theoretical work by Harker et al. (1977) concerning the liberation of HNO_3 from non-volatile nitrates due to strong acids was supported experimentally by Pierson et al. (1980). Further supporting the theory of relative humidity effects on filter collection media in the Stelson and Harker studies, Fellin et al. (1980), Cadle et al. (1982), Spicer and Schumacher (1983) and Goldan et al. (1983), showed that relative humidity causes loss of HNO_3 from nylon

filters, with the Goldan study indicating nearly 55% loss of HNO_3 from nylon filters. In an effort to reduce these problems, Mulawa and Cadle (1985) have shown the penetration method (nylon-coated interior wall tubes) can be used in a difference experiment which achieve significant reductions in nitric acid and non-volatile particulate nitrate interferences.

There are non-filter measurement techniques for atmospheric nitric acid. Miller and Spicer (1975) used a modified Mast microcoulumb meter adapted for sensing acids rather than oxidants and integrated this analysis with a chromatropic acid method. HCOOH (formic acid) and HNO_2 (nitrous acid) were interferents and the system required a long response time with only a 5.0 ppb detection limit. Tuazon et al. (1980) used Fourier Transform Spectroscopy Long Path Infrared Absorption (FTS-LPIR) to detect ambient HNO_3 concentration of greater than 1.0 ppb. This system is too large (23 meters) and too sensitive to vibrations for in-flight purposes. A tunable diode laser absorption spectroscopy (TDLAS) system has been successfully field tested by Schiff et al. (1983). It has high resolution for trace gas analysis, and can measure nitric acid without interference from other gases at laser absorption wavelength 5.8 μm with 0.5 ppb detection capability.

Dual channel chemiluninescence oxides of nitrogen (NO_x) analyzers have been modified by Joseph and Spicer (1978) and Kelly et al. (1979) to measure nitric acid. Nylon is used as an absorbing medium (scrubber) to remove nitric acid from a sample air stream in one of the two channels. The difference between the unscrubbed and scrubbed air

samples, then, is equal to ambient nitric acid. A commercial NO_x analyzer, when modified as in the Kelly study, can detect nitric acid to 0.3 ppb.

The Denuder Difference Experiment mentioned earlier stimulated interest in other denuder techniques because of the selective nature of this method for gaseous measurement. Gaseous HNO_3 diffuses to the interior walls of chemically coated tubes where it is chemisorbed. Once nitric acid is collected, it can be analyzed through various techniques. The analytical sensitivity of these systems is dependent upon denuder collection efficiency, chemical interferents and analyzer detection limitations. Ferm (1982) used sodium carbonate (Na_2CO_3 coated) denuders and IC analysis to measure nitric acid (as NO_3^-). An annular (Na_2CO_3/Glycerine coated) denuder was shown by Possanzini (1983) to effectively collect nitric acid. Again, IC analysis was used, with nitric acid sensitivity approximately 0.04 ppb.

Braman et al. (1982 and 1985), McClenny et al. (1982) and Eatough et al. (1985) used tungsten oxide (WO_3 coated) denuders to collect HNO_3 and analyzed, after thermal desorption, (as NO) with commercial chemiluminescence NO_x analyzers. The sensitivity of this technique for nitric acid is approximately 0.05 ppb. Aluminum sulfate ($Al_2(SO_4)_3$ coated) denuders have been used similarly by Lindqvist (1985) with gas chromatography/photoionization detection. This system's sensitivity is described to be 0.006 ppb for nitric acid.

There has been some question as to the effectiveness of denuders in humidified environments. The concern is based on the ability of nitric

acid to form hydrated species (Lloyd and Wyatt, 1955) which may cause a decrease in the efficiency of denuder tube collection capability. Wartburg et al. (1984) reports a 20% loss of efficiency when humidified conditions exist while collecting HNO_3 with a WO_3 coated denuder. Eatough et al. (1985) supports these claims when WO_3-coated tubes were compared to other HNO_3 measurement techniques. These findings are opposite to that of Braman et al. (1982 and 1985), who found no significant loss using the Tungstic Acid Technique. Therefore, the need arises for further research on the effects of relative humidity for collection media in general, and more specifically for denuder methods.

3. Tungstic Acid Technique

The tungstic acid technique (TAT) used in the Braman and McClenny studies was chosen for this study to measure nitric acid, because the TAT facilitates measurement of HNO_3, NH_3, and their aerosols (NO_3^-, NH_4^+). This method clearly differentiates between gaseous nitric acid and its aerosols, therefore, there is little error in specifically measuring HNO_3. Also, Table III shows the technique is shown to be relatively free of potential interferents (Braman, 1985). In addition to this, the method is relatively inexpensive, because it is an add-on collection system to commercially available chemiluminescent NO_x analyzers. An automated system has been successfully operated in field (McClenny et al., 1982) and in flight measurement (LeBel et al., 1983). The contradictory results mentioned earlier concerning relative humidity effects warrants the need for further research with the tungstic acid technique.

Table III. Interference effects of various compounds on tungsten oxide denuder (TOD) measurement of NH_3 and HNO_3 [Braman et al., 1982].

Compound	Concentration	Effect
Mono-, di-, tri-methylamines	(specify)	significant (specify)
NO_2	50N.M.	<1%
O_3	100ppb	Decreased NH_3 adsorption by 5%
PAN	50-500MG	Not adsorbed
Organics (e.g., ethanol, benzene, methylene chloride, formaldehyde, etc.)	MG	No response
HCN	MG	No response
SO_2	MG	No response
H_2S	MG	No response
NO	MG	No response
DMS	MG	No response

The key to the TAT is the tungstic acid-coated tube shown in Figure 12. Forty-five cm length Vycor tubes were coated with Tungsten VI oxide once treated with benzene, hot 50% NaOH, water, HF and oven drying (as described by Braman et al., 1982). Figure 13 shows the vacuum deposition apparatus used for coating the tubes. The tungsten wire inside the sampling tube is heated by passing through it a 12 ampere current for 2 hours, while the tube is under a vacuum of 10 Torr. The tube is then oxidized by passing oxygen through the heated tubes yielding the WO_3 coating.

Figure 14 shows a sample collection and analysis system using the preconditioned WO_3-coated tubes for gases (HNO_3 and NH_3) only. The operation of a more elaborate, automated system used in this study is described in the Materials and Method section. A cooling system was added as part of this research also.

The tungstic acid technique follows the principles of trace gas diffusion within a hollow tube addressed by Gormely and Kennedy (1949). The following equation was developed in that study which relates diffusion to interior tube walls and collection tube efficiency,

$$C/Co = 0.819\exp(-11.488(D)(L)/F) + \ldots + \ldots \qquad (2)$$

where C is concentration of gas that passes through the tube and Co is the initial concentration, C/Co (in percent) is tube leakage (therefore, tube efficiency is 1-C/Co), L is tube length (cm), F is sample flow (cm^3/sec) and D (cm^2/sec) is the diffusion coefficient of a trace

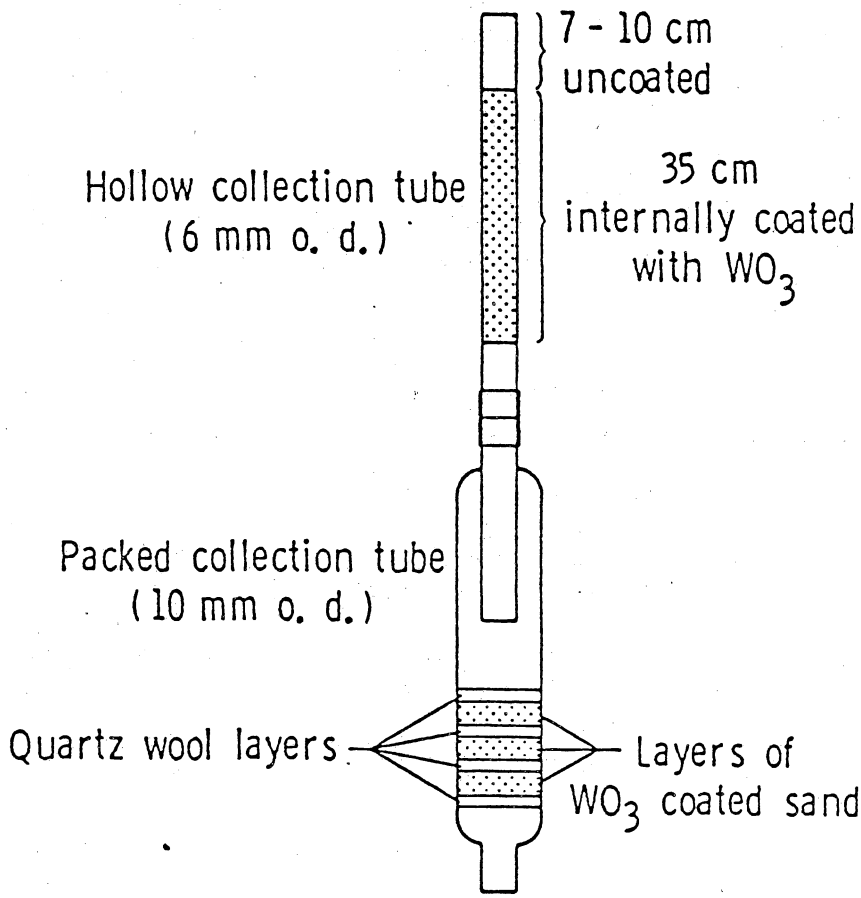

Figure 12. Schematic diagram of tungsten oxide denuder and packed collection tubes. Hoell et al., 1984

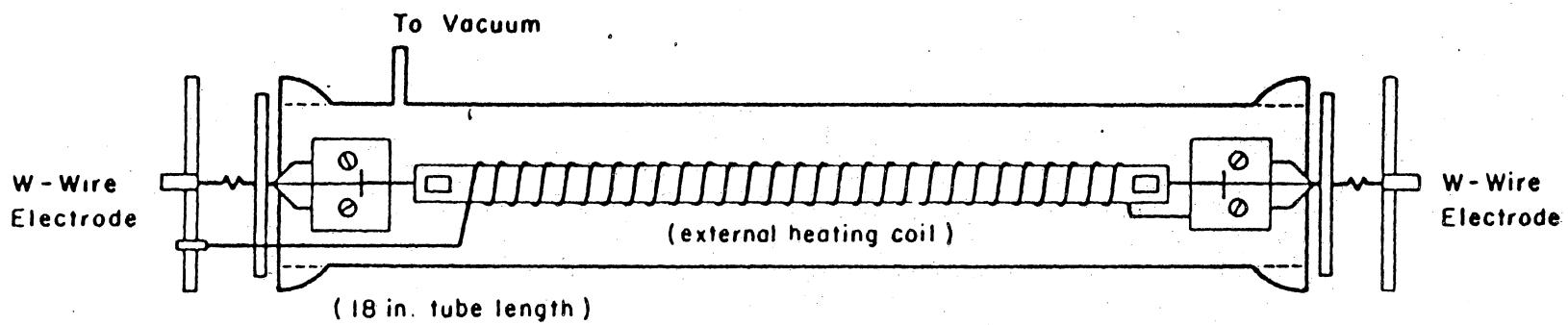

Figure 13. Apparatus for coating hollow tubes. Braman et al., 1982

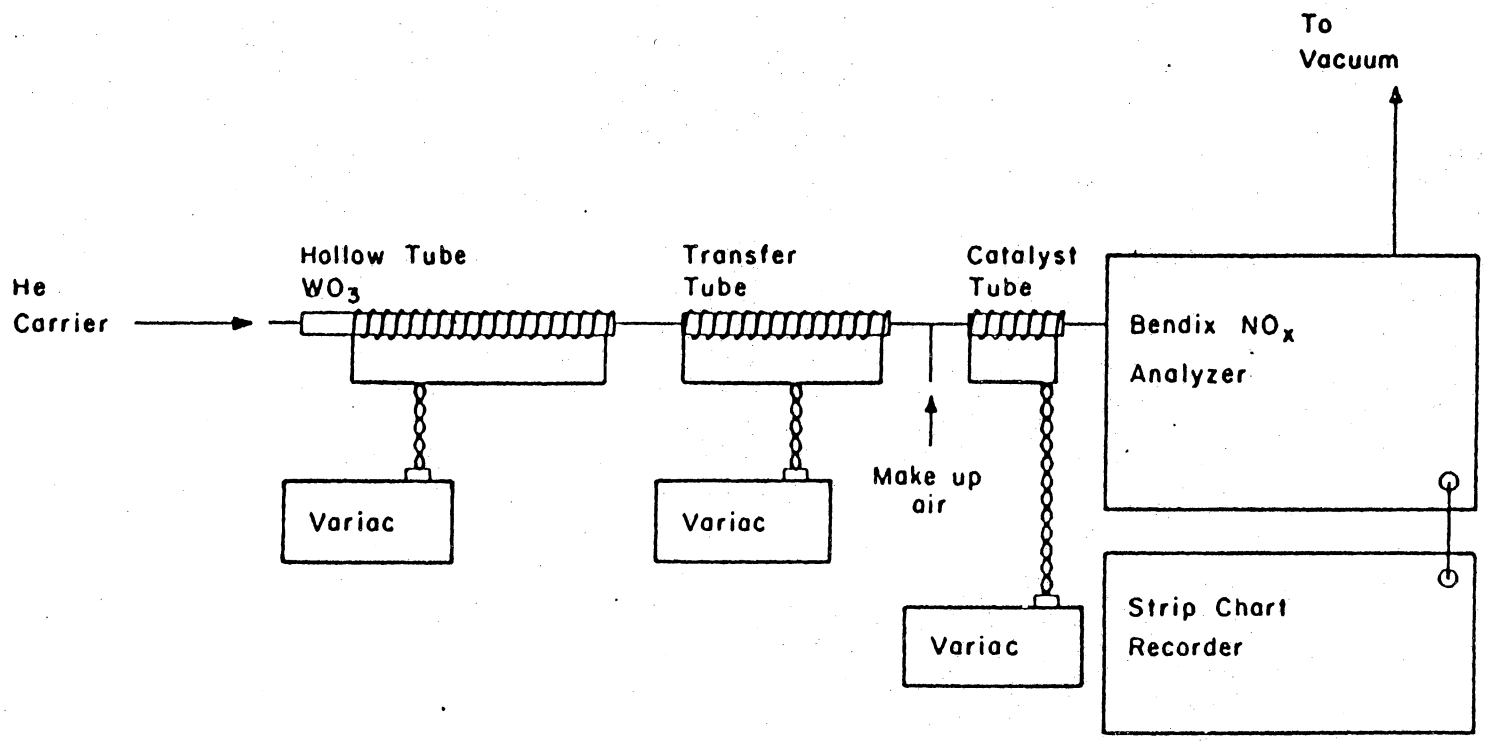

Figure 14. Apparatus for gaseous preconcentration tube analysis. Braman et al., 1982

compound at temperature, T (K), and pressure, P (mm Hg) described by the following,

$$D = Do(T/273)(760/P) \quad (3)$$

Do = 0.150 cm^2/sec for dry nitric acid (Wilke and Lee, 1955). Hydrated forms of nitric acid yield slightly lower diffusion coefficients with increased hydration number (i.e., the number of H_2O molecules associated with a hygroscopic molecule). Braman et al. (1982 and 1985) did extensive theoretical work and established load capacities and WO_3-coated tube lengths used in the TAT for atmospheric HNO_3 concentrations. An efficiency range of 80-95% for gaseous HNO_3 collection was determined depending on flow rate, tube length and hydration number.

The mechanism of nitric acid absorption is not clearly understood but experimental work indicates that irreversible chemisorption is involved. Absorption may take place due to formation of the inorganic acyl nitrate.

$$WO_2(OH)_2 + 2HNO_3 \longrightarrow WO_2(NO_3)_2 + 2H_2O$$

or

$$WO_2(OH)_2 + HNO_3 \longrightarrow WO_2(OH)(NO_3) + H_2O$$

Thermal decomposition of this type of compound would then occur in a manner similar to that of other nitrates.

$$WO_2(NO_3)_2 \longrightarrow 3/2\ O_2 + 2NO + WO_3$$

Thermal decomposition of nitrates appears to occur at temperatures just below the temperature needed for ammonia release from the tungstic acid tubes. Generally, only a single broad peak is observed in nitric acid desorption.

4. Summary

Tables I and II (reactions 3a,b, 6, 10, 13) show that the formation of HNO_3 is dependent on the presence of H_2O. Therefore, the practical application of a measurement technique for HNO_3 should not be subject to effects due to changes in atmospheric water vapor. The objective of this study is to further understanding of the ability of TAT to effectively measure nitric acid with respect to relative humidity.

CHAPTER III

MATERIALS AND METHODS

1. Instrumentation

Figure 15 shows the integrated system built by NASA for the automated TAT used in this study. The sampling and analysis system is controlled by a Hewlett Packard 85 personal computer, which also records the data and integrates the area under the signal generated by an NO_x analyzer. The computer controls the electronic relays which are used to turn valves and heaters on/off for the proper collection and analysis processes (described in the Procedures section) in the sample collection apparatus including coolant and carrier flows. The nitric oxide (NO) generated in the analysis cycle is detected by a modified chemiluminescent oxides of nitrogen (NO_x) analyzer, which is described subsequently. The NO_x analyzer signal from the photomultiplier tube (PMT) is amplified, then measured by an electronic photon counter. A digital voltmeter/analog data controller (DVM/ADC) is used to send the electronic signal from the PMT to the HP85.

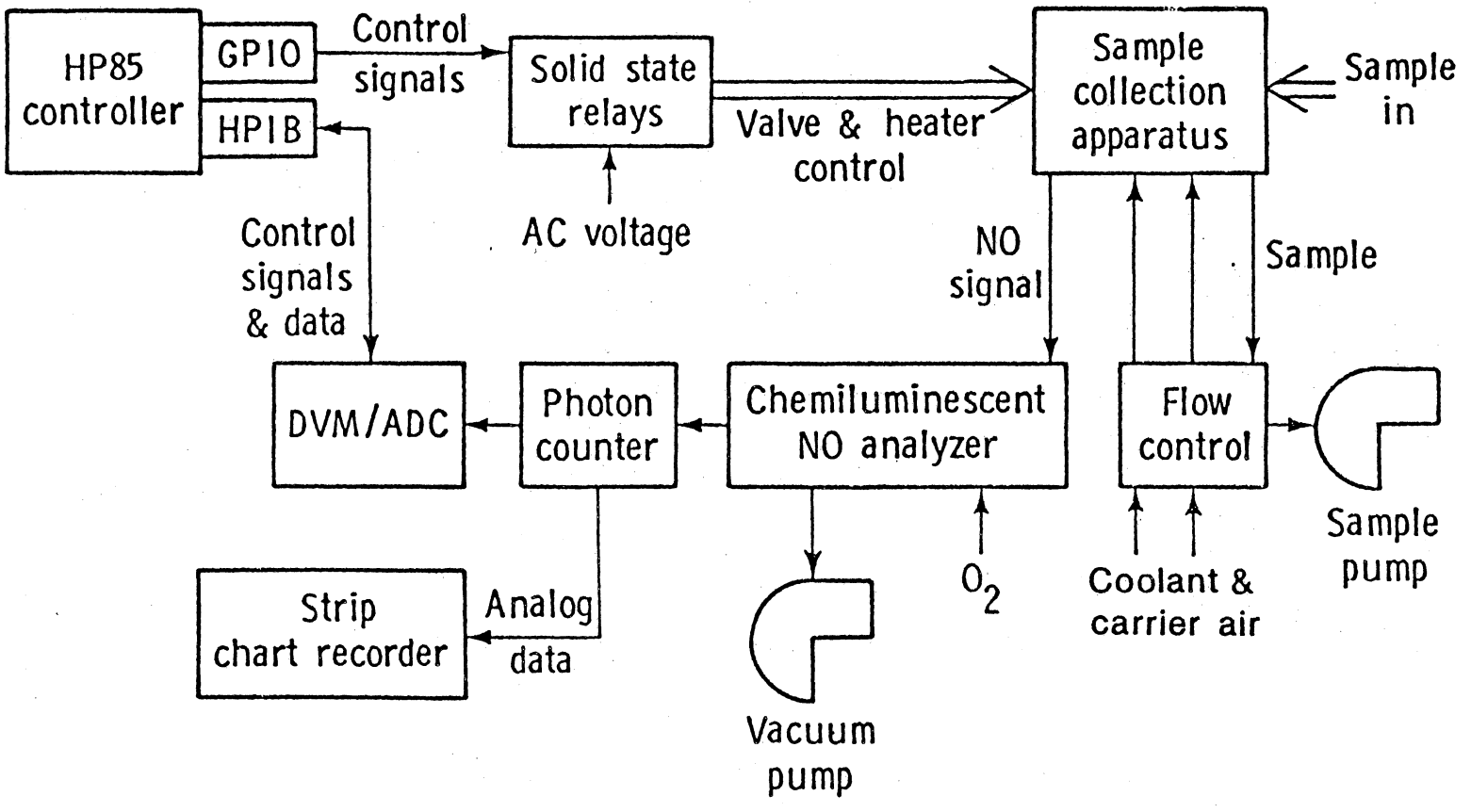

Figure 15. Automated HNO_3, NH_3, NO_3^-, and NH_4^+ collection and analysis system.

A "super" NO_x analyzer was built for increased sensitivity to measure HNO_3. Shown schematically in Figure 16, this modified analyzer has a larger reaction chamber as in Figure 17, which is gold coated, and increased ozone (O_3) input due to the larger chamber size. It utilizes the principle of photometric detection of the chemiluminescence of the reaction of NO with ozone ($NO + O_3$ to form activated NO_2). A portion of the energy of the activated NO_2 gives off light by fluorescence to reach ground state. The intensity of emitted light measured by the photomultiplier tube (PMT) and counting system is proportional to the concentration of NO.

2. Procedures

The measurement of HNO_3 vapor with the TAT is a two-step process; sampling with treated tubes and analysis of the tubes. Figure 18 is a schematic of the sample collection unit used to collect the analysis constituents (sample) and desorb them as a detectable gas (NO), measured with a chemiluminescence NO_x analyzer, which constitutes the second step in the procedure (analysis). Figure 19 illustrates the overall process for desorbing and analyzing the collected gas samples from the chemisorbed tubes.

Sample collection is done by pumping sampled gas (i.e., air) through the hollow and packed tubes with a 1 liter per minute (1/min) flow-controlled sample pump shown in Figure 18. Gases (HNO_3 and NH_3) chemisorb on the hollow tube and aerosols pass to the packed tube (see Figure 19 and Literature Review section) by the Gormley-Kennedy diffusion equation (Braman et al., 1982, Eatough et al., 1985).

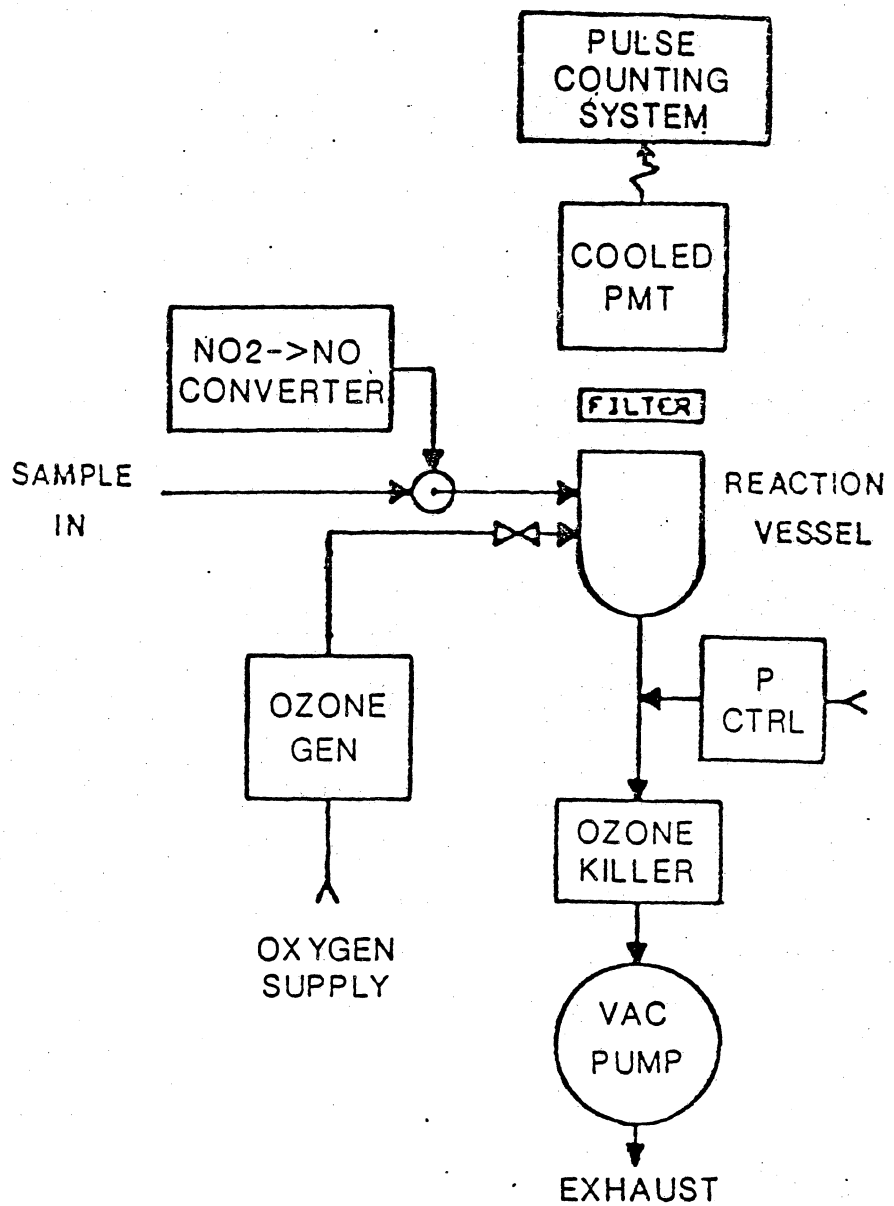

Figure 16. Schematic diagram of "super" NO_x analyzer configuration. Torres, 1985.

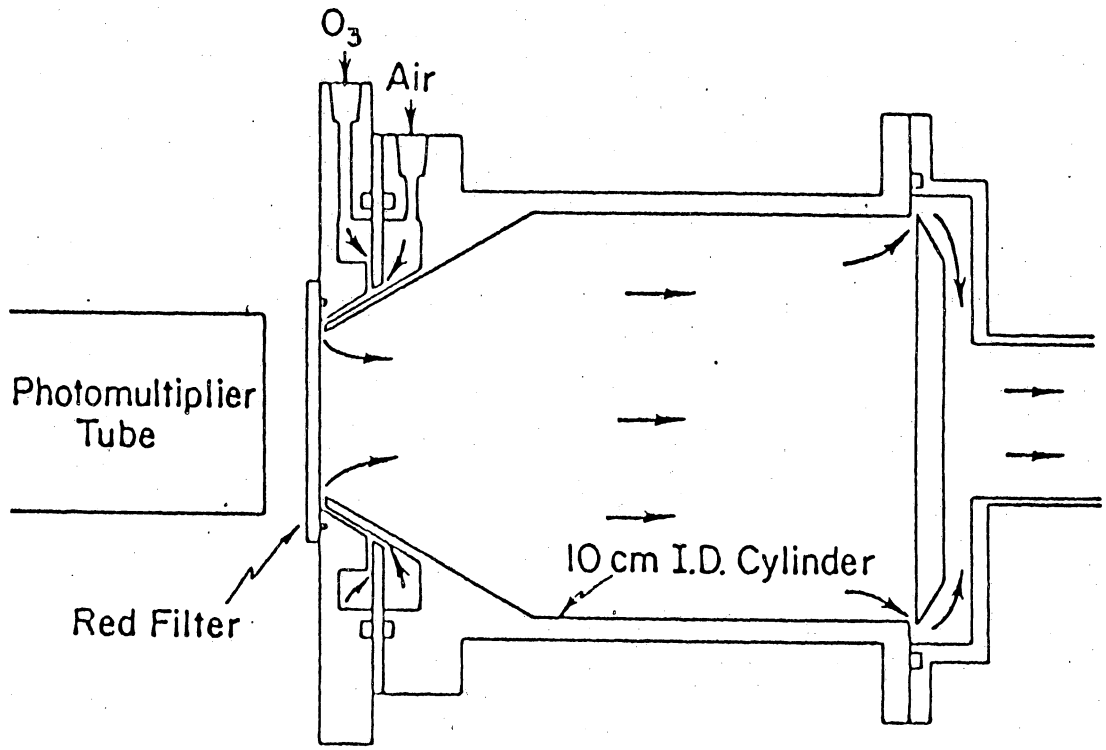

Figure 17. Schematic diagram of gold interior coated reaction vessel (Bollinger, 1982).

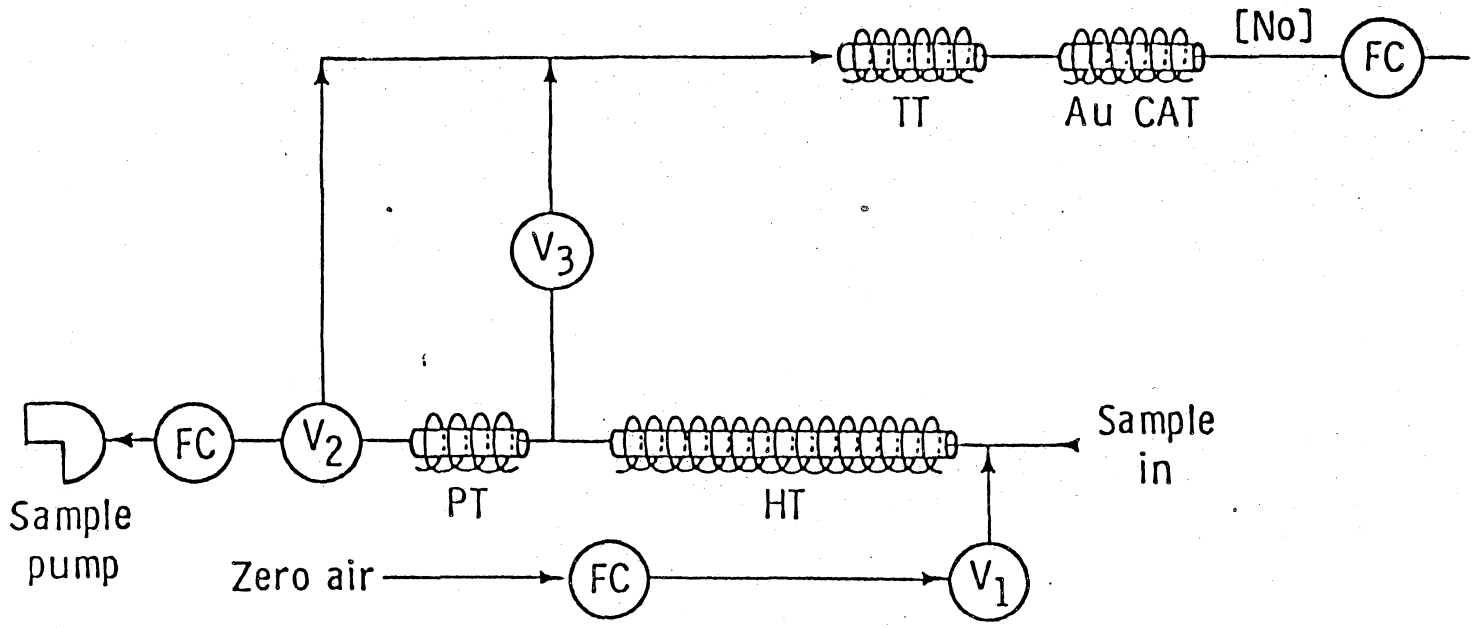

V_1, V_2, V_3	Teflon solenoid valves
FC	Flow controller
HT	WO_3 coated hollow tube
PT	WO_3 coated sand-packed tube
TT	WO_3 coated transfer tube

Figure 18. Schematic flow diagram of the sample collection and analysis system.

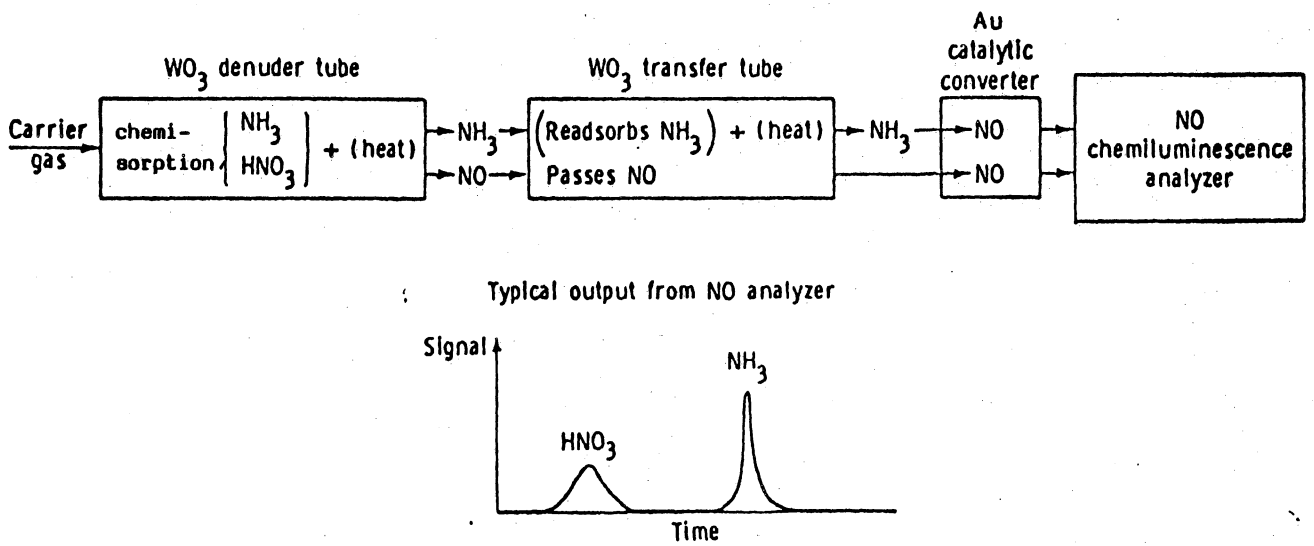

Figure 19. Schematic diagram and typical output of analysis process for hollow denuder tubes (gaseous HNO_3 and NH_3) Hoell, 1984.

The HP85 computer controls the flows for either collection or analysis. Flow controllers regulate the amount of flow of the carrier, sample and analysis gases. The flow sequence is as follows:

(1) Sampling - valve one (V1) and valve three (V3) are closed, three way valve (V2) is open to the sample pump. Gases and aerosols collect on the hollow (HT) and packed (PT) tubes.

(2) Gas analysis - V2 closes to the pump, when the sample period is over, and opens to the analyzer direction. Simultaneously, the carrier valve, V1 opens and provides excess zero air (in relation to the demand of the NO_x analyzer), while V3 also opens. The PT restricts flow in its direction. Gases are analyzed in this sequence; HNO_3, then NH_3.

(3) Aerosol analysis - same as above but V3 is closed, forcing carrier through the PT. Aerosols are analyzed in this sequence; NO_3^-, then NH_4^+.

Analysis begins as the hollow tube is heated to approximately 350°C, while the transfer tube remains cool. The nitric acid collected on the hollow tube is converted to NO which is not re-adsorbed by the transfer tube (see Figure 19 and Literature Review section). Nitric acid (as NO) is detected immediately by a modified Monitor Labs Oxides of Nitrogen Analyzer. The integrated peak area recorded by the NO_x analyzer is proportional to the ambient concentration of gaseous HNO_3 (see Figure 19). Ammonia released at the same time (as HNO_3) in the heating of the hollow tube is re-adsorbed onto the transfer tube. After the nitric

acid signal has decreased to baseline, the transfer tube is heated to drive off the adsorbed ammonia. A gold catalyst (see Figure 18) is used to convert ammonia to NO (see Figure 19). This is done by heating the catalyst bed to 600°C, and oxidizing the ammonia with carrier gas (zero air). Thus, the separation between nitric acid and ammonia can be made as shown in Figure 19.

Nitrate aerosols collected on the packed tube are analyzed the same way as hollow tubes as shown in Figure 20, after the gas analyses are completed. Nitrate is converted to NO_2 and NO upon heating, while ammonium is converted to ammonia.Again, the transfer tube collects only the ammonia (i.e., ammonium ion), so that the NO_X analyzer detects only NO (i.e., NO_3^-). Later, the transfer tube is heated producing a signal proportional to the ammonium present.

The determination of peak area to nitric acid and other collected constituent concentrations depends on calibration of the system with known gaseous concentrations. Calibration of the TAT system is described subsequently.

3. Calibration

Calibration was done in two parts; the calibration of the NO_X analyzer and the calibration of the tungstic acid tubes. Calibration of the NO_X analyzer was achieved using a dilution system and a NBS traceable NO gas source (99 ppm NO in N_2) described in Figure 21. The tungstic acid tubes were calibrated using the permeation tube/dilution system shown in Figure 22.

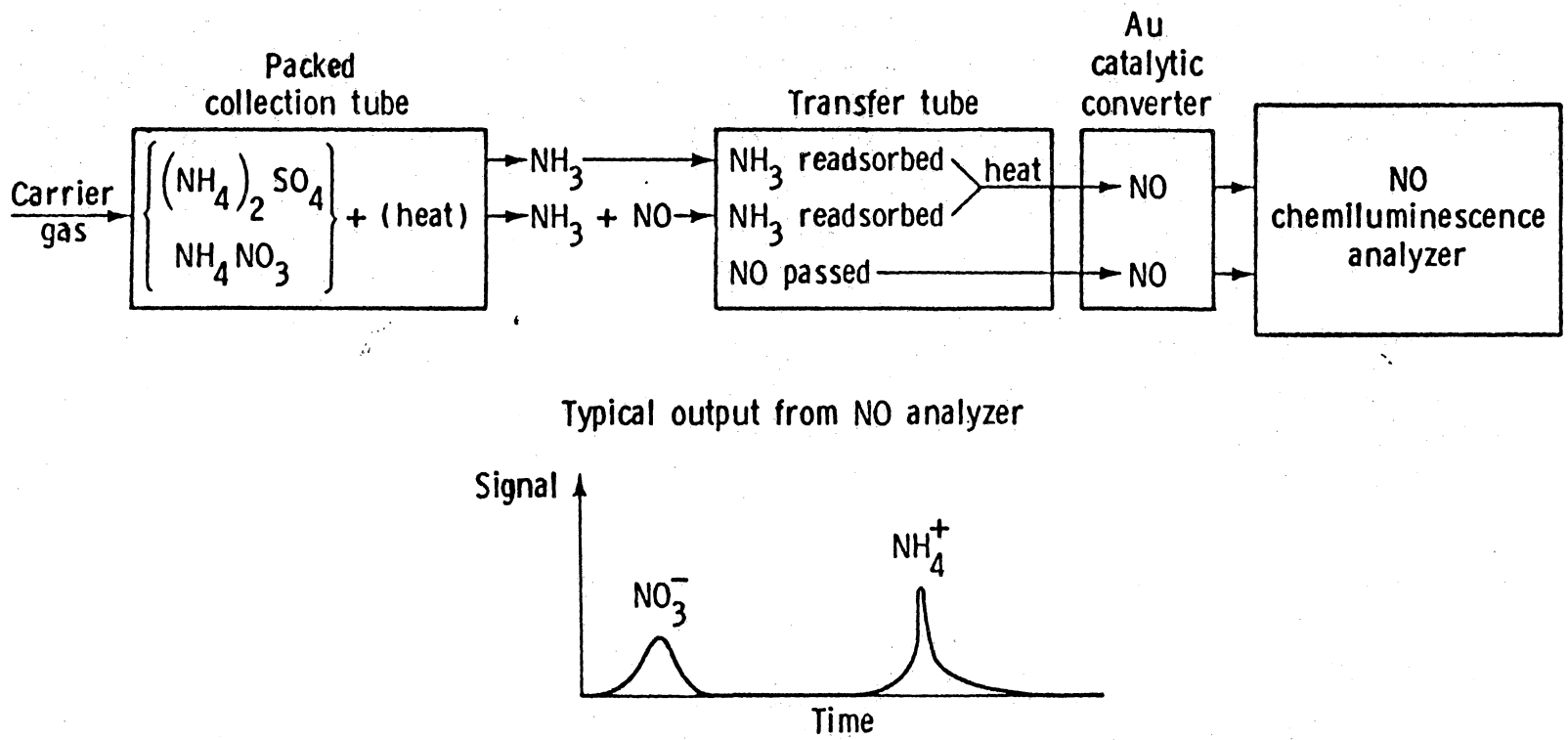

Figure 20. Schematic diagram and typical output of analysis process for packed collection tubes (NO_3^- and NH_4^+ aerosols).

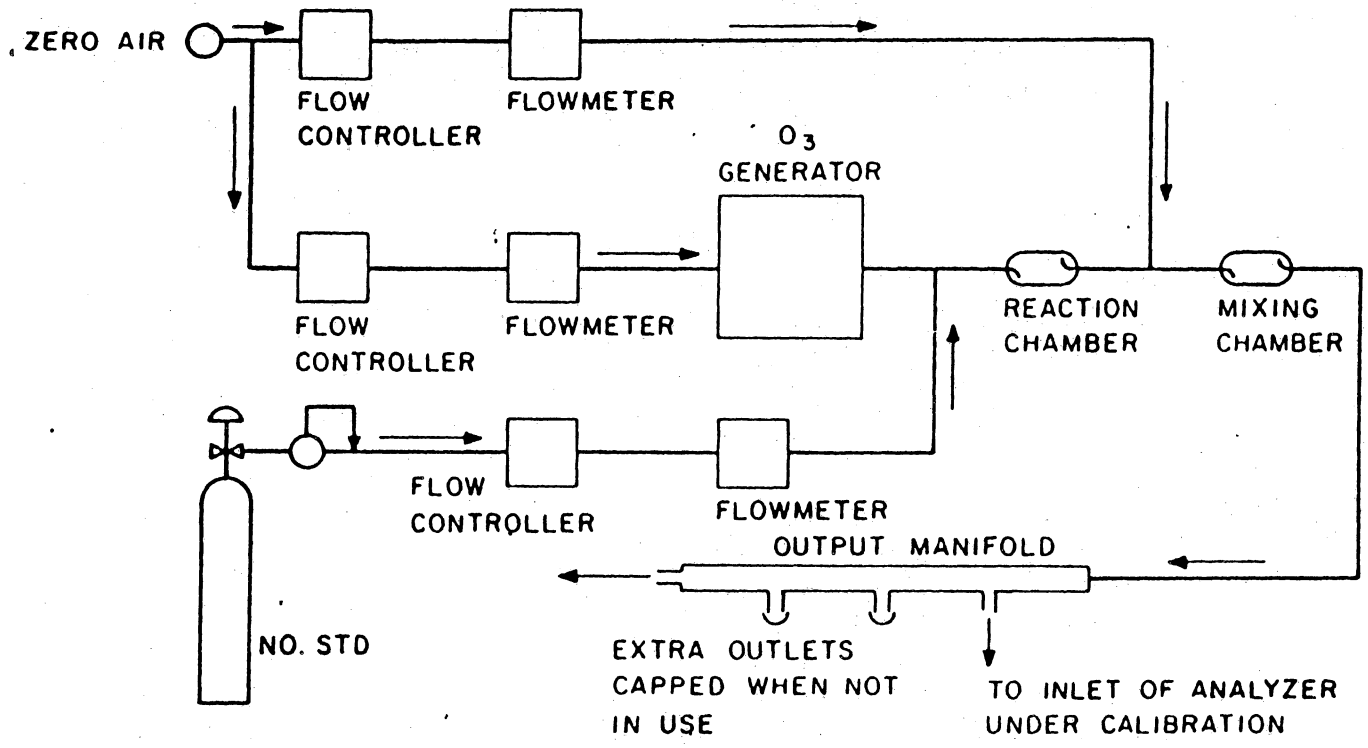

Figure 21. Schematic diagram of the gas phase titration calibration system used for the NO_x analyzer (Ellis, 1975).

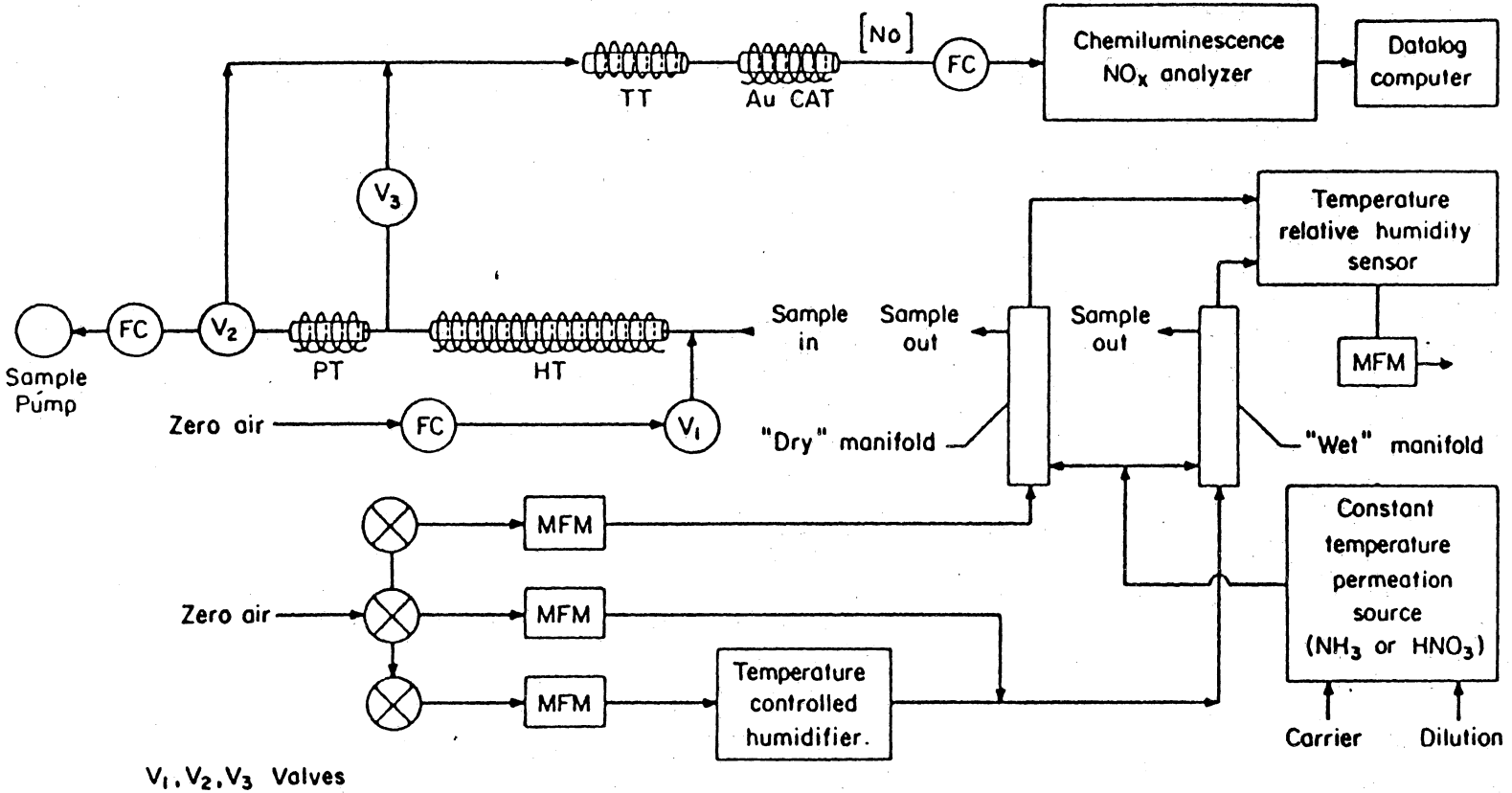

V_1, V_2, V_3 Valves

FC Flow controller

MFM Mass flow meter

Figure 22. Schematic diagram of the calibration system used for the tungstic acid technique.

The NO_x analyzer calibration followed standard procedures described by Ellis (1975).

Permeation tubes of a 2:1 concentrated sulfuric acid to nitric acid solution (Bowermaster and Shaw, 1981) made and certified by Kin-Tech Corporation were used as the nitric acid source. These tubes were kept in constant temperature (30°C), voltage regulated ovens (see Figure 22) and a known permeation rate was determined gravimetrically. Independent (Bionetics Corporation) wet-chemical analysis measurements (ion chromatography, IC) of the permeation devices were also performed. The results of the two methods were found to be in good agreement within experimental error (55 nanograms per minute (ng/min) by weight and 62 ng/min by IC).

The mass concentration, ρ, in micrograms per cubic meter ($\mu g/m^3$) of the gaseous nitric acid generated by the dilution system was given by

$$\rho = \dot{m}/Q_1 \tag{4}$$

where $\dot{m}$ is the permeation rate of HNO_3 vapor ($\mu g/sec$) and Q_1 the zero air flow rate in cubic meters per second (m^3/sec).

The concentration, C_1, in parts per million by volume (ppm) is given by

$$C_1 = \frac{\rho \times Vm \times T}{(MW \times 1000 \times Ts)} \tag{5}$$

where Vm is the molar volume (liters, L) at temperature, T (degrees Kelvin, K), MW is the molecular weight of nitric acid (grams per mole, g/mole), Ts is standard temperature (K) and C_1 is nitric acid concentration before dilution.

The nitric acid concentration after dilution is given by

$$C_2 = (C_1 \times Q_1)/Q_2 \tag{6}$$

Q_2 is the total flow rate (m^3/sec) and C_2 is the nitric acid concentration after dilution (ppm).

The sample box collection tubes are exposed to the diluted nitric acid, C_2, by drawing the sample gas from the manifolds indicated in Figure 22. Response curves were then generated at several concentration levels and relative humidities.

Relative humidities were generated from a humidifier by blowing zero air over a deionized water reservoir. Relative humidity (in percent) was monitored with a General Eastern Instrument Corporation Model 400-E temperature/relative humidity sensor. The sensor operates by the reaction of H_2O with sulfonated polystyrene, sulfonation occurs mobilizing sulfate ions which produces an electrical charge across a large electrical resistance. The electronic charge is amplified and RH determined proportional to the voltage signal. A temperature thermistor is used to correct humidity measurements induced by changes in temperature. Electronic calibration of this sensor was performed by Wyle Laboratories, NASA's instrument calibration contractor.

The RH sensor has a 5 - 95% RH range for measurement of humid environments. Due to the difficulty to maintain a low RH (< 15% RH) experimentally and the sensor's lower limitation, RH values greater than 15% RH were used. Also, high relative humidities (> 81% RH) formed mists in the glass manifold due to condensation. In order to insure against aerosol formation, visible mists were avoided and a 78% RH was appropriate for an upper RH limit.

The HNO_3 concentrations and relative humidities are varied by changing the zero air (house air scrubbed with Drierite for H_2O removal, activated charcoal for organic chemical removal and molecular sieve for particle removal) flows through the humidifier and dilution/dry air lines prior to entering the glass sampling manifolds. The total flow Q_2 in equation (6) is measured at the exhaust of the manifolds, and is compared to the individual flows measured by the flow meters prior to entering the sample manifold to insure a leak free system.

Samples are collected by programming the computer for varying sample pump durations. Repetitive analyses (five) per load time at one minute intervals, up to five minutes, are used to ensure the precision of the measurements. Therefore, a total of twenty-five data points per concentration/RH change are taken per response curve.

4. Materials

Bowermaster and Shaw (1981) and Goldan et al. (1983) indicated that materials used in transfer lines had to be selected with minimum affinity for nitric acid. Their results were supported by material

tests for this study. Stainless steel and glass should be used sparingly if at all, since teflon appears to be best suited for gaseous transport.

Originally, a single glass manifold was used to provide both dry and humid nitric acid/air mixtures. The nitric acid retention (adsorption) on this glass manifold caused many problems when changes in experimental conditions occurred (i.e., a "memory" effect of nitric acid retained from the previous equilibrium condition within the manifold). This was remedied by using the dual manifold system indicated and allowing sufficient time (hours) for equilibrium to be reached within the entire calibraton system (as indicated by a constant HNO_3 signal).

In addition to this, a purge cycle was incorporated into the programmed analysis, because HNO_3 was found in the carrier gas (zero air). As carrier gas was used after hollow tube heating, it also was denuded of trace nitric acid as the other analyses continued. Therefore, upon subsequent sample collection, a small amount of signal could be attributed to the carrier gas from the previous analysis cycle. This would have given higher than actual values for HNO_3, an undesirable systematic error.

CHAPTER IV

RESULTS AND DISCUSSION

The data collected in this study are presented to show the effects of relative humidity on the Tungstic Acid Technique. All plotted points from these data show the mean of the data per sample load interval. The error bars associated with each mean represent the standard deviation for that data. In some cases, when data from different sample conditions fall on the same curve, the plotted points are the mean for that entire group of sample conditions and the standard deviation is similarly derived.

1. Relative Humidity

Figure 23 illustrates typical response curves showing the difference in TAT HNO_3 response between the dry (◊) and humid (o) conditions indicated at a constant sample box collection temperature of 60°C and HNO_3 concentration of 4.7 ppb. Sample size (in ng of HNO_3) is defined as concentration, C_2 (in ng/L), times the sample flow rate (always 1.0 L/min) and sample duration (1 to 5 minutes). Signal (V x sec) represents the area under the peak plotted by the HP85 as shown in Figures 19

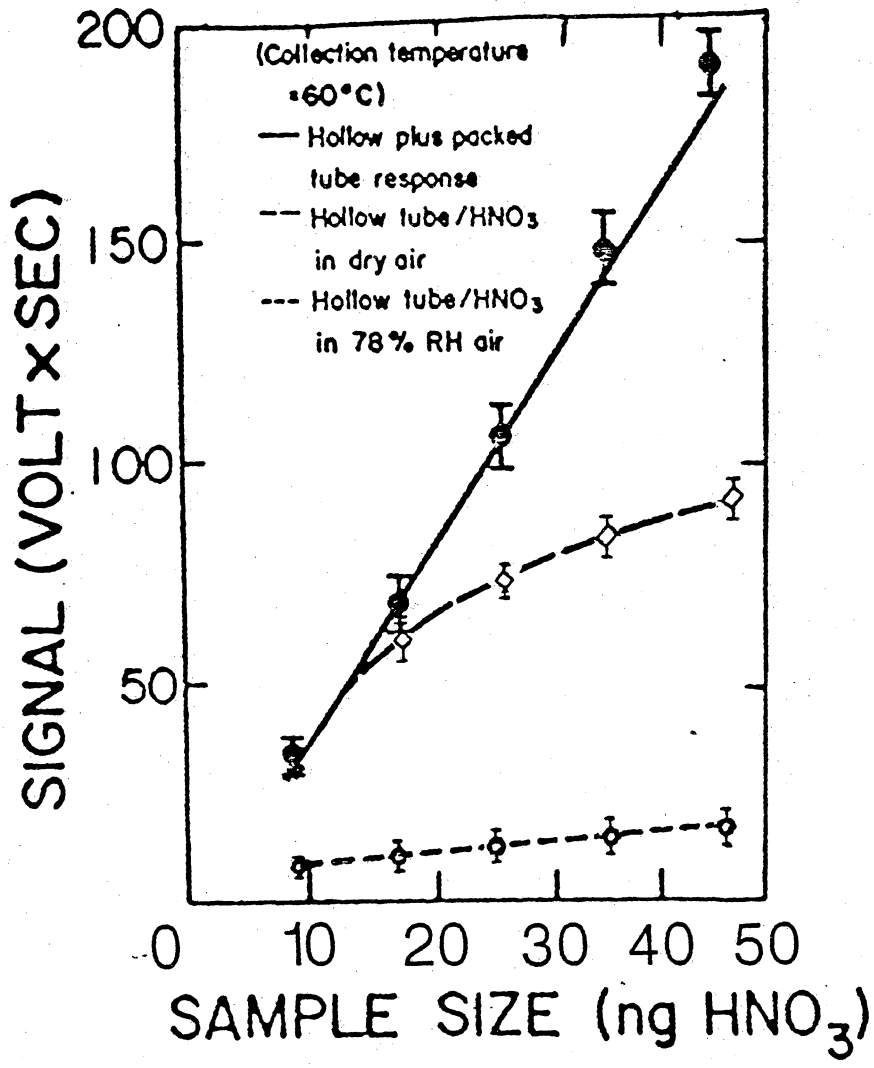

Figure 23. Plot of TAT HNO_3 and total "nitrate", TNO_3, (solid line) response (V x sec) versus calibration HNO_3 (ng) for dry (broken line) and humid (dashed line) condition (78% RH). Sample box collection temperature is 60 °C.

and 20. The obvious problem with these results is that the dry condition is not linear and there is nearly total loss of signal when water vapor was added. The possibility arose that calibration curves for a range of relative humidities would be required. These results generated concern about the effectiveness of the TAT system to measure HNO_3 vapor at typical atmospheric conditions, which provided the impetus to carry out this research to relate the effect of RH on the tungstic acid technique.

Initially, only gases were analyzed, until the apparent RH problem developed as shown in Figure 23. When both HNO_3 and NO_3^- components were analyzed, there appeared to be a correlation between loss of HNO_3 signal and gain of a NO_3^- response. Thus, a new term called total nitrate, TNO_3, was quantified which equaled the sum of the HNO_3 and NO_3^- signals. The solid line on Figure 23 represents the sums of those responses, each point representing the average of 10 data points (5 dry, 5 at 78% RH). It can be seen from this plot that although there was vast differences between dry and humid HNO_3 signals, the TNO_3 values for both those conditions are conservative, linear, and experimentally equivalent.

At a sample box collection temperature of 60°C and a HNO_3 concentration of 24 ppb, the data presented in Tables A1-1 through A1-5 were generated at relative humidities ranging from 0-78% RH as indicated using the automated TAT and gas/RH delivery systems described in the Methods and Material section. Figures A1-1 through A1-5 are the plots of the HNO_3 responses from those tables. At a sample box temperature of

60°C there appeared little variability at other than 0% (dry) relative humidity between the four RH conditions tested (17, 41, 52, 78% RH). Therefore, although water vapor content affected HNO_3 collection it did not appear variable (i.e, systematic for RH).

Figure 24 is a composite representation of the relative humidity data just described. In this plot, HNO_3 collection efficiency is defined as the HNO_3 response divided by the sum of the HNO_3 and NO_3^- responses (HNO_3/TNO_3). HNO_3 collection efficiency is plotted against sample load and shows a decrease in efficiency with increased sample size. This decrease in efficiency was not due to an overloading of the hollow tube (re: breakthrough), because similar results were obtained at a lower HNO_3 concentration (4.7 ppb) as shown in Figures A2-1 through A2-3 from data collected in Tables A2-1 through A2-3 at 17, 52, 78% RH. It was concluded that either some other physical factor was contributing to the systematic loss of HNO_3 signal or water vapor was forming aerosol nitrate (Eatough et al., 1985).

2. Temperature

The sample collection box had been maintained at a warm temperature (60°C) because NH_3 was believed to be less likely to adsorb onto surfaces at warmer temperatures. Since the analysis process is one of thermal desorption, temperature seemed to be a physical property easily varied. Cooling of the sample box was achieved using a fan and varying the position of the lid covering the sample box. Tables A3-1 through A3-3 contain the data used to plot Figure 25 at constant relative

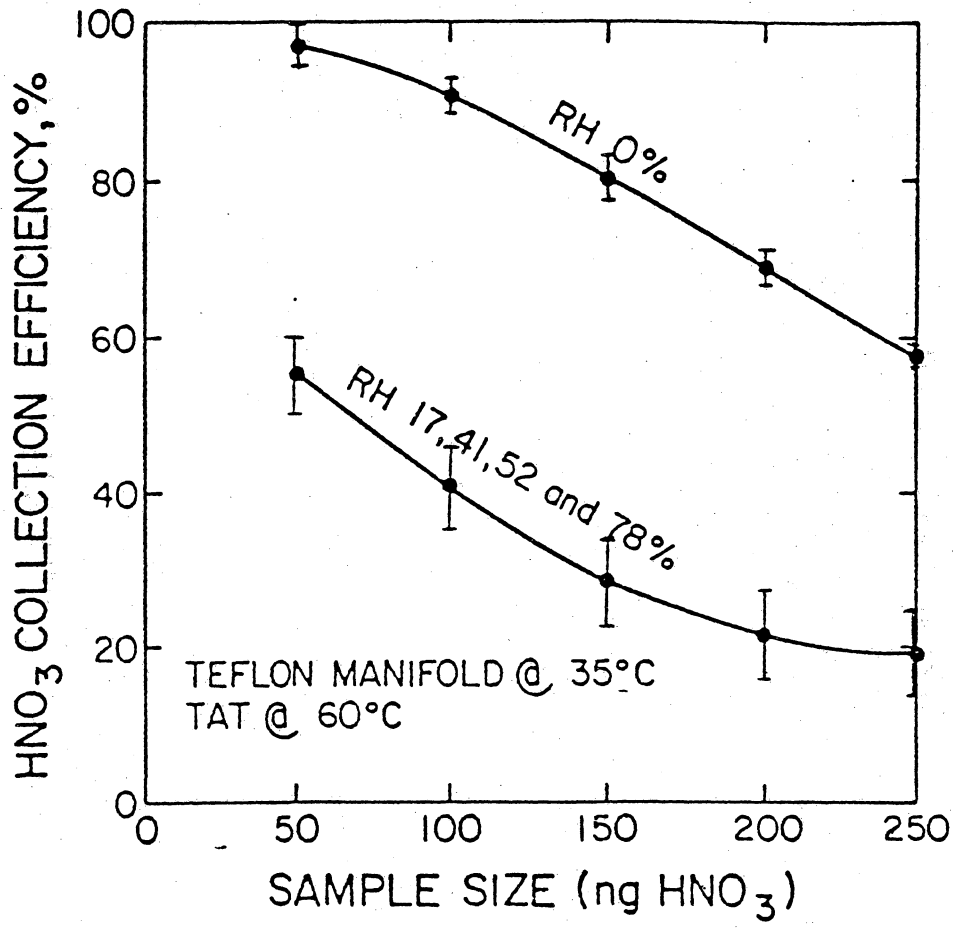

Figure 24. Plot of TAT HNO_3 percent collection efficiency (%) versus calibration HNO_3 (ng) for various relative humidities at constant sample box collection temperature (60 °C).

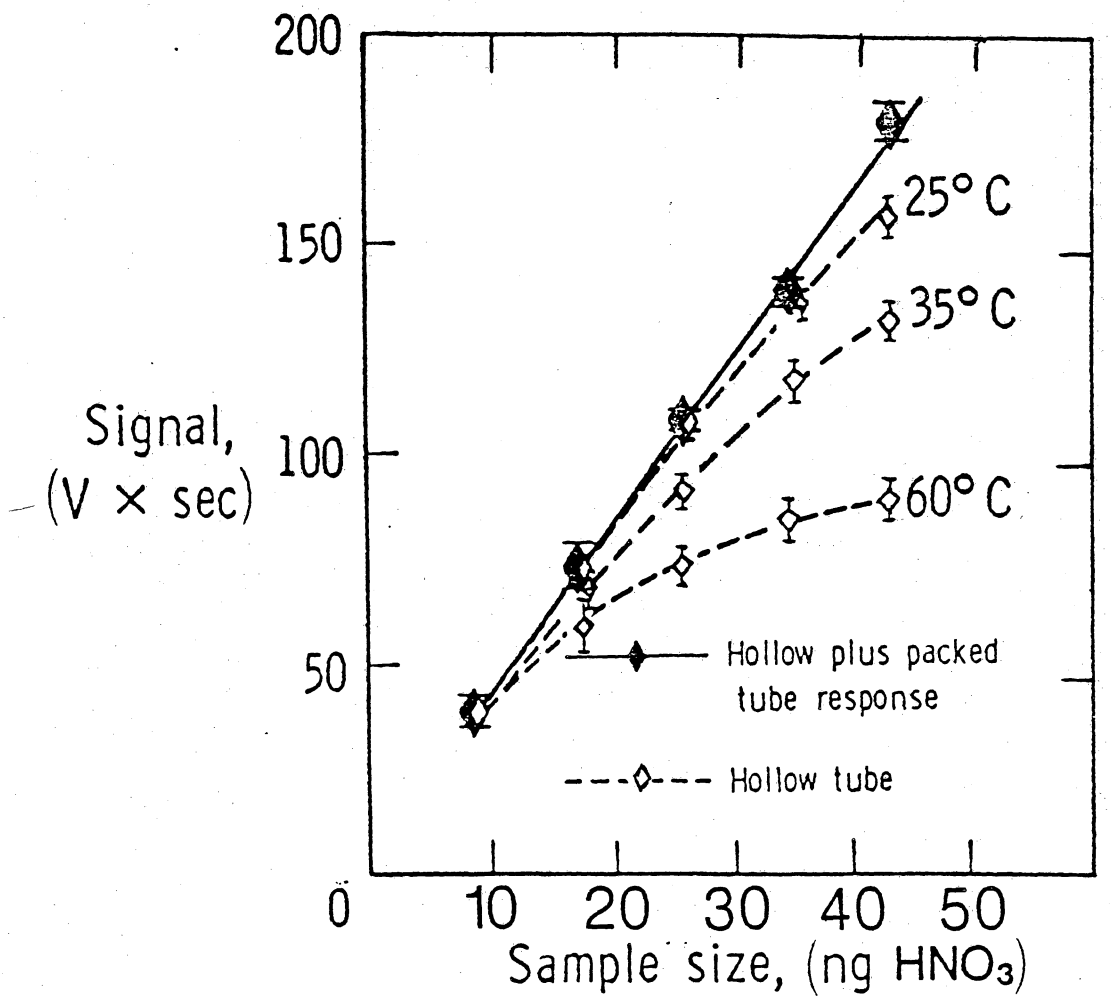

Figure 25. Plot of TAT HNO_3 (dashed lines) and total "nitrate" (solid line) responses (V x sec) for various sample box collection temperatures at constant relative humidity (0% RH).

humidity (0% RH) and HNO_3 concentration (4.7 ppb), while varying temperature, 25°C, 35°C, and 60°C, respectively. As temperature decreases the HNO_3 signal approaches the solid line which again represents the hollow plus packed tube response, TNO_3. Each TNO_3 point plotted represents the mean of 15 data (5 data from each temperature). From these plots it can be seen that temperature has an effect and is also variable.

Figure 26 is a plot of the 4 data sets from Tables A4-1 through A4-4 at constant relative humidity of 78% RH and HNO_3 concentration (4.7 ppb), again with varying temperatures of 60°C, 45°C, 30°C, and 25°C, respectively. At 78% RH, a similar effect to dry conditions can be seen. As temperature decreases, the HNO_3 signal increases approaching the solid line representing TNO_3. In this plot, TNO_3 data points represent the mean of 20 data (5 data from each of the temperatures). Temperature has an effect on HNO_3 signal.

The temperature effect may be expanded by activation energy theory. The rate of reactions, k', are temperature dependent and can be represented by the Arrhenius equation

$$k' = A\exp\left(\frac{-Ea}{RT}\right) \tag{7}$$

here A is the frequency constant, Ea is the activation energy (required for the reaction to occur) in kilocalories (kcal) per mole, R is the universal gas constant, and T is the temperature. Therefore, depending on the value for Ea, the rate of reaction, k' can vary enormously with temperature. This variation in the rate of reaction could support the results presented in this research.

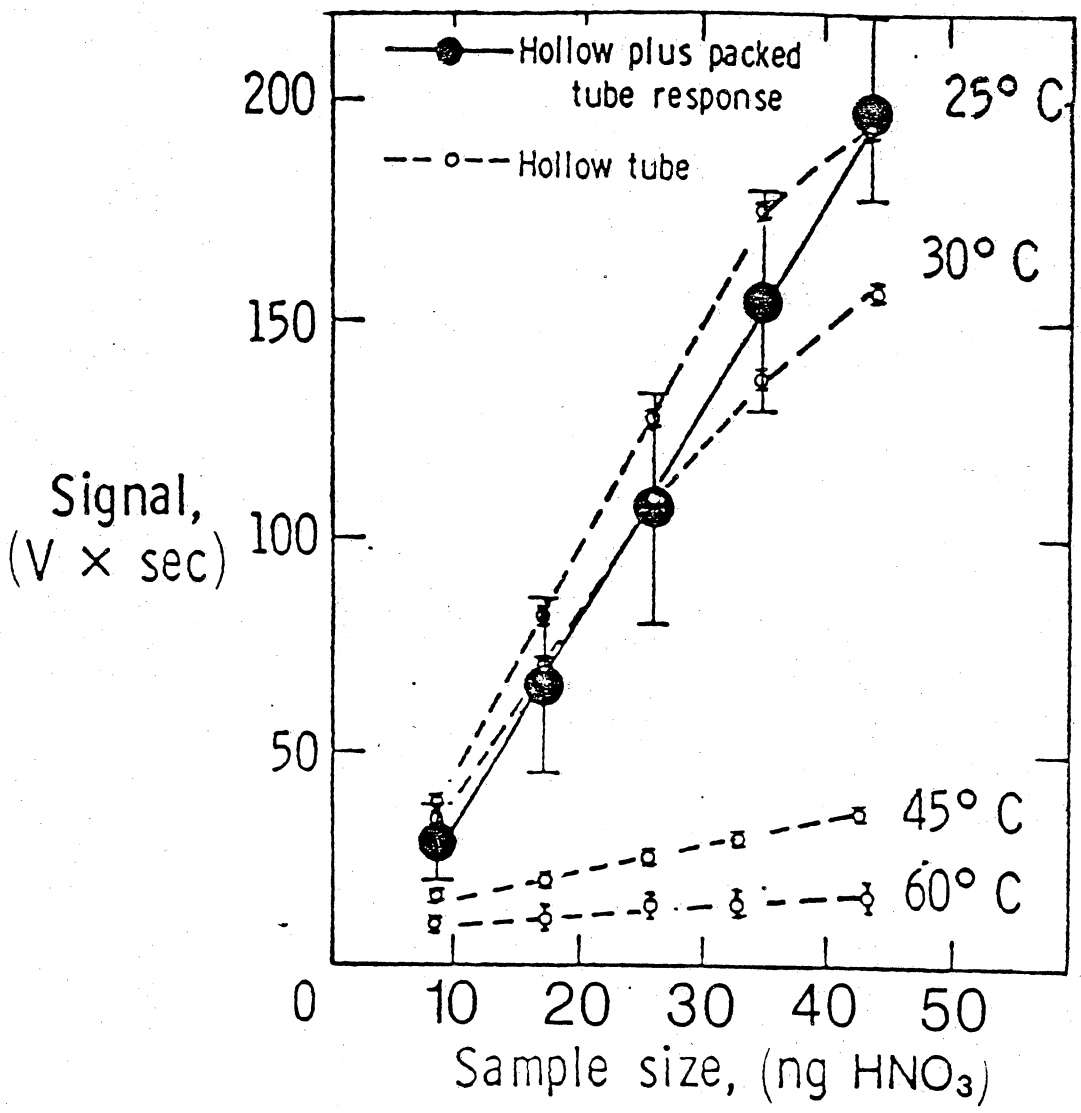

Figure 26. Plot of TAT HNO_3 (dashed lines) and total "nitrate" (solid line) responses (V x sec) for various sample box collection temperatures at constant relative humidity (78% RH).

3. Combined Relative Humidity and Temperature

Blanks of zero air (dry and humid) were tested also. Tables A5-1 through A5-6 contain the data collected for these blanks. Only humidified air showed similar effects to temperature. The HNO_3 data in Tables A5-1 and A5-2 are compared in Figures A5-1 and A5-2. Figure A5-1 is at 60°C and Figure A5-2 is at 25°C. The TAT system, again collects more HNO_3 at the cooler temperature, but there is still a significant NO_3^- response. The data in Tables A5-3 through A5-6 were taken at 25°C and various relative humidities (0, 17, 52, and 78% RH, respectively). These data show a general trend to increase NO_3^-, while HNO_3 shows only a slight increase in signal over that RH range.

The explanation of the increase in NO_3^- with increasing RH is straight forward. Periodic IC analysis of the deionized H_2O, used in this study's humidifier, by the supplier (Bionetics Corporation) at NASA indicate trace NO_3^- (sub ppm). Therefore, the NO_3^- signal is actual nitrate being collected by the packed tube, and increases at high RH as would be expected (i.e., the higher the relative humidity the greater the formation of aerosols). The HNO_3 (0.0 ppb) responses shown in Tables A5-1 through A5-6 must be from gas/liquid phase equilibria and therefore only moderately increased. The one dry air sample presented in Table A5-3 shows no variation with sample load, therefore, zero air was deemed free of analysis constituents, and an excellent carrier source. Based on these data, corrections were made to HNO_3 results when conditions varied.

Figure 27 summarizes the effects of relative humidity and temperature on HNO_3 collection efficiency (HNO_3/TNO_3) using the TAT system. The data for the dry (0% RH) curves which are plotted in this figure are from Tables A3-1 through A3-3. The data for the relative humidity (78% RH) curves which are plotted come from Tables A4-1 through A4-4. As temperature increases from 25°C to 60°C under dry conditions, the efficiency of HNO_3 collection decreases from ≈ 95% to ≈ 50% at 43 ng HNO_3. Under humid conditions, the effect of temperature on collection efficiency is enhanced from ≈ 92% at 25°C to ≈ 10% for 60°C (43 ng HNO_3). Therefore, unless the hollow tube temperature is elevated above standard temperature, relative humidity has a neglible effect on the HNO_3 collection capability of the TAT system.

4. Sample Collection Apparatus Modification

As a result of the data presented in this research, a sample collection box was designed as shown in Figure 28, which includes the cooling system shown in Figure 29. Modifications were made to the sample collection apparatus were to remove unnecessary sources of heat. Since thermal desorption and dissocation are processes by which analysis occurs, the task to bring temperature below 25°C was difficult and required special attention.

The sample cooling system shown was the result of six months of varying designs. Constraints on the design (specifically for flight) required careful consideration. Problems developed with choice of cooling solution, while amount of coolant flow was also a problem.

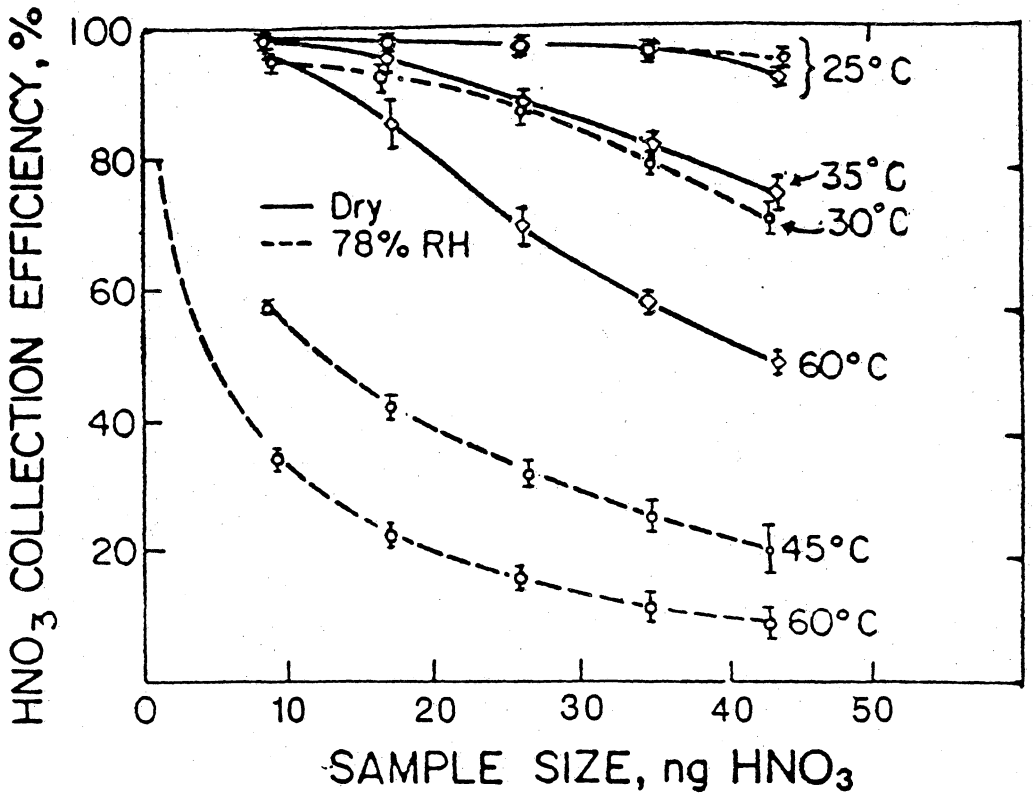

Figure 27. Plot of TAT HNO_3 percent collection efficiency (%) versus calibration HNO_3 (ng) for 0 (solid lines) and 78 (dashed lines % RH and various sample bbx temperatures.

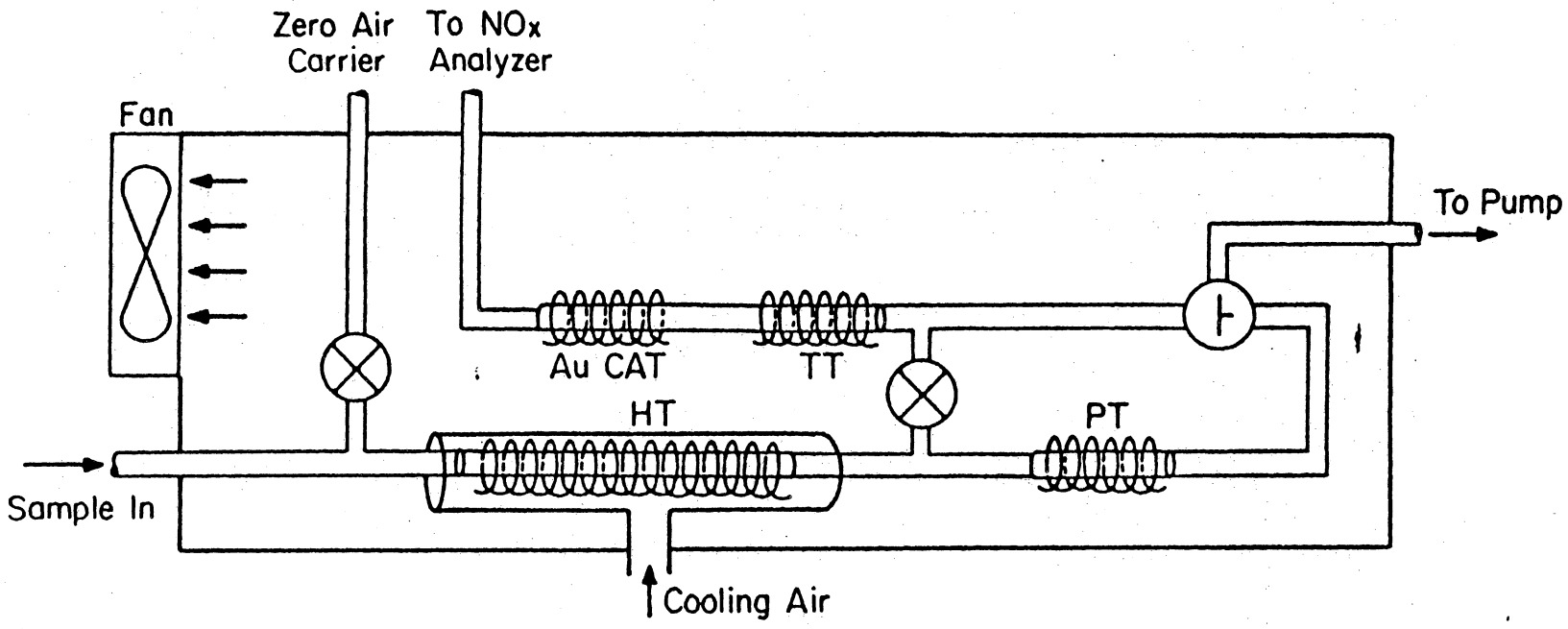

Au Cat Gold Catalyst
HT WO_3 coated hollow tube
PT WO_3 coated sand-packed tube
TT WO_3 coated transfer tube

Figure 28. Schematic diagram of new sample box collection design with coolant system added.

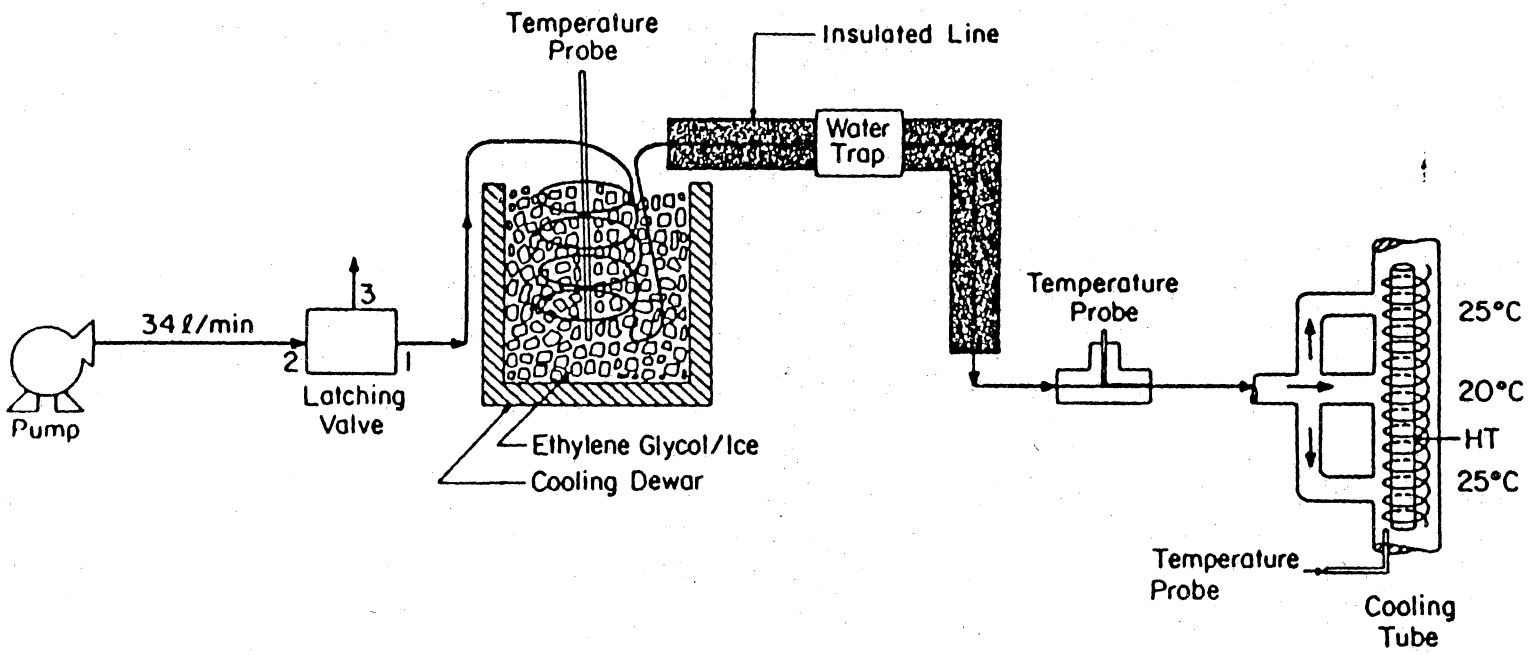

Figure 29. Ethylene Glycol/Ice cooling system.

Liquid nitrogen (LN_2) and "dry" ice/alcohol coolant solutions caused coolant lines to freeze shut. When H_2O was removed from the coolant air stream, CO_2 would still solidify in the coolant lines. The eventual use of ethylene glycol ("antifreeze") and ice solution proved most effective to maintain hollow tube collection temperatures for long durations (> 5 hrs) without service.

Large volumes of air (in excess of 15 l/min) would be required as the coolant carrier source. Therefore, due to limited aircraft space compressed gas cylinders were replaced with a compressor (diaphragm) pump.

Special "latching" valves replaced continuous voltage solenoid valves to reduce heat generated by these devices and thus reduce temperature in the sample box.

Finally, additional cooling was provided by moving warm stagnant air through the box with a "cooling" fan and out a screened section. This cooling method served a dual purpose, because heat build-up in the sample box, also caused difficulty in pulling a sample through the packed tubes due to expansion of the WO_3-coated sand in the packed tubes.

In addition to cooling the sample collection apparatus, materials were selected to minimize chemiscorption onto transfer lines and component connections. Glass or stainless steel tubing and connections were replaced with teflon to ensure transport of HNO_3.

5. Modified Sample Collection Apparatus Results

With temperature conditions properly controlled, much lower sample loads (sic HNO_3 concentrations) could be measured without significant loss, which is the ultimate goal of background measurements for ambient gaseous nitric acid. Sub part per billion levels have been measured and have only been limited by the sensitivity of the detection system (NO_x analyzer) with part per trillion levels desirable.

Figures 30 and 31 were plotted using the modified sample collection apparatus. Figure 30 is a plot of HNO_3 at 0% RH and 25°C for a concentration of 0.73 ppb. The packed tube did not give a response upon analysis, therefore, a TNO_3 was not plotted. Figure 31 shows the plots of HNO_3 and TNO_3 for 78% relative humidity.

There is still some apparent loss of nitric acid or actual nitrate gain between dry and humidified conditions at 25°C as shown in Figures 27, 30, and 31 which may be a result of any single or combined effect of the following:

(1) efficiency of hollow tubes to collect nitric acid is not 100%.

(2) aerosol formation within the sample manifold may occur prior to taking a sample.

(3) material/"memory" effect in the manifold.

(4) NO_3^- from the humidifier water.

(5) experiment error limitations.

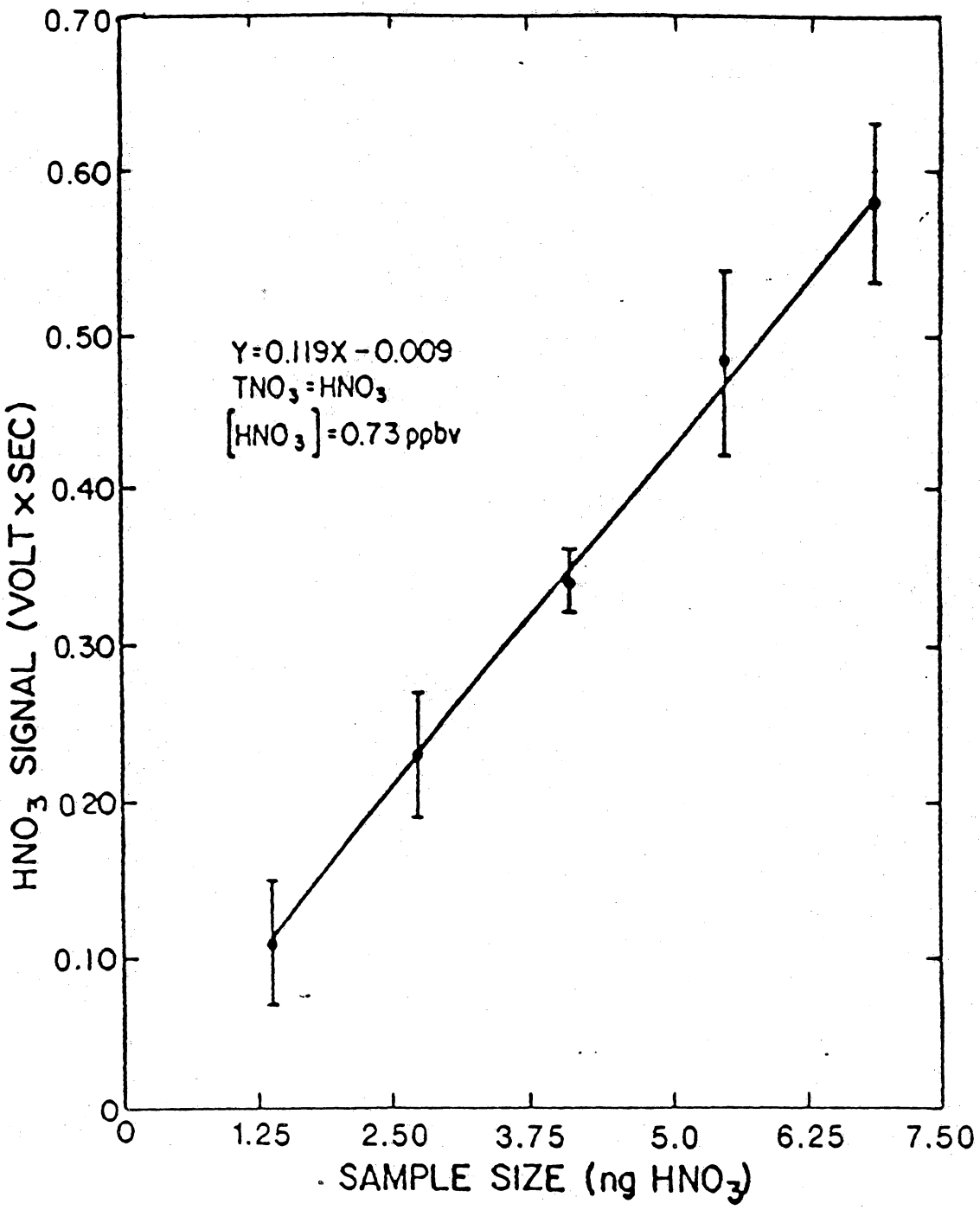

Figure 30. Plot of TAT HNO_3 response (V x sec) versus calibration HNO_3 (ng) at 0% relative humidity with least squares linear regression line (TAT HNO_3 = 0.119(CAL HNO_3) - 0.009, r^2 = 0.999). Sample box collection temperature is 25°C.

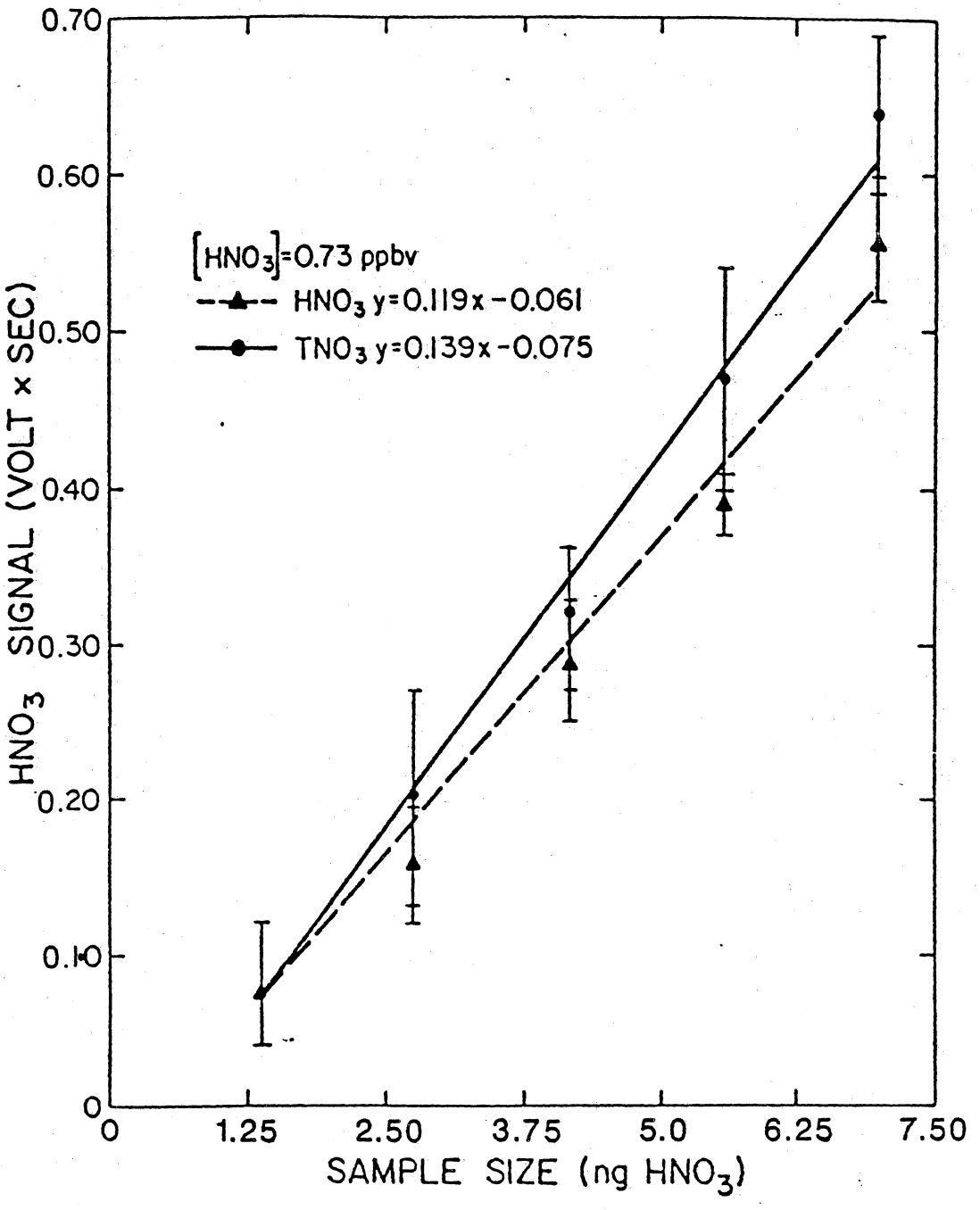

Figure 31. Plot of TAT HNO_3 (▲) and total "nitrate" (●), TNO_3, responses (V x sec) versus calibration HNO_3 (ng) at 35% relative humidity with least squares linear regression lines (TAT HNO_3 = 0.119(CAL HNO_3) - 0.061, r^2 = 0.993 and TAT TNO_3 = 0.139(CAL HNO_3) - 0.075, r^2 = 0.997). Sample box collection temperature is 25 °C.

Even with these possible problems, the experimental results indicate an effective system has been further enhanced for the measurement of gaseous nitric acid.

6. Summary

Figures 32, 33, and 34 summarize the results presented here. Figure 32 is the signal responses for HNO_3 and NO_3^- at 60°C and 78% RH. The NO_3^- response is clearly greater than the HNO_3 signal. Figure 33 is the same response for the dry condition (0% RH). The signals in this figure are relatively equal. At 25°C, under either 0 or 78% RH, nearly all the HNO_3 is collected on the hollow tube as shown in Figure 34. Such an increase in efficiency enables measurement sensitivity to increase. Therefore, lower concentrations of HNO_3 are more effectively measured enhancing the TAT HNO_3 analysis capability.

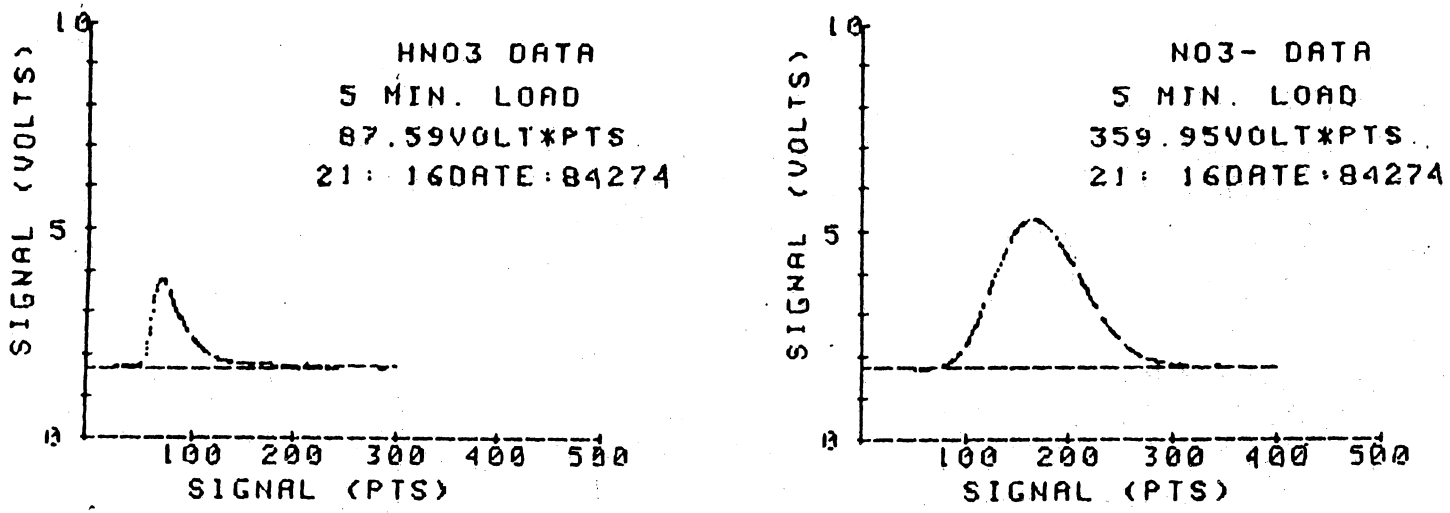

Figure 32. TAT HNO_3 and TAT NO_3- signal responses for sample collection apparatus temperature of 60 °C and 78% sample relative humidity.

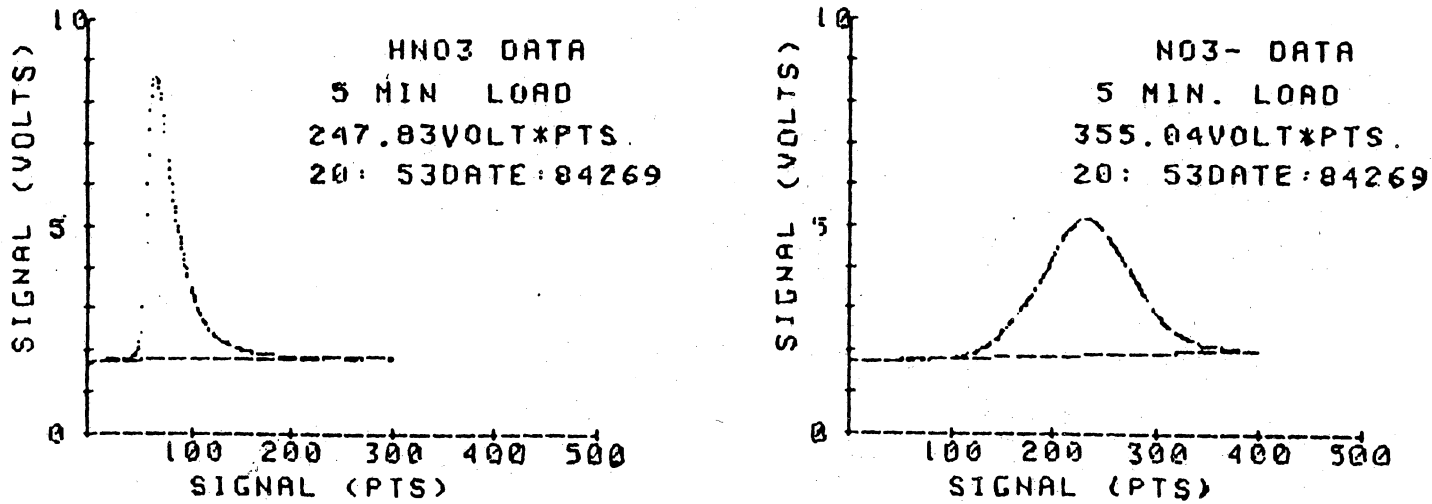

Figure 33. TAT HNO_3 and TAT NO_3^- signal responses for sample collection apparatus temperature of 60 °C and 0% sample relative humidity.

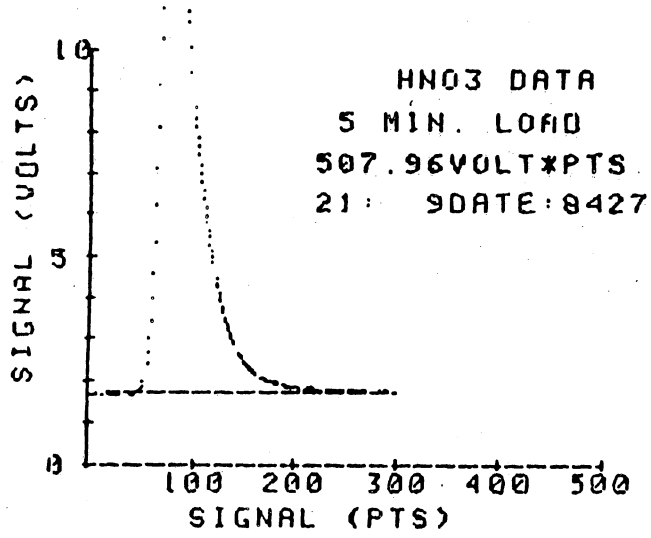

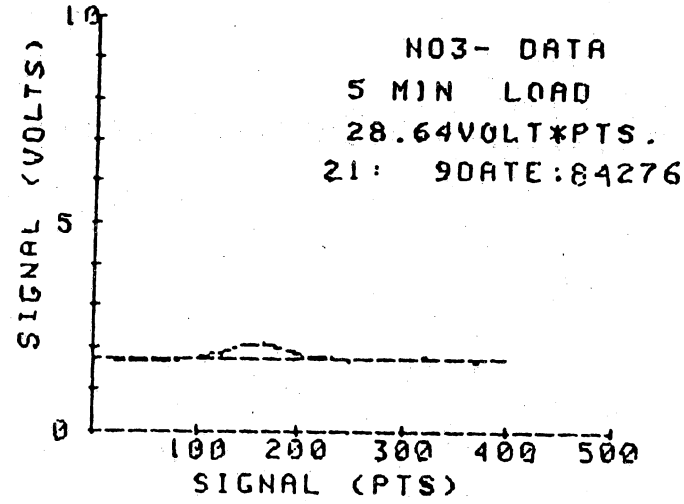

Figure 34. TAT HNO_3 and TAT NO_3^- signal responses for sample collection apparatus temperature of 25°C and either 0 or 78% sample relative humidities.

CHAPTER V

CONCLUSIONS

The hypothesis that relative humidity does not affect HNO_3 measurements using the Tungstic Acid Technique (TAT) is valid at temperatures below 25°C. Therefore, temperature is the controlling factor in collection efficiency, and can be supported by activation energy theory with the Arrhenius equation. The apparent effect of H_2O on collection efficiency initially indicated by the data was a consequence of the temperature of the collection medium prior to the sample collection cycle. Relative humidity enhances this temperature effect as the temperature of the medium increases.

With the changes made in this work, the TAT system has been redesigned with successful enhancement of the collection efficiency of nitric acid on the WO_3-coated tubes and overall sampling performance by ensuring complete aerosol and gas separation. Without this research and these improved modifications, the TAT system would have been subject to large errors in collection and subsequent evaluation of HNO_3 and NO_3^- data. Also, at the controlled reduced temperature indicated, there is

an increase in HNO_3 signal due to this complete separation (i.e., efficient collection). The sensitivity reported by others for HNO_3 with the TAT system (0.05 ppb) can be achieved with proper temperature control.

The importance of a controlled sample environment has been shown to be of major consequence. Such a consequence may have even broader significance than just for this technique, when applied to other techniques using similar (chemisorption, thermal desorption) analytical procedures.

CHAPTER VI

RECOMMENDATIONS

The sampling system used in this study has shown that control over the sample collection temperature is an important factor for nitric acid measurement using the Tungstic Acid Technique, especially at ambient relative humidity conditions. Therefore, it is recommended that temperature control below 25°C be done to maintain the integrity of HNO_3 gas sampled, otherwise, complete separation of the gases and aerosols collected by the TAT will not occur. A lack of separation will cause misinterpretation of the results and lead to false conclusions.

Future research with the Tungstic Acid Technique will be necessary to define temperature effects for the other analyzed species, particularly NH_3. Ammonia is the other gas analyzed by the TAT. Its thermal desorption occurs at much warmer temperatures (≈ 350°C) and thereby may not be as affected by, or sensitive to, temperature collection variation. Once the gases are collected with known efficiency, the analyses of the aerosols can be ascertained. In this way, the TAT can be used to simultaneously measure four species of atmospheric chemical importance, and prove to be a useful instrument to provide data for atmospheric chemical models.

REFERENCES

Adams, D. D. (1986) Acid deposition: Environmental, Economic and Policy Issues. Plenum Press, ISBN 030 6420627.

Anlauf, K. G., Fellin, P., Wiebe, H. A., Schiff, H. I., MacKay, G. I., Braman, R. S., and Gilbert, R. (1985), A comparison of three methods for measurement of atmospheric nitric acid and aerosol nitrate and ammonium. Atmospheric Environment, 19: 325-333.

Appel, B. R., Wall, S. M., Tokiwa, Y., and Haik, M. (1980) Simultaneous nitric acid, particulate and acidity measurements in ambient air. Atmospheric Environment, 14: 549-554.

Appel, B. R., Tokiwa, Y., and Haik. M. (1981) Sampling of nitrates in ambient air. Atmospheric Environment, 15: 283-289.

Appel, B. R. and Tokiwa, Y. (1981) Atmospheric particulate nitrate sampling errors due to reactions with particulate and gaseous strong acids. Atmospheric Environment, 15: 1987-1089.

Barnes, R. A. (1979) The long range transport of air pollutants: A review of European experience. J. Air Poll. Control Assoc., 29: 1213.

Bollinger, M. J. (1982) Chemiluminescent Measurements of the Oxides of Nitrogen in the Clean Troposphere and Atmospheric Chemistry Implications. Dissertation, University of Colorado at Boulder.

Bowermaster, J. and Shaw, R. W. Jr. (1981) A source of gaseous HNO and its transmission efficiency through various materials. J. Air Pollution Control Assoc. 31: 787-788.

Braman, Robert S., Shelley, Timothy J., McClenny, William A., Tungstic acid for preconcentration and determination of gaseous and particulated ammonia and nitric acid in ambient air. Analytical Chemistry, 54: 358.

Braman, R. S. and Llywellyn, J. A. (1985) Fabrication and test of a monitor for NH_3, HNO_3, NH_4^+, and NO_3^-. NASA No. 16844, University of South Florida at Tampa.

Cadle, S. H., Countess, R. J. and Kelly, N. A (1982) Nitric acid and ammonia in urban and rural locations. Atmospheric Environment, 10: 2501-2506.

Cadle, S. H. (1985) Seasonal variation in nitric acid, nitrate strong aerosol acidity and ammonia in an urban area. Atmospheric Environment, 19: 181-188.

Eatough, D. J., White, V. F., Hansen, L. D., Eatough, N. L., and Ellis, E. C. (1985) Hydration of nitric acid and its collection in the atmosphere by diffusion denuders. Analytical Chemistry, 57: 743-748.

REFERENCES (continued)

Ellis, E. C. (1975) Technical assistance document for chemiluminescence measurement of nitrogen dioxide. EPA-600/4-75-003.

Fellin, P., Wiebe, H. A., and Anlauf, K. G. (1980) Design and characterization of a low volume sampling system for the simultaneous sampling of atmospheric particulates and vapor phase nitric acid. 63rd Chemical Institute of Canada Conference: Report ARQA 83-80.

Ferm, M. and Sjodin, A. (1985) A sodium carbonate coated denuder for determination of a nitrous acid in the atmosphere. Atmospheric Environment, 19: 979-983.

Fishman, J., and Crutzen, P. J. (1977) A numerical study of tropospheric photochemistry using a one-dimensional model. Journal Geophysical Research, 82: 5897-5906.

Goldan, P. D., Kuster, W. LC., Albritton, D. L., Fehsenfeld, F. C., Connell, P. S., Norton, R. B., and Huebert, B. J. (1983) Calibration and tests of the filter collection method for measuring clean-air levels of nitric acid. Atmospheric Environment, 17: 1355-1364.

Gormley, P. and Kennedy, M. (1949) Diffusion from a stream flowing through a cylindical tube. Proceedings Royal Irish Academy, 52A: 163.

Hampson, R. F. (1973) Chemical kinetics data survey VII. Photochemical and rate data for twelve gas phase reactions of interest for atmospheric chemistry. NBS Rep. NBSIR, pp. 73-207.

Hampson, R. F. and Garvin, D. (1977) Reaction rate and photochemical data for atmospheric chemistry. NBS special publication 513, pp. 17-19.

Harker, A. B., Richards, L. W., and Clark, W. F. (1977) The effect of atmospheric SO_2 photochemistry upon observed nitrate concentrations in aerosols. Atmospheric Environment: 11:87-91.

Hildemann, L. M., Russell, A. G., and Cass, G. R. (1984) Ammonia and nitric acid concentrations in equilibrium with atmospheric aerosols: Experiment vs. Theory. Atmospheric Environment, 18: 1737-1750.

Hoell, J. M., LeBel, P. J., and Braman, R. S. (1983) Simultaneous measurements of tropospheric ammonia and nitric acid. Personal communication, unpublished.

Holzworth, G. C. (1972) Mixing heights, wind speeds, and potential for urban air pollution throughout the continuous United States. U.S. Environmental Protection Agency, U.S. Government Printing Office, Washington D.C.

REFERENCES (continued)

Huebert, B. J. and Lazrus, A. L. (1979) Tropospheric measurements of nitric acid vapor and particulate nitrate. Nitrogenous Air Pollutants. Ann Arbor Science, Ann Arbor, Mich., p: 307-315.

Huebert, B. J. and Lazrus, A. L. (1980a) Tropospheric gas-phase particulate nitrate measurements. Journal Geophysical Research, 85: 7322-7328.

Huebert, B. J. and Lazrus, A. L. (1980b) Bulk composition of aerosols in remote troposphere. Journal Geophysical Research, 85: 7337-7344.

Joseph, D. W., and Spicer, C. W. (1978) Chemiluminescence method for atomspheric monitoring of nitric acid and nitrogen oxides. Anal. Chem., 50: 1400-1403.

Knapp, K. T., Durham, J. L. and Ellestad, T. G. (1986) Pollutant sampler for measurements of atmospheric acidic dry deposition. Evironmental Science and Technology, 20: 633-637.

Kelly, T. J. and Stedman, D. H. (1979) Chemiluminescence measurements of HNO_3 in air. NTIS PB-294098, U.S. Environmental Protection Agency.

Lazrus, A. L., Haagenson, P. L., Kok, G. L., Kreitberg, C. W., Likens, G. E., Mohnen, V. A., Wilson, W. E., and Winchester, J. W. (1981) Acidity in air and water in warm frontal precipitation. 74th Air Pollution Control Association Conference.

LeBel, P. J., Hoell, J. M., Levine, J. S., and Vay, S. A. (1985) Aircraft measurements of ammonia and nitric acid in the lower troposphere. Geophysical Research Letters, 12: 401-404.

Leighton, P. A. (1961) The Photochemistry of Air Pollution. Academy Press, New York.

Lindqvist, F. (1985) Determination of nitric acid in ambient air by gas chromatography/photoionization detection after collection in a denuder. Journal Air Pollution Control Association, 35: 19-23.

Liu, S. and Cicerone, J. (1984) Fixed nitrogen cycle. Global NH_3. Analytical Chemistry, 54: 365-369.

Lloyd, L. and Wyatt, P. A. (1955) Vapor pressures of HNO_3 solutions, Part 1. Journal Chemical Society: 2248-2252.

McClenny, W. A., Gailey, P. C., Braman, R. S., and Shelley, t. J. (1982) Tungstic acid technique for monitoring nitric acid and ammonia in ambient air. Analytical Chemistry, 54: 365-369.

Miller, D. F. and Spicer, C. W. (1975) Measurement of nitric acid in smog. Journal Air Pollution Control Association, 25: 940-942.

REFERENCES (continued)

Mulawa, P. A. and Cadle, S. H. (1985) A comparison of nitric acid and particulate nitrate measurements by the penetration and denuder methods. Atmospheric Environment, 19: 1317-1324.

National Academy of Science (1977) Nitrogen Oxides. NAS Printing and Publishing Office, Washington, D.C.

National Oceanic and Atmospheric Administration (1984) National Acid Precipitation Assessment Program: Summary, NTIS N85-21820.

Okita, T., Morinoto, S., Izawa, M. and Konns, S. (1976) Measurement of gaseous and particulate nitrate in the atmosphere. Atmospheric Environment, 10: 1085-1089.

Okita, T. and Ohta, S. (1976) Measurements of nitrogenous and other compounds in the atmosphere and in cloud water: A study of the mechanism of formation of acid precipitation. Nitrogeneous Air Pollutants. D. Grosjean, Ed., Ann Arbor Science, Michigan, pp. 289-305.

Pierson, W. R., Brachaczek, W. W., Korniski, T. J., Truex, T. J., and Butler, J. W. (1980) Artifact formation of sulfate, nitrate, and hydrogen ion on backup filters: Allegheny Mountain Experiment. Journal Air Pollution Control Association, 30: 30-45.

Possanzini, M., Febo, A., and Liberti, A. (1983) New design of high-performance denuder for the sampling of atmospheric pollutants. Atmospheric Environment, 17: 2605-2610.

Ross, W. D., Butler, G. W., Duffy, T. G., Rehg, W. R., Wininger, M. T., and Sievers, R. E. (1975) Analysis for gaseous nitrates and nitrites and gaseous nitrogen by electron capture gas chromatography. Journal Chromatography, 112: 719-727.

Russell, A. G., McRae, G. J., and Cass, G. R. (1983) Mathematical modeling of the formation and transport of ammonium nitrate aerosol. Atmospheric Environment, 17: 1315-1329.

Russell, A. G., McRae, G. J., and Cass, G. R. (1985) The dynamics of nitric acid production and the fate of nitrogen oxides. Atmospheric Environment, 19: 893-903.

Saxena, P. and Seigneur, C. (1983) Modeling of multiphase atmospheric aerosols. Atmospheric Environment, 17: 1315-1329.

Schiff, H. J., Hastie, D. R., MacKay, G. I., Iguchi, T. and Ridley, B. A. (1983) Tunable diode laser systems for measuring trace gases in tropospheric air. Environmental Science and Technology, 17: 352A-364A.

REFERENCES (continued)

Seigneur, C. and Saxena, P. (1984) A study of atmospheric acid formation in different environments. Atmospheric Environment, 18: 2109-2124.

Seinfeld, J. H. (1975) Air Pollutions: physical and chemical fundamental. McGraw-Hill, Inc., New York.

Shaw, R. W., Dzubay, T. G., and Stevens, R. K. (1979) The denuder difference experiment. NTIS PB-294098, U.S. Environmental Protection Agency.

Shaw, R. W., Stevens, R. K., Bowermaster, J., Tesch, J. W., and Tew, E. (1982) Measurements of atmospheric nitrate and nitric acid: The Denuder Difference Experiment. Atmospheric Environment, 16: 845-853.

Spicer, C. W., Howes, J. E., Bishop, T. A., and Arnold, L. H. (1982) Nitric acid measurement methods: An intercomparison. Atmospheric Environment, 16: 1487-1500.

Spicer, C. W. and Miller, D. F. (1976) Nitrogen balance in smog chamber studies. Journal Air Pollution Control Association, 26: 45-50.

Spicer, C. W. and Schumacher, P. M. (1979) Particulate nitrate: laboratory and field studies of major sampling interferences. Atmospheric Environment, 13: 543-552.

Spicer, C. W., Schumacher, P. M., Konyoumjian, J. A., and Joseph, D. W. (1978) Sampling and analytical methodolgy for atmospheric particulate nitrates. EPA 600/2-78-067, U.S. Environmental Protection Agency.

Stedman, D. H., Chameides, W. H., and Cicerone, R. J. (1975) The vertical distribution of soluble gases in the troposphere. Geophysical Research Letters, 2: 333-336.

Stelson, A. W., Friedlander, S. K. and Seinfeld, J. H. (1979) A note on the equilibrium relationship between ammonia and nitric acid and particulate ammonium nitrate. Atmospheric Environment, 13: 369-371.

Stevens, R. K. (1979) Current methods to measure atmospheric nitric acid and nitrate artifacts. NTIS PB-294098, U.S. Environmental Protection Agency.

Torres, A. L. (1985) Nitric oxide measurement at a nonurban eastern United States site - Wallops instrument results from July 1983 GTE-CITE mission. Journal of Geophysical Research, 90: 12,875-12,880.

REFERENCES (continued)

Tuazon, E. C., Graham, R. A., Winer, A. M., Easton, R. R., Pitts, J. N. Jr., and Hanst, P. L. (1978) A kilometer pathlength Fourier-transform infrared system for the study of trace pollutants in ambient and synthetic atmosphere. Atmospheric Environment, 12: 865-875.

Vermeulen, A. J. (1979) The acidic precipitation phenomenon. A study of this phenomenon and of a relationship between the acid content of precipitation and the emission of sulfur dioxide and nitrogen oxides in the Netherlands. Polluted Rain, Plenum Press, N. Y., pp. 4-12.

Wartburg, A., Rael R. and Ridley, B. A. (1984) Laboratory tests of a tungstic acid coated diffusion denuder tube for measurements of atmospheric nitric acid. National Center of Atmospheric Research, personal communication.

Wilke, C. R. and Lee, C. Y (1955) Estimation of diffusion coefficients for gases and vapors. Industrial and Engineering Chemistry, 47: 1253-1257.

APPENDIX A1

APPENDIX A1

Table A1-1. TAT Signal Data for HNO3, NH3, NO3- and NH4+ at 60°C, 0% RH and [HNO_3] = 24 ppb.

FILE NAME IS HNO33
****
No. OF DATA SETS IN FILE = 25
JULIAN DATE FILE = 84209
RELATIVE HUMIDITY= 0
TEMPERATURE = 23.4
****

DATA PT	SAMPLE TIME	HNO3	NH3	NO3-	NH4+
1	1.00	58.40	1.80	.80	0.00
2	1.00	56.40	9.30	.60	0.00
3	1.00	61.60	3.20	3.20	0.00
4	1.00	60.00	9.00	1.60	11.00
5	1.00	66.40	10.70	3.40	0.00
6	2.00	118.00	21.00	9.20	2.80
7	2.00	119.00	33.00	11.00	1.10
8	2.00	120.00	29.00	10.00	7.40
9	2.00	123.00	41.00	15.00	1.80
10	2.00	122.00	37.00	12.00	0.00
11	3.00	144.00	70.00	32.40	4.60
12	3.00	141.00	67.00	33.20	1.60
13	3.00	144.00	68.00	37.00	5.00
14	3.00	158.00	70.00	40.00	2.50
15	3.00	155.00	73.00	38.00	2.50
16	4.00	178.00	105.00	78.00	10.00
17	4.00	179.00	100.00	81.00	5.50
18	4.00	180.00	100.00	83.00	11.00
19	4.00	186.00	108.00	90.00	4.30
20	4.00	180.00	108.00	90.00	11.00
21	5.00	190.00	120.00	142.00	13.00
22	5.00	187.00	130.00	140.00	12.00
23	5.00	182.00	140.00	146.00	7.00
24	5.00	189.00	140.00	145.00	6.00
25	5.00	185.00	143.00	149.00	9.00

Table A1-2. TAT Signal Data for HNO3, NH3, NO3- and NH4+ at 60°C, 17% RH and [HNO_3] = 24. ppb.

FILE NAME IS HNO32
****
No. OF DATA SETS IN FILE = 25
JULIAN DATE FILE = 84206
RELATIVE HUMIDITY= 16.9
TEMPERATURE = 25.9
****

DATA PT	SAMPLE TIME	HNO3	NH3	NO3-	NH4+
1	1.00	52.80	18.00	47.50	1.20
2	1.00	52.40	8.30	47.60	5.00
3	1.00	53.20	17.00	40.80	5.00
4	1.00	54.40	18.00	42.00	4.00
5	1.00	54.00	12.00	35.60	4.10
6	2.00	69.20	20.00	87.60	1.60
7	2.00	67.20	24.00	100.00	3.70
8	2.00	68.40	26.00	102.00	6.10
9	2.00	68.80	19.00	102.00	2.00
10	2.00	68.80	19.00	105.00	0.00
11	3.00	76.80	30.00	202.00	6.30
12	3.00	78.40	30.00	199.00	2.50
13	3.00	76.40	24.00	196.00	11.00
14	3.00	73.20	24.00	196.00	2.90
15	3.00	77.20	25.00	178.00	9.00
16	4.00	81.20	31.00	295.00	7.00
17	4.00	84.00	26.00	299.00	5.30
18	4.00	81.20	18.00	295.00	10.00
19	4.00	81.60	29.00	302.00	9.50
20	4.00	81.20	32.00	288.00	5.20
21	5.00	88.80	31.00	388.00	4.70
22	5.00	86.40	29.00	396.00	8.30
23	5.00	85.20	28.00	392.00	8.20
24	5.00	89.20	28.00	385.00	2.10
25	5.00	88.00	31.00	384.00	3.20

Table A1-3. TAT Signal Data for HNO3, NH3, NO3- and NH4+ at 60°C, 41% RH and [HNO_3] = 24 ppb.

****
No. OF DATA SETS IN FILE = 25
JULIAN DATE FILE = 84204
RELATIVE HUMIDITY= 41
TEMPERATURE = 25.9
****

DATA PT	SAMPLE TIME	HNO3	NH3	NO3-	NH4+
1	1.00	40.50	10.90	41.90	2.70
2	1.00	50.00	7.00	39.30	1.20
3	1.00	45.40	6.00	38.70	2.00
4	1.00	48.10	5.70	39.30	3.30
5	1.00	40.40	9.00	43.30	2.30
6	2.00	62.80	6.90	86.90	2.60
7	2.00	61.50	10.50	93.30	3.40
8	2.00	64.10	9.20	94.50	3.80
9	2.00	65.60	9.50	97.40	2.00
10	2.00	60.90	9.10	94.90	1.70
11	3.00	70.70	12.70	153.60	2.40
12	3.00	75.80	12.10	154.60	1.00
13	3.00	73.60	7.40	156.70	2.90
14	3.00	72.10	10.00	159.40	4.10
15	3.00	72.40	9.90	161.80	2.80
16	4.00	81.10	12.00	226.10	2.90
17	4.00	83.10	9.50	230.50	1.00
18	4.00	79.80	11.40	239.40	3.00
19	4.00	78.90	10.00	241.10	.90
20	4.00	79.70	9.00	238.00	4.50
21	5.00	87.00	13.30	305.40	2.60
22	5.00	86.80	10.70	317.40	1.60
23	5.00	86.00	13.30	310.30	3.30
24	5.00	84.30	12.60	316.80	3.20
25	5.00	86.50	12.60	309.40	1.20

Table A1-4. TAT Signal Data for HNO3, NH3, NO3- and NH4+ at 60°C, 52% RH and [HNO_3] = 24 ppb.

FILE NAME IS HNO35
****
No. OF DATA SETS IN FILE = 25
JULIAN DATE FILE = 84206
RELATIVE HUMIDITY= 52
TEMPERATURE = 26.2
****

DATA PT	SAMPLE TIME	HNO3	NH3	NO3-	NH4+
1	1.00	47.60	8.70	42.80	7.60
2	1.00	48.80	15.00	37.60	5.10
3	1.00	46.80	17.00	34.40	5.00
4	1.00	47.60	15.00	33.60	2.50
5	1.00	43.60	15.00	35.60	4.60
6	2.00	59.20	20.00	107.00	4.30
7	2.00	59.20	21.00	108.00	2.40
8	2.00	58.40	11.00	100.00	3.90
9	2.00	59.60	21.00	94.00	3.10
10	2.00	59.60	15.00	93.00	6.90
11	3.00	66.40	29.00	194.00	7.00
12	3.00	67.20	21.00	190.00	6.00
13	3.00	68.40	24.00	190.00	12.00
14	3.00	69.20	26.00	177.00	8.20
15	3.00	66.80	24.00	182.00	11.00
16	4.00	75.60	25.00	282.00	10.00
17	4.00	75.20	24.00	264.00	5.00
18	4.00	78.40	29.00	274.00	10.00
19	4.00	77.20	28.00	273.00	7.00
20	4.00	77.60	26.00	270.00	6.00
21	5.00	75.60	30.00	354.00	11.50
22	5.00	79.60	21.00	360.00	0.00
23	5.00	82.00	27.00	368.00	4.00
24	5.00	84.00	26.00	361.00	7.00
25	5.00	80.40	25.00	354.00	8.00

Table A1-5. TAT Signal Data for HNO3, NH3, NO3- and NH4+ at 60°C, 78% RH and [HNO_3] = 24 ppb.

FILE NAME IS HNO34
****
No. OF DATA SETS IN FILE = 25
JULIAN DATE FILE = 84204
RELATIVE HUMIDITY= 78
TEMPERATURE = 25.9
****

DATA PT	SAMPLE TIME	HNO3	NH3	NO3-	NH4+
1	1.00	40.00	6.00	15.80	0.00
2	1.00	37.60	10.00	15.60	2.20
3	1.00	39.20	15.00	25.60	9.40
4	1.00	44.00	11.00	22.40	9.90
5	1.00	50.00	16.00	22.40	7.40
6	2.00	62.00	18.00	73.20	0.00
7	2.00	63.60	18.00	70.00	5.20
8	2.00	60.40	15.00	83.20	1.10
9	2.00	56.80	17.00	84.40	1.40
10	2.00	60.40	19.00	86.80	0.00
11	3.00	71.20	21.00	152.40	0.00
12	3.00	70.00	19.00	145.20	11.00
13	3.00	69.20	22.00	156.00	10.00
14	3.00	70.40	24.00	161.00	.40
15	3.00	71.60	27.00	163.00	6.50
16	4.00	79.20	23.00	233.00	6.50
17	4.00	75.60	21.00	229.00	10.00
18	4.00	75.60	21.00	227.00	4.20
19	4.00	80.00	20.00	241.00	4.30
20	4.00	79.20	24.00	245.00	8.60
21	5.00	82.80	26.00	310.00	4.00
22	5.00	88.00	24.00	315.00	6.90
23	5.00	87.20	31.00	323.00	12.00
24	5.00	86.40	22.00	336.00	14.00
25	5.00	84.40	20.00	334.00	2.20

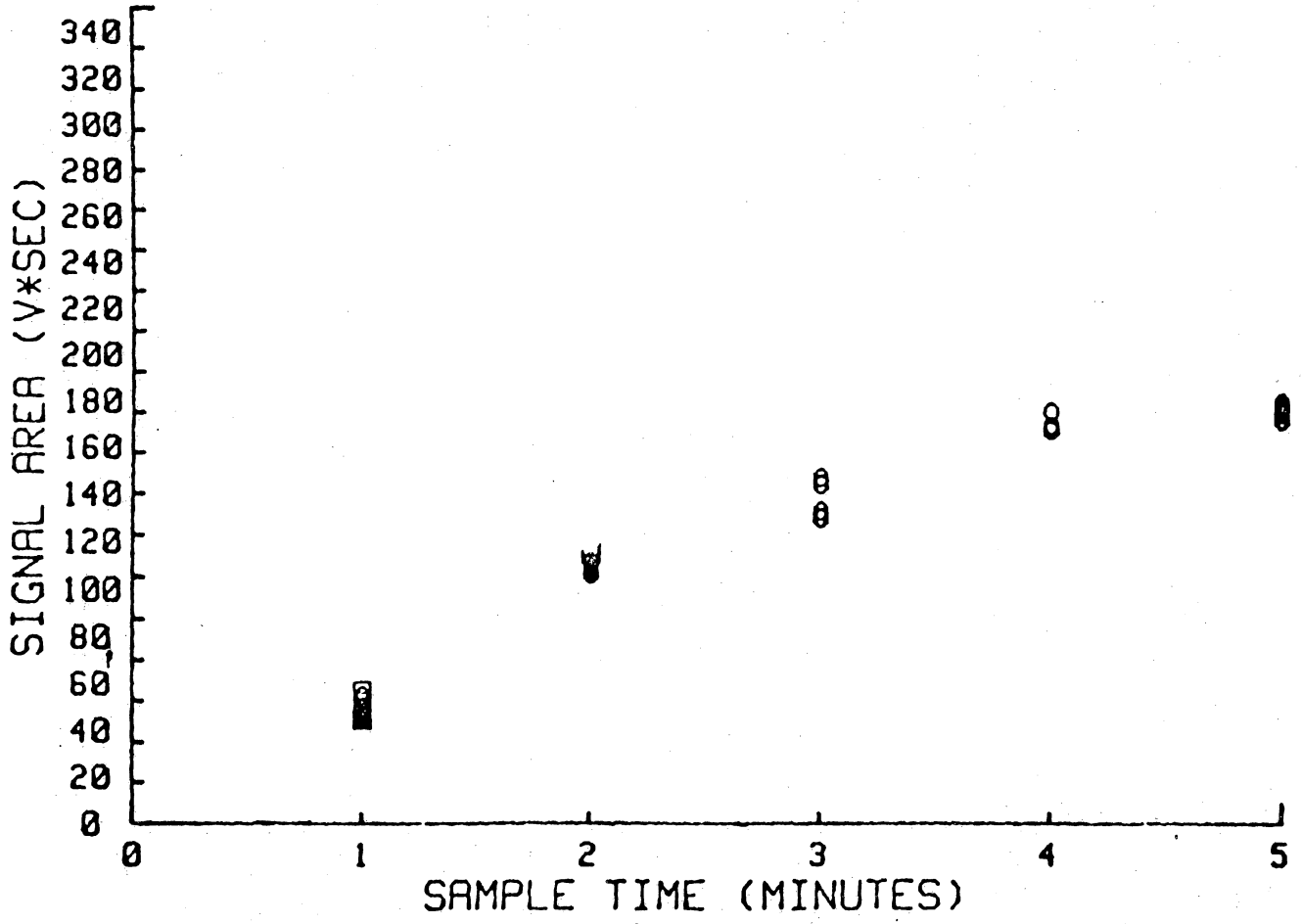

Figure A1-1. TAT Signal Area for HNO_3 (volt x sec) versus sample time (minutes) at 60°C, 0% RH and [HNO_3] = 24 ppb.

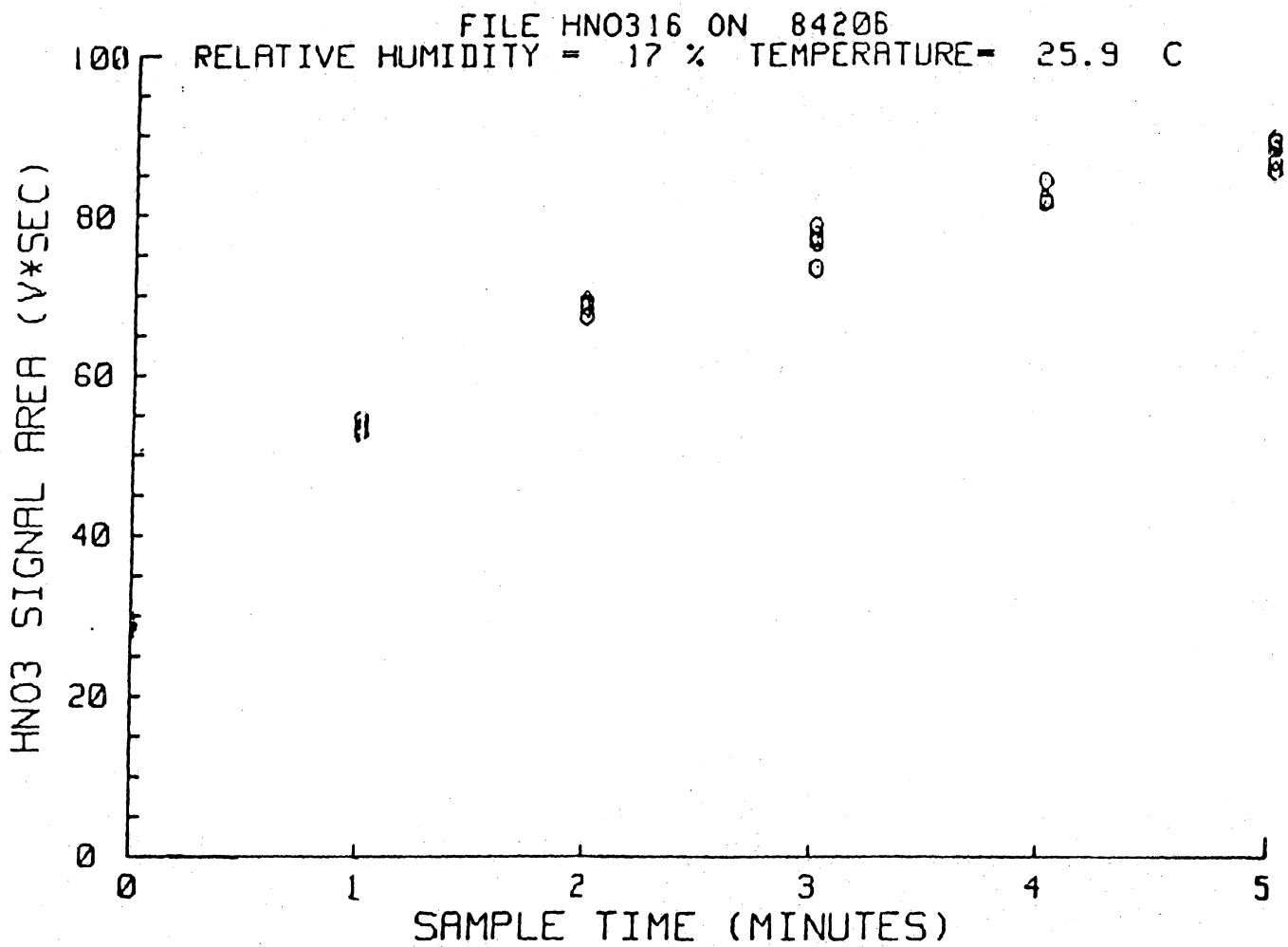

Figure A1-2. TAT Signal Area for HNO_3 (volt x sec) versus sample time (minutes) at 60°C, 17% RH and $[HNO_3]$ = 24 ppb.

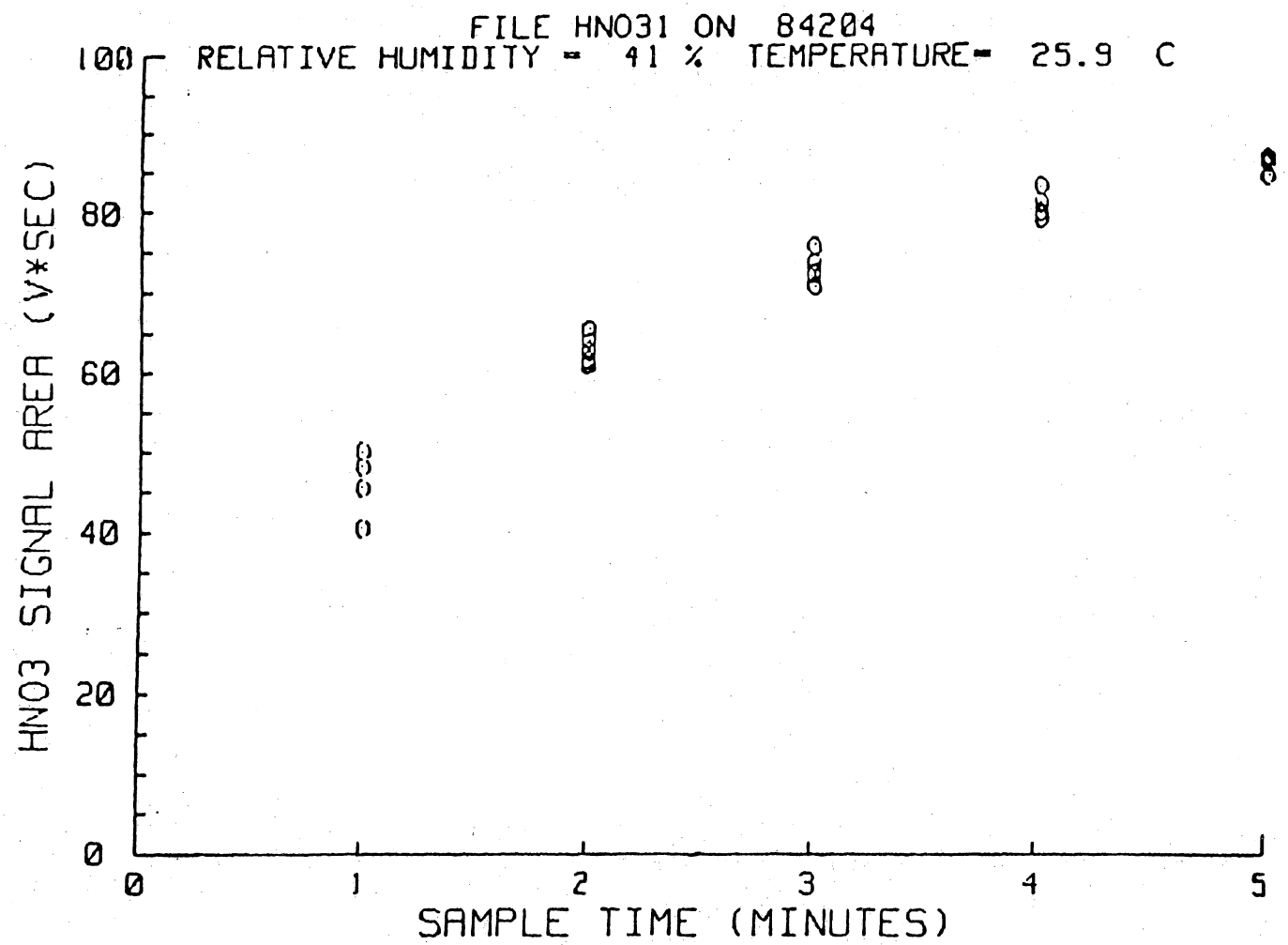

Figure A1-3. TAT Signal Area for HNO_3 (volt x sec) versus sample time (minutes) at 60°C, 41% RH and $[HNO_3]$ = 24 ppb.

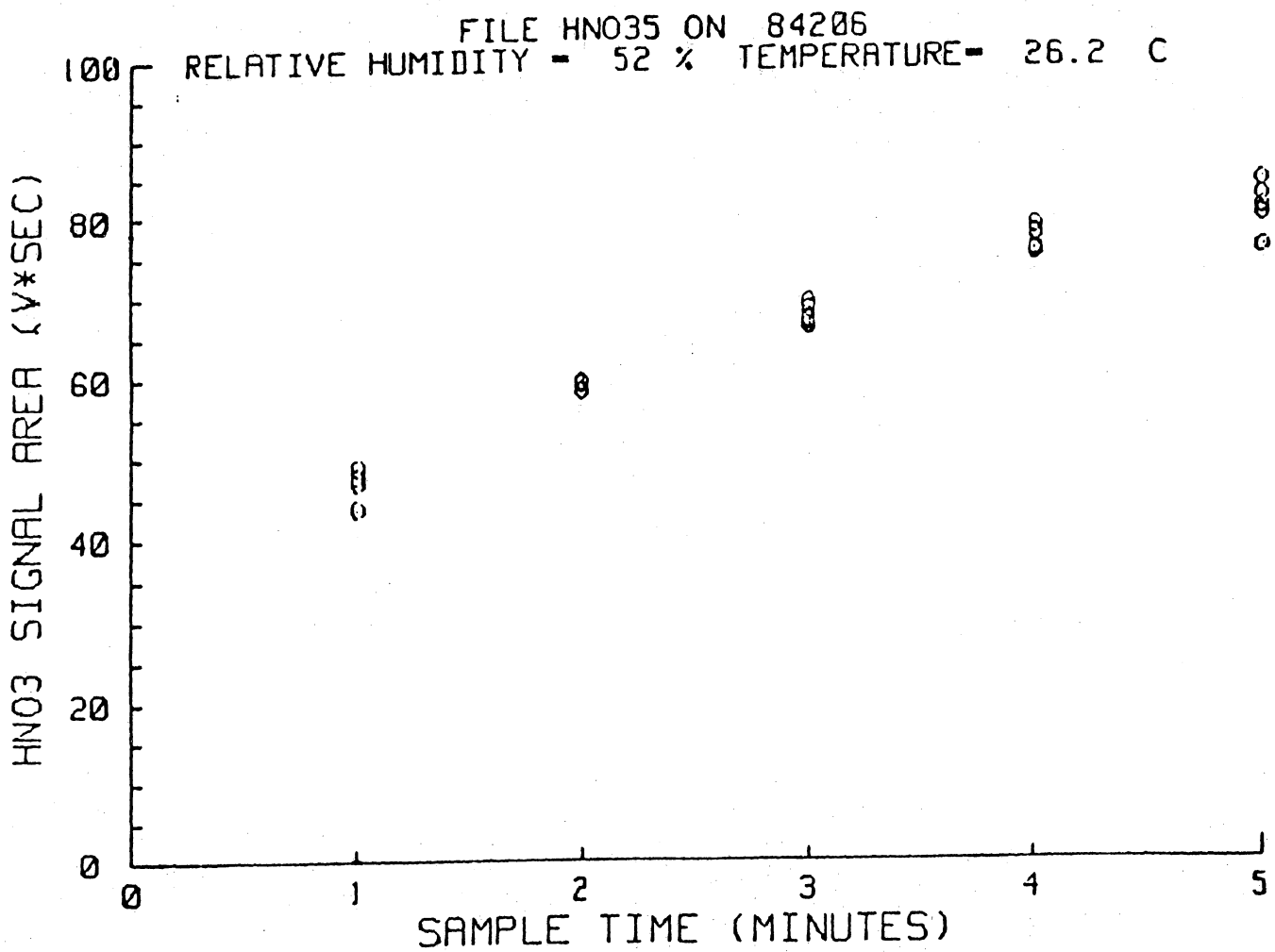

Figure A1-4. TAT Signal Area for HNO_3 (volt x sec) versus sample time (minutes) at 60°C, 52% RH and $[HNO_3]$ = 24 ppb.

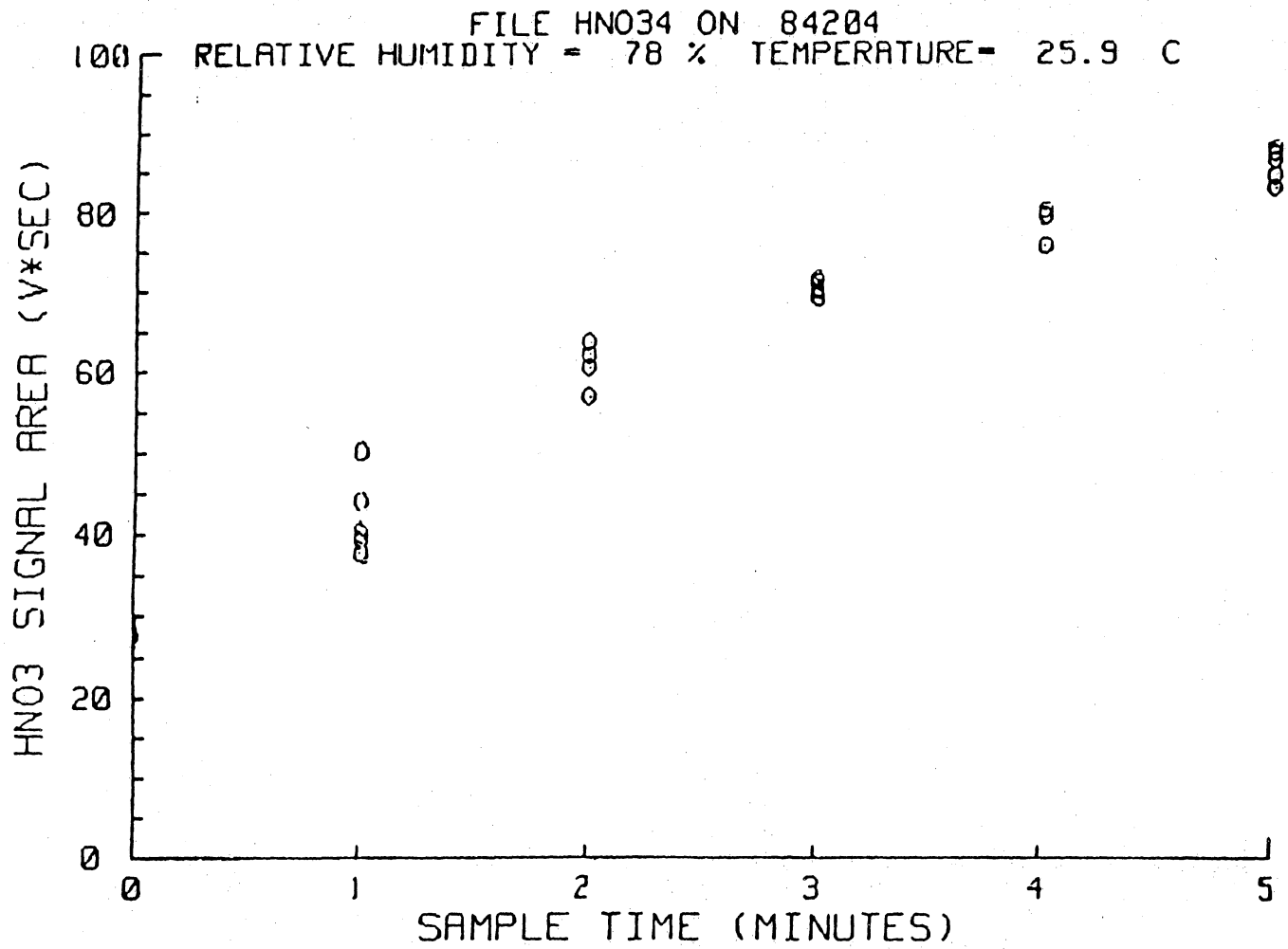

Figure A1-5. TAT Signal Area for HNO_3 (volt x sec) versus sample time (minutes) at 60°C, 78% RH and $[HNO_3]$ = 24 ppb.

APPENDIX A2

APPENDIX A2

Table A2-1. TAT Signal Data for HNO3, NH3, NO3- and NH4+ at 60°C, 17% RH and [HNO_3] = 4.7 ppb.

FILE NAME IS HNO317
****
No. OF DATA SETS IN FILE = 25
JULIAN DATE FILE = 84227
RELATIVE HUMIDITY= 17
TEMPERATURE = 27.5
****

DATA PT	SAMPLE TIME	HNO3	NH3	NO3-	NH4+
1	1.00	10.00	15.00	2.00	1.80
2	1.00	9.60	6.60	3.00	0.00
3	1.00	13.00	0.00	4.80	0.00
4	1.00	13.00	2.10	1.60	0.00
5	1.00	11.00	9.80	2.80	0.00
6	2.00	13.00	4.80	8.00	0.00
7	2.00	18.00	0.00	10.00	0.00
8	2.00	16.00	2.60	8.20	1.20
9	2.00	20.00	0.00	10.00	8.70
10	2.00	15.00	5.20	7.20	4.00
11	3.00	18.00	7.70	16.00	8.90
12	3.00	18.00	7.40	16.00	3.40
13	3.00	18.00	3.20	17.00	0.00
14	3.00	18.00	2.40	17.00	3.10
15	3.00	20.60	4.90	16.00	2.10
16	4.00	21.00	0.00	30.40	1.40
17	4.00	18.00	1.90	27.40	2.20
18	4.00	18.00	0.00	32.20	1.40
19	4.00	22.20	0.00	28.20	4.60
20	4.00	19.00	3.90	29.00	14.00
21	5.00	20.00	7.10	41.20	2.10
22	5.00	22.20	4.60	38.20	0.00
23	5.00	24.00	3.10	39.00	11.00
24	5.00	21.60	4.40	38.60	3.10
25	5.00	21.40	6.00	40.00	.40

Table A2-2. TAT Signal Data for HNO3, NH3, NO3- and NH4+ at 60°C, 52% RH and [HNO_3] = 4.7 ppb.

FILE NAME IS HNO352
****
No. OF DATA SETS IN FILE = 25
JULIAN DATE FILE = 84227
RELATIVE HUMIDITY= 52
TEMPERATURE = 26.5
****

DATA PT	SAMPLE TIME	HNO3	NH3	NO3-	NH4+
1	1.00	10.00	16.00	.60	2.60
2	1.00	9.20	10.00	2.30	.70
3	1.00	7.30	3.00	4.70	0.00
4	1.00	11.40	0.00	3.90	0.00
5	1.00	9.90	3.00	4.10	0.00
6	2.00	13.40	11.00	10.70	0.00
7	2.00	16.10	19.00	9.00	0.00
8	2.00	15.60	0.00	10.60	0.00
9	2.00	12.70	0.00	9.50	0.00
10	2.00	13.50	0.00	11.30	0.00
11	3.00	15.20	0.00	15.90	0.00
12	3.00	14.20	0.00	18.90	0.00
13	3.00	17.50	2.40	20.00	4.20
14	3.00	14.40	13.00	20.00	17.00
15	3.00	16.70	14.00	18.30	0.00
16	4.00	17.30	0.00	28.70	5.70
17	4.00	17.10	0.00	29.80	0.00
18	4.00	17.70	.60	28.20	0.00
19	4.00	17.00	22.00	29.20	0.00
20	4.00	18.70	9.30	31.30	3.60
21	5.00	18.90	0.00	38.40	0.00
22	5.00	18.10	31.00	38.90	6.00
23	5.00	18.50	32.00	38.70	15.00
24	5.00	18.80	8.60	38.10	0.00
25	5.00	19.10	0.00	41.10	0.00

Table A2-3. TAT Signal Data for HNO3, NH3, NO3- and NH4+ at 60°C, 78% RH and [HNO_3] = 4.7 ppb.

FILE NAME IS HNO378
****
No. OF DATA SETS IN FILE = 25
JULIAN DATE FILE = 84224
RELATIVE HUMIDITY= 78
TEMPERATURE = 27.5
****

DATA PT	SAMPLE TIME	HNO3	NH3	NO3-	NH4+
1	1.00	30.00	13.00	3.40	10.00
2	1.00	27.00	10.00	8.80	3.20
3	1.00	26.00	0.00	8.60	0.00
4	1.00	28.00	2.80	7.20	0.00
5	1.00	25.00	8.30	6.80	3.40
6	2.00	34.00	2.70	17.20	0.00
7	2.00	26.00	.90	20.00	0.00
8	2.00	29.00	5.20	21.00	0.00
9	2.00	29.00	0.00	16.00	1.00
10	2.00	27.00	2.70	17.00	3.80
11	3.00	29.20	4.50	28.00	0.00
12	3.00	27.00	1.40	24.00	3.00
13	3.00	27.00	0.00	29.00	3.30
14	3.00	27.00	3.60	29.00	5.80
15	3.00	26.00	1.00	28.00	0.00
16	4.00	27.00	5.60	41.00	0.00
17	4.00	27.00	3.30	37.00	0.00
18	4.00	27.00	6.70	41.00	0.00
19	4.00	28.00	2.90	37.00	0.00
20	4.00	27.00	0.00	38.00	2.60
21	5.00	28.00	2.70	52.00	4.00
22	5.00	29.00	.80	55.00	.50
23	5.00	30.40	0.00	55.00	0.00
24	5.00	28.00	1.60	53.00	9.50
25	5.00	28.00	6.70	56.00	0.00

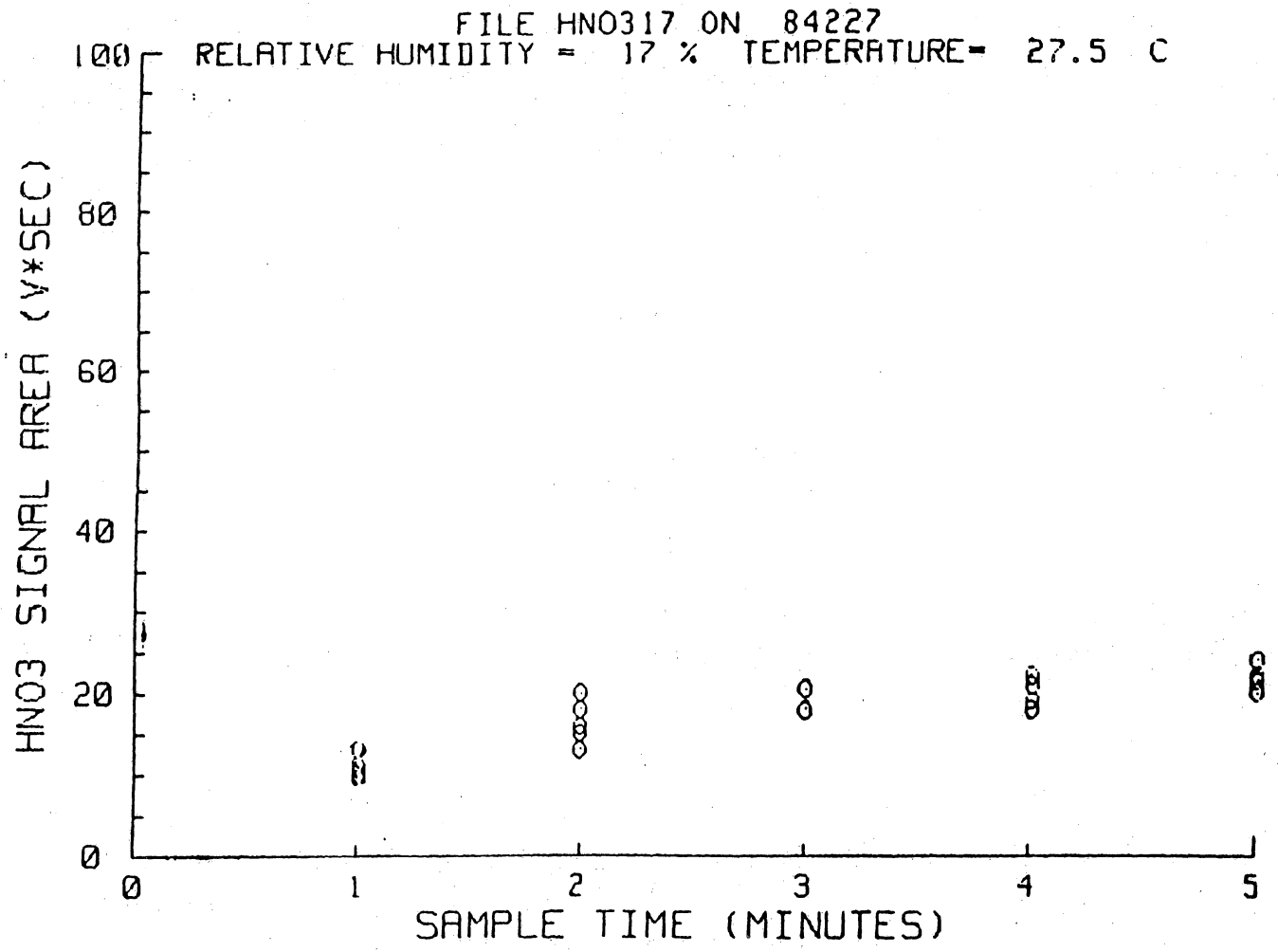

Figure A2-1. TAI Signal Area for HNO_3 (volt x sec) versus sample time (minutes) at 60°C, 17% RH and $[HNO_3]$ = 4.7 ppb.

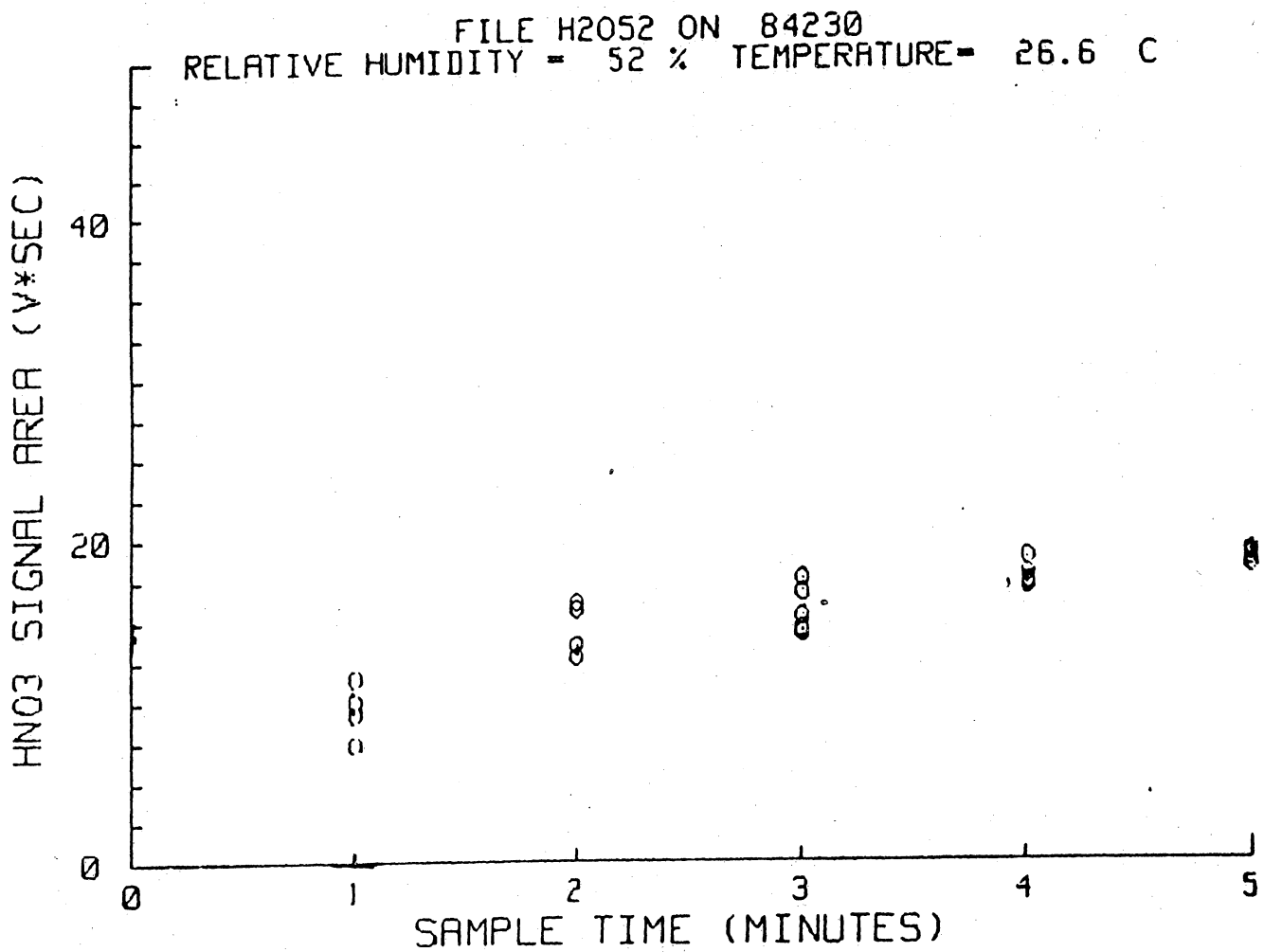

Figure A2-2. TAT Signal Area for HNO_3 (volt x sec) versus sample time (minutes) at 60°C, 52% RH and $[HNO_3]$ = 4.7 ppb.

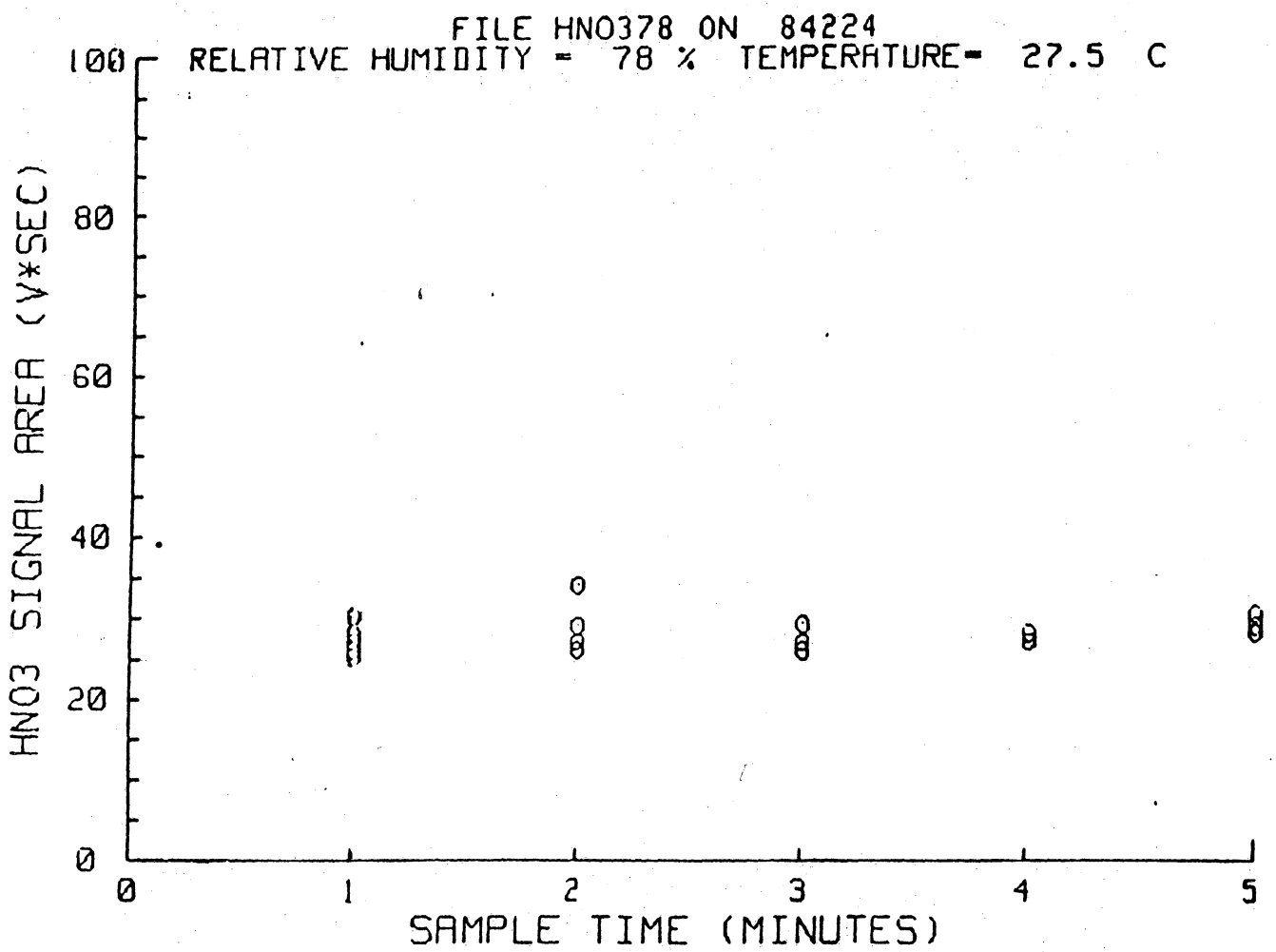

Figure A2-3. TAT Signal Area for HNO_3 (volt x sec) versus sample time (minutes) at 60°C, 78% RH and $[HNO_3]$ = 4.7 ppb.

APPENDIX A3

APPENDIX A3

Table A3-1. TAT Signal Data for HNO3, NH3, NO3- and NH4+ at 60°C, 0% RH and [HNO_3] = 4.7 ppb.

```
*****************************************
No. OF VALUES IN FILE  TO BE STORED=    29
JULIAN DATE FILE =  270
RELATIVE HUMIDITY=  0
TEMPERATURE       = 22.4
*************DATA STORE IN FILE*************
```

DATA PT	SAMPLE TIME	HNO3	NH3	NO3-	NH4+
1	1.00	38.00	0.00	0.00	0.00
2	1.00	33.00	0.00	0.00	0.00
3	1.00	34.00	0.00	0.00	0.00
4	1.00	36.00	0.00	3.90	0.00
5	1.00	34.00	0.00	2.70	0.00
6	2.00	56.00	0.00	5.70	0.00
7	2.00	59.00	0.00	10.00	0.00
8	2.00	70.00	0.00	10.00	0.00
9	2.00	62.00	0.00	12.00	0.00
10	2.00	61.00	0.00	12.00	0.00
11	3.00	74.00	0.00	29.00	0.00
12	3.00	72.00	0.00	30.00	0.00
13	3.00	71.00	0.00	34.00	0.00
14	3.00	76.00	0.00	35.00	0.00
15	3.00	75.00	0.00	33.00	0.00
16	4.00	82.00	0.00	57.00	0.00
17	4.00	79.00	0.00	57.00	0.00
18	4.00	84.00	0.00	57.00	0.00
19	4.00	79.00	0.00	60.00	0.00
20	4.00	85.00	0.00	61.00	0.00
21	5.00	88.00	0.00	91.00	0.00
22	5.00	88.00	0.00	93.00	0.00
23	5.00	90.00	0.00	95.00	0.00
24	5.00	91.00	0.00	95.00	0.00
25	5.00	88.00	0.00	99.00	0.00

FILE NAME IS 00HNO3
****
No. OF VALUES IN FILE TO BE STORED= 29

Table A3-2. TAT Signal Data for HNO3, NH3, NO3- and NH4+ at 35°C, 0% RH and [HNO_3] = 4.7 ppb.

JULIAN DATE FILE = 268
RELATIVE HUMIDITY= 0
TEMPERATURE = 23
**********DATA STORE IN FILE**********

DATA	SAMPLE TIME	HNO3	NH3	NO3-	NH4+
1	1.00	36.00	0.00	1.00	0.00
2	1.00	36.00	0.00	1.20	0.00
3	1.00	36.00	0.00	0.00	0.00
4	1.00	36.00	0.00	0.00	0.00
5	1.00	35.00	0.00	1.40	0.00
6	2.00	55.00	0.00	1.60	0.00
7	2.00	57.00	0.00	2.70	0.00
8	2.00	60.00	0.00	3.70	0.00
9	2.00	62.00	0.00	1.00	0.00
10	2.00	62.00	0.00	4.40	0.00
11	3.00	88.00	0.00	10.00	0.00
12	3.00	90.00	0.00	10.00	0.00
13	3.00	92.00	0.00	12.00	0.00
14	3.00	92.00	0.00	10.00	0.00
15	3.00	93.00	0.00	12.00	0.00
16	4.00	111.00	0.00	26.00	0.00
17	4.00	113.00	0.00	22.00	0.00
18	4.00	112.00	0.00	25.00	0.00
19	4.00	117.00	0.00	26.00	0.00
20	4.00	110.00	0.00	24.00	0.00
21	5.00	129.00	0.00	40.00	0.00
22	5.00	131.00	0.00	41.00	0.00
23	5.00	136.00	0.00	45.00	0.00
24	5.00	133.00	0.00	45.00	0.00
25	5.00	136.00	0.00	46.00	0.00

Table A3-3. TAT Signal Data for HNO3, NH3, NO3- and NH4+ at 25°C, 0% RH and [HNO_3] = 4.7 ppb.

FILE NAME IS 25/DRY
****
No. OF VALUES IN FILE TO BE STORED= 9
JULIAN DATE FILE = 276
RELATIVE HUMIDITY= 0
TEMPERATURE = 22.5
**********DATA STORE IN FILE**********

DATA PT	SAMPLE TIME	HNO3	NH3	NO3-	NH4+
1	1.00	43.00	25.00	1.70	28.00
2	2.00	81.00	0.00	.76	0.00
3	3.00	105.00	0.00	2.30	0.00
4	4.00	133.00	0.00	3.20	0.00
5	5.00	158.00	0.00	12.00	0.00

APPENDIX A4

APPENDIX A4

Table A4-1. TAT Signal Data for HNO3, NH3, NO3- and NH4+ at 60°C, 78% RH and [HNO_3] = 4.7 ppb.

FILE NAME IS C78MIX
****
No. OF DATA SETS IN FILE = 24
JULIAN DATE FILE = 272
RELATIVE HUMIDITY= 78
TEMPERATURE = 22.5
****

DATA PT	SAMPLE TIME	HNO3	NH3	NO3-	NH4+
1	1.00	10.00	55.00	10.00	65.00
2	1.00	10.00	0.00	8.00	0.00
3	1.00	8.40	0.00	11.00	0.00
4	1.00	7.60	0.00	14.00	0.00
5	1.00	7.60	0.00	13.00	0.00
6	2.00	11.00	0.00	31.00	0.00
7	2.00	12.00	0.00	37.00	0.00
8	2.00	12.00	0.00	38.00	0.00
9	2.00	10.00	0.00	38.00	0.00
10	2.00	11.00	0.00	42.00	0.00
11	3.00	13.00	0.00	71.00	0.00
12	3.00	13.00	0.00	76.00	0.00
13	3.00	12.00	0.00	76.00	0.00
14	3.00	14.00	0.00	79.00	0.00
15	3.00	13.00	0.00	80.00	0.00
16	4.00	15.00	0.00	117.00	0.00
17	4.00	14.00	0.00	121.00	0.00
18	4.00	16.00	0.00	128.00	0.00
19	4.00	16.00	0.00	126.00	0.00
20	4.00	14.00	0.00	128.00	0.00
21	5.00	17.00	0.00	166.00	0.00
22	5.00	16.00	0.00	169.00	0.00
23	5.00	17.00	0.00	171.00	0.00
24	5.00	16.00	0.00	179.00	0.00

Table A4-2. TAT Signal Data for HNO3, NH3, NO3- and NH4+ at 45°C, 78% RH and [HNO_3] = 4.7 ppb.

FILE NAME IS MROMIX
****
No. OF DATA SETS IN FILE = 24
JULIAN DATE FILE = 273
RELATIVE HUMIDITY= 78
TEMPERATURE = 22.5
****

DATA PT	SAMPLE TIME		HNO3	NH3	NO3-	NH4+
1	1.00	14.00		45.00	9.00	45.00
2	1.00	13.00		0.00	10.00	0.00
3	1.00	14.00		0.00	10.00	0.00
4	1.00	14.00		0.00	10.00	0.00
5	2.00	22.00		0.00	24.00	0.00
6	2.00	20.00		0.00	26.00	0.00
7	2.00	19.00		0.00	28.00	0.00
8	2.00	21.00		0.00	26.00	0.00
9	2.00	22.00		0.00	31.00	0.00
10	3.00	26.00		0.00	46.00	0.00
11	3.00	27.00		0.00	50.00	0.00
12	3.00	28.00		0.00	54.00	0.00
13	3.00	26.00		0.00	59.00	0.00
14	3.00	26.00		0.00	60.00	0.00
15	4.00	30.00		0.00	86.00	0.00
16	4.00	32.00		0.00	89.00	0.00
17	4.00	33.00		0.00	91.00	0.00
18	4.00	31.00		0.00	96.00	0.00
19	4.00	33.00		0.00	101.00	0.00
20	5.00	35.00		0.00	131.00	0.00
21	5.00	36.00		0.00	129.00	0.00
22	5.00	36.00		0.00	135.00	0.00
23	5.00	37.00		0.00	144.00	0.00
24	5.00	37.00		0.00	149.00	0.00

Table A4-3. TAT Signal Data for HNO3, NH3, NO3- and NH4+ at 30°C, 78% RH and [HNO_3] = 4.7 ppb.

FILE NAME IS 78%MIX
****
No. OF DATA SETS IN FILE = 25
JULIAN DATE FILE = 270
RELATIVE HUMIDITY= 78
TEMPERATURE = 23.9
****

DATA PT	SAMPLE TIME	HNO3	NH3	NO3-	NH4+
1	1.00	33.00	0.00	4.00	0.00
2	1.00	32.00	0.00	.90	0.00
3	1.00	34.00	0.00	1.20	0.00
4	1.00	31.00	0.00	.80	0.00
5	1.00	34.00	0.00	1.80	0.00
6	2.00	66.00	0.00	2.70	0.00
7	2.00	72.00	0.00	6.40	0.00
8	2.00	75.00	0.00	4.40	0.00
9	2.00	74.00	0.00	6.80	0.00
10	2.00	76.00	0.00	8.00	0.00
11	3.00	103.00	0.00	11.00	0.00
12	3.00	103.00	0.00	13.00	0.00
13	3.00	110.00	0.00	13.00	0.00
14	3.00	112.00	0.00	17.00	0.00
15	3.00	111.00	0.00	16.00	0.00
16	4.00	132.00	0.00	28.00	0.00
17	4.00	137.00	0.00	28.00	0.00
18	4.00	138.00	0.00	34.00	0.00
19	4.00	136.00	0.00	38.00	0.00
20	4.00	138.00	0.00	44.00	0.00
21	5.00	160.00	0.00	77.00	0.00
22	5.00	156.00	0.00	72.00	0.00
23	5.00	158.00	0.00	64.00	0.00
24	5.00	156.00	0.00	62.00	0.00
25	5.00	154.00	0.00	57.00	0.00

Table A4-4. TAT Signal Data for HNO3, NH3, NO3- and NH4+ at 25°C, 78% RH and [HNO_3] = 4.7 ppb.

FILE NAME IS REMIX2
****
No. OF VALUES IN FILE, TO BE STORED= 29
JULIAN DATE FILE = 277
RELATIVE HUMIDITY= 78
TEMPERATURE = 23
**********DATA STORE IN FILE**********

DATA PT	SAMPLE TIME	HNO3	NH3	NO3-	NH4+
1	1.00	41.00	.00	1.10	.00
2	1.00	34.00	0.00	.76	0.00
3	1.00	38.00	0.00	0.00	0.00
4	1.00	38.00	0.00	0.00	0.00
5	1.00	40.00	0.00	.56	0.00
6	2.00	80.00	0.00	3.60	0.00
7	2.00	83.00	0.00	3.10	0.00
8	2.00	83.00	0.00	3.40	0.00
9	2.00	85.00	0.00	2.00	0.00
10	2.00	86.00	0.00	3.40	0.00
11	3.00	125.00	0.00	4.00	0.00
12	3.00	129.00	0.00	5.60	0.00
13	3.00	131.00	0.00	4.00	0.00
14	3.00	132.00	0.00	3.10	0.00
15	3.00	131.00	0.00	4.60	0.00
16	4.00	176.00	0.00	4.00	0.00
17	4.00	172.00	0.00	4.00	0.00
18	4.00	176.00	0.00	6.00	0.00
19	4.00	174.00	0.00	6.00	0.00
20	4.00	179.00	0.00	4.00	0.00
21	5.00	196.00	0.00	9.60	0.00
22	5.00	196.00	0.00	9.60	0.00
23	5.00	196.00	0.00	10.00	0.00
24	5.00	200.00	0.00	11.00	0.00
25	5.00	200.00	0.00	13.00	0.00

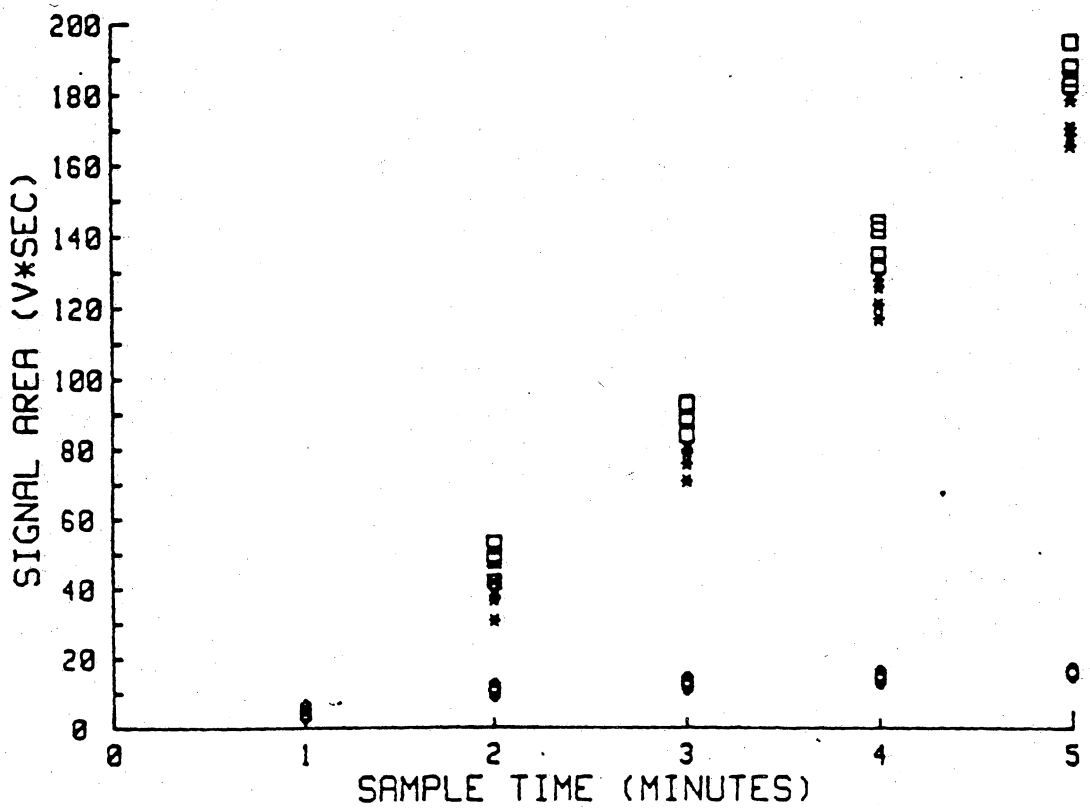

Figure A4-1. TAT Signal Area for HNO_3 (ϕ), "NO_3-" (*) and TNO_3 (□) (volt x sec) versus sample time (minutes) at 60 C, 78% RH and [HNO_3] = 4.7 ppb.

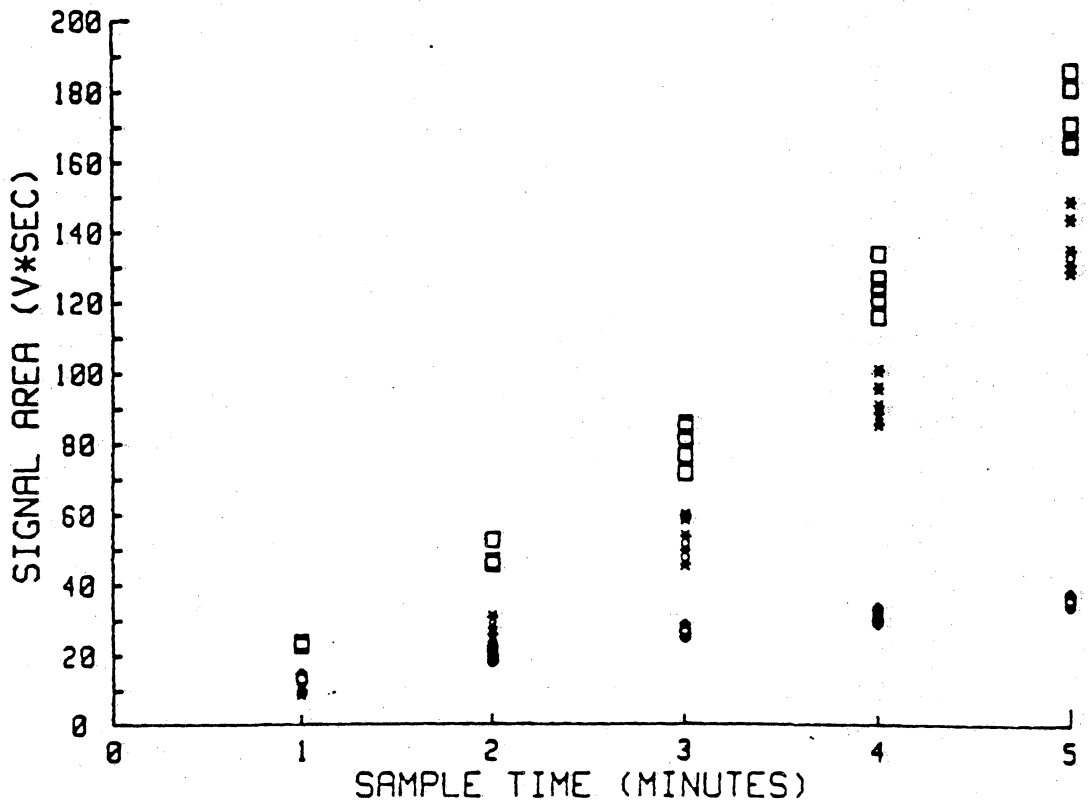

Figure A4-2. TAT Signal Area for HNO_3 (δ), "NO_3^-" (*) and TNO_3 (□) (volt x sec) versus sample time (minutes) at 45°C, 78% RH and [HNO_3] = 4.7 ppb.

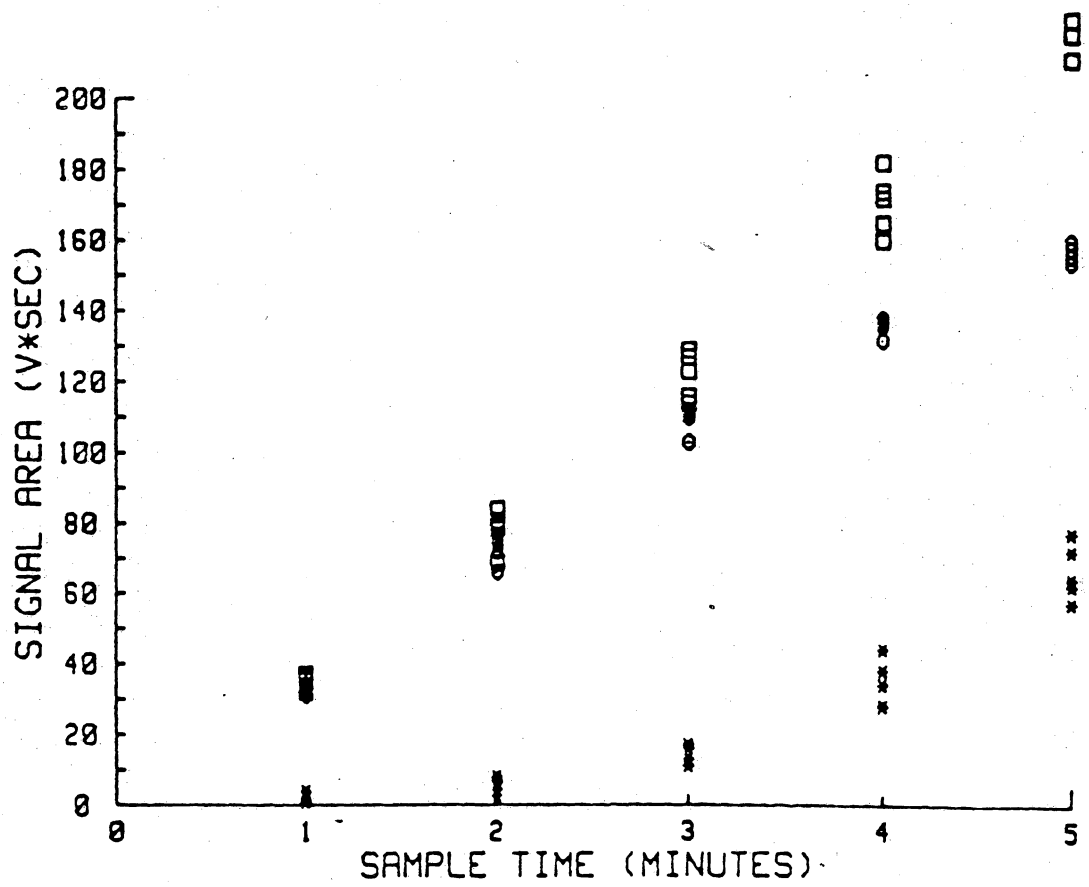

Figure A4-3. TAT Signal Area for HNO_3 (⊖), "NO_3^-" (✱) and TNO_3 (□) (volt x sec) versus sample time (minutes) at 30 °C, 78% RH and [HNO_3] = 4.7 ppb.

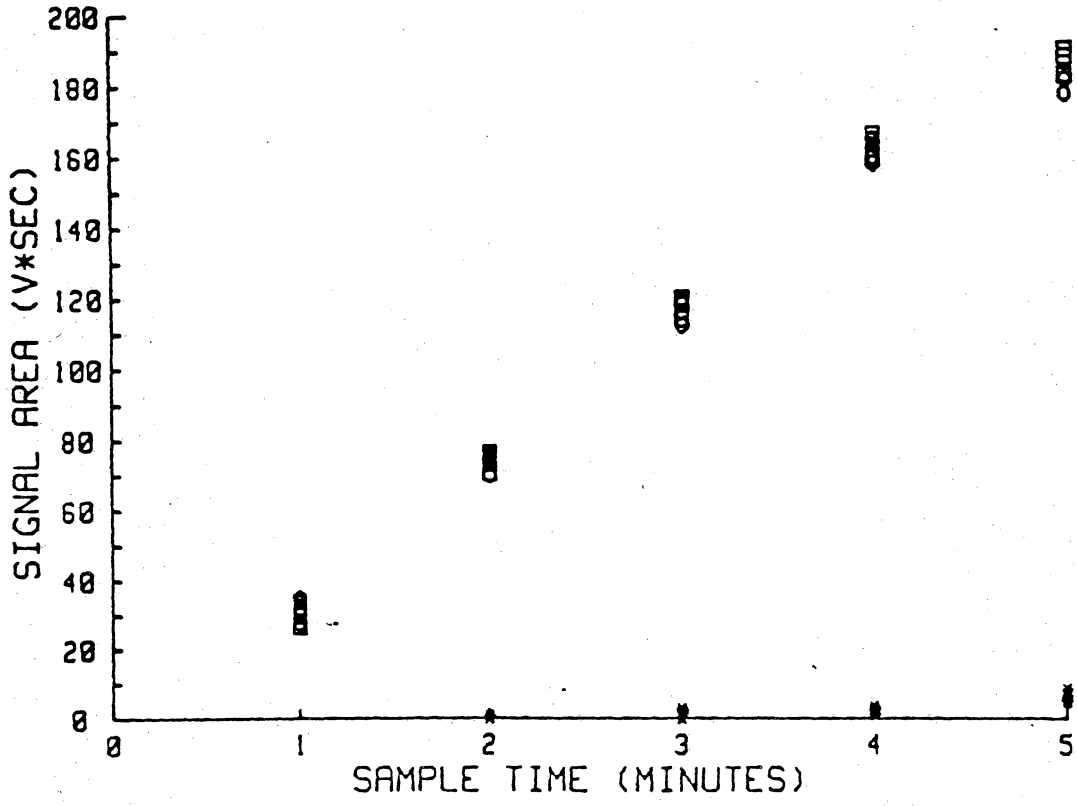

Figure A4-4. TAT Signal Area for HNO_3 (0), "NO_3-" (*) and TNO_3 (□) (volt x sec) versus sample time (minutes) at 25°C, 78% RH and [HNO_3] = 4.7 ppb.

APPENDIX A5

APPENDIX A5

Table A5-1. TAT Signal Area for HNO3, NH3, NO3- and NH4+ (volt x sec) versus sample time (minutes) at 60°C, 78% RH and [HNO_3] = 0.0 ppb.

FILE NAME IS C078RH
****
No. OF DATA SETS IN FILE = 5
JULIAN DATE FILE = 272
RELATIVE HUMIDITY= 78
TEMPERATURE = 23.2
****

DATA PT	SAMPLE TIME	HNO3	NH3	NO3-	NH4+
1	1.00	3.60	0.00	8.00	0.00
2	2.00	3.80	0.00	17.00	0.00
3	3.00	3.70	0.00	22.00	0.00
4	4.00	4.20	0.00	23.00	0.00
5	5.00	4.40	0.00	24.00	0.00

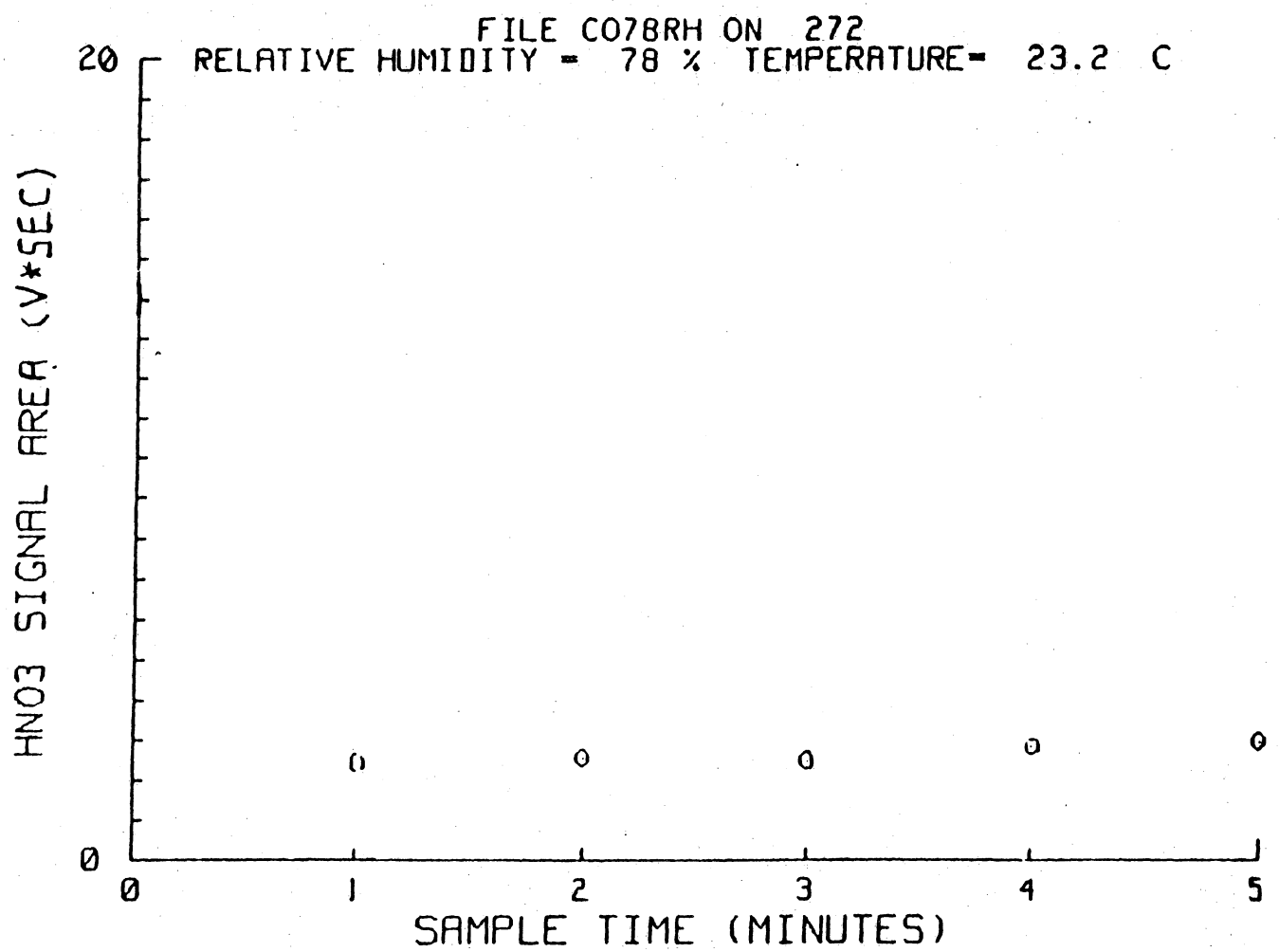

Figure A5-1. TAT Signal Area for HNO_3 (volt x sec) versus sample time (minutes) at 25 C, 78% RH and $[HNO_3]$ = 0.0 ppb.

Table A5-2. TAT Signal Area for HNO3, NH3, NO3- and NH4+ (volt x sec) versus sample time (minutes) at 25°C, 78% RH and [HNO_3] = 0.0 ppb.

FILE NAME IS 78%RH
****
No. OF DATA SETS IN FILE = 5
JULIAN DATE FILE = 271
RELATIVE HUMIDITY= 78
TEMPERATURE = 22.4
****

DATA PT	SAMPLE TIME	HNO3	NH3	NO3-	NH4+
1	1.00	3.00	0.00	3.20	0.00
2	2.00	4.20	0.00	7.80	0.00
3	3.00	5.80	0.00	9.20	0.00
4	4.00	7.60	0.00	11.00	0.00
5	5.00	8.80	0.00	14.00	0.00

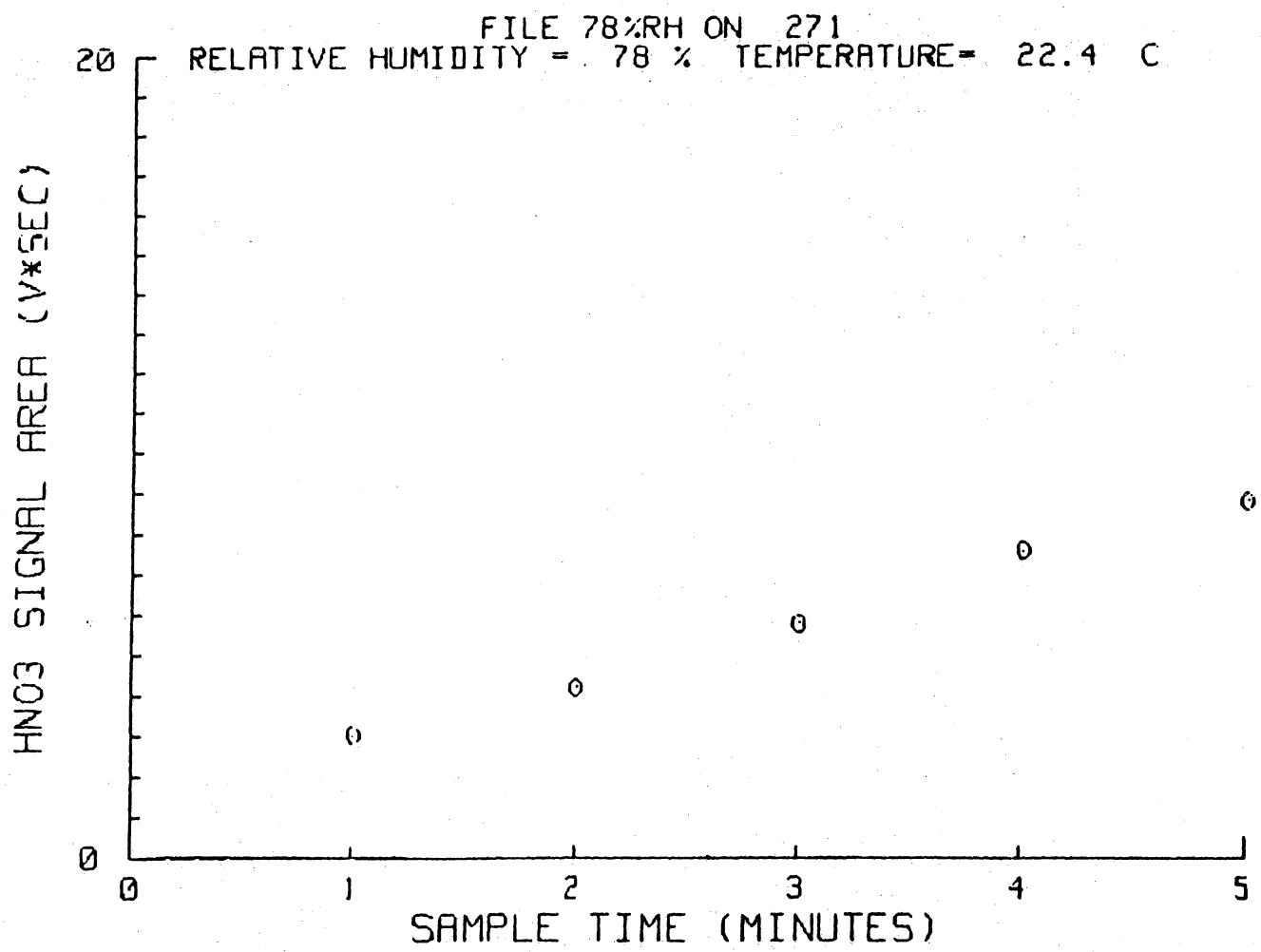

Figure A5-2. TAT Signal Area for HNO_3 (volt x sec) versus sample time (minutes) at 60 C, 78% RH and $[HNO_3]$ = 0.0 ppb.

Table A5-3. TAT Signal Area for HNO3, NH3, NO3- and NH4+ (volt x sec) versus sample time (minutes) at 25°C, 0% RH and [HNO_3] = 0.0 ppb.

FILE NAME IS NEWDRY
****
No. OF VALUES IN FILE TO BE STORED= 9
JULIAN DATE FILE = 84223
RELATIVE HUMIDITY= 0
TEMPERATURE = 27.8
**********DATA STORE IN FILE**********

DATA PT	SAMPLE TIME	HNO3	NH3	NO3-	NH4+
1	1.00	5.00	.20	1.80	.10
2	2.00	5.00	.20	1.80	.10
3	3.00	5.00	.20	1.80	.10
4	4.00	5.00	.20	1.80	.10
5	5.00	5.00	.20	1.80	.10

Table A5-4. TAT Signal Area for HNO3, NH3, NO3- and NH4+ (volt x sec) versus sample time (minutes) at 25 °C, 17% RH and [HNO3] = 0.0 ppb.

FILE NAME IS M2017
****
No. OF VALUES IN FILE TO BE STORED= 9
JULIAN DATE FILE = 84227
RELATIVE HUMIDITY= 17
TEMPERATURE = 27.5
**********DATA STORE IN FILE**********

DATA PT	SAMPLE TIME	HNO3	NH3	NO3-	NH4+
1	1.00	8.00	0.00	4.00	.20
2	2.00	8.80	1.50	5.60	.40
3	3.00	10.00	.70	11.00	1.50
4	4.00	9.00	.40	11.00	.30
5	5.00	9.00	.60	11.00	.80

Table A5-5. TAT Signal Area for HNO3, NH3, NO3- and NH4+ (volt x sec) versus sample time (minutes) at 25 °C, 52% RH and [HNO_3] = 0.0 ppb.

FILE NAME IS H2052
****
No. OF VALUES IN FILE TO BE STORED= 9
JULIAN DATE FILE = 84230
RELATIVE HUMIDITY= 52
TEMPERATURE = 26.6
**********DATA STORE IN FILE**********

DATA PT	SAMPLE TIME	HNO3	NH3	NO3-	NH4+
1	1.00	9.70	14.00	.80	9.00
2	2.00	11.00	1.30	6.30	0.00
3	3.00	12.10	.50	11.90	4.30
4	4.00	12.50	0.00	20.00	4.10
5	5.00	11.00	8.00	18.50	0.00

Table A5-6. TAT Signal Area for HNO3, NH3, NO3- and NH4+ (volt x sec) versus sample time (minutes) at 25 °C, 78% RH and [HNO_3] = 0.0 ppb.

FILE NAME IS H2078H
****
No. OF VALUES IN FILE TO BE STORED= 9
JULIAN DATE FILE = 84225
RELATIVE HUMIDITY= 78

TEMPERATURE = 27.5
**********DATA STORE IN FILE**********

DATA PT	SAMPLE TIME	HNO3	NH3	NO3-	NH4+
1	1.00	14.00	4.30	5.50	4.70
2	2.00	16.00	7.20	13.00	5.50
3	3.00	16.00	4.00	20.00	5.00
4	4.00	14.00	.30	26.00	3.00
5	5.00	13.00	8.00	32.00	7.00

The vita has been removed from the scanned document

INVESTIGATION OF WATER VAPOR EFFECTS

ON THE DETECTION OF NITRIC ACID VAPOR

WITH THE TUNGSTIC ACID TECHNIQUE

BY

RALPH MICHAEL MARINARO JR.

(ABSTRACT)

An automated tungstic acid technique (TAT) has been successfully used to measure gaseous HNO_3 in the presense of water vapor. The TAT is based on the diffusion of gaseous HNO_3 to the interior walls of a tube coated with tungsten VI oxide (WO_3), where it is selectively chemisorbed. The collected HNO_3 sample is thermally desorbed from the WO_3 surface, as NO, and measured by a chemiluminescent oxides of nitrogen analyzer. The integrated analyzer response is directly proportional to the nitric acid collected.

Based on nitric acid hydration characteristics, a decrease in the diffusion coefficient and thus collection efficiency for denuder type measurement techniques may result with increased atmospheric water vapor (i.e., relative humidity). This study emphasizes the effect of water vapor (i.e., relative humidity) as a potential interferent for HNO_3 collection with the TAT system.

The effect of water vapor (< 78% RH) on the collection efficiency for HNO_3 with the tungstic acid technique is negligible at 25°C, but is significant only at elevated sampling temperatures. This threshold effect is further substantiated and eliminated when a modified sampling collection system was designed with coolant capabilities. The new design has been tested to sub-part-per-billion (NO_x analyzer detection limit) levels with minimal loss of gaseous HNO_3 signal, thereby increasing sensitivity to atmospheric HNO_3 concentrations and maintaining the gas/aerosol sample integrity.